DEVELOPMENT OF A FLUORESCENT DRUG SCREENING TOOL FROM THE TEM-1 BETA-LACTAMASE

CHEONG WING LAM

M. Phil

The Hong Kong Polytechnic University

2011

The Hong Kong Polytechnic University

Department of Applied Biology and Chemical Technology

Development of a Fluorescent Drug Screening Tool from the TEM-1 Beta-Lactamase

Cheong Wing Lam

A Thesis Submitted

in

Partial Fulfillment of the Requirements

for

The Degree of Master of Philosophy

August, 2010

Certificate of Originality

I hereby declare that this thesis is my own work and that, to the best of my knowledge and belief, it reproduces no material previously published or written, nor material that has been accepted for the award of any other degree or diploma, except where due acknowledgement has been made in the text.

Cheong Wing Lam

August, 2010

Abstract

Beta-lactamases are bacterial enzymes which can destroy beta-lactam antibiotics. These enzymes function by hydrolyzing the four-membered beta-lactam ring into clinically inactive carboxylic acid. The increasing emergence of new beta-lactamases has compromised the utility of many beta-lactam antibiotics. As such, extensive efforts have been made to discover new drugs, such as new-generation beta-lactam antibiotics and non-beta-lactam inhibitors. To this end, computational drug screening has been increasingly used to search for potential drug compounds capable of binding to the enzyme's active site. Despite its high efficiency, recent studies have shown that some compounds selected by computational drug screening can form aggregates *in vitro* to inhibit beta-lactamase activity via non-specific protein adsorption/absorption instead of blocking the enzyme's active site specifically. These 'false-positive' compounds may mislead drug discovery teams and therefore result in a huge waste of capital and resources. As such, it is highly desirable to develop a reliable drug screening tool that can screen for active-site-binding drugs *in vitro*. In this project, we developed a fluorescent drug screening tool from the TEM-1 beta-lactamase. This clinically significant enzyme is regarded as the ancestor from which various TEM variants have been derived. Thus, TEM-1 represents a good protein model for the development of *in vitro* drug screening tools from other clinically relevant TEM

variants. The non-catalytic residue Val216 (at the top of the active site) of TEM-1 was first replaced by a cysteine and then labeled by thiol-reactive fluorescein. Despite these modifications, the labelled mutant remains similar in catalytic activity to the wild-type enzyme. The labelled mutant can distinguish compounds capable of binding to the active site from drug aggregates and non-binding compounds by giving characteristic fluorescence changes. Moreover, the labelled mutant can differentiate beta-lactam antibiotics with different potency by giving different fluorescence profiles. Mass spectrometric studies showed that the fluorescence changes are induced by the binding interactions of compounds to the active site. These findings indicate that the labelled V216C mutant can act as an *in vitro* drug screening tool to identify active-site-binding compounds and facilitate the drug development against TEM-type beta-lactamases.

Acknowledgements

I am deeply indebted to my chief supervisor Dr. P. H. Chan for his invaluable suggestions, encouragement, supervision and discussions during the course of my MPhil study. My appreciation is also given to my co-supervisor Prof. Y. C. Leung for his guidance and encouragement. His professional knowledge inspired my interest in biological science.

I would like to thank Dr. W. H. Chung for his guidance in molecular modeling and Ms. M. S. Tsang for her guidance in molecular biology work. I would also like to thank Dr. L. Zou, Ms. F. Y. Chan and Mr. N. Sun for their support in TEM experiments. I deeply appreciate Dr. P. K. So for his assistance in mass spectrometric studies and Dr. Y. J. Lu for his support in circular dichroism experiments.

I would also like to thank my colleagues, Dr. W. L. Wong, Dr. K. P. Ho, Dr. K. C. Cheung, Dr. B. Qiu, Dr. C. Y. Li, Dr. H. Z. Zheng, Dr. Z. H. Liu, Dr. Lawrence Y. S. Lee, Mr. K. M. Lam, Ms. K. Y. Chow and Mr. M. H. So for their support and encouragement in the course of my study.

Furthermore, I would like to acknowledge the Research Committee of the Hong Kong Polytechnic University for supporting my MPhil study.

Last but not least, I would like to express my deepest appreciation to my family for their support and care.

Table of Contents

Abbreviations

α	Alpha
β	Beta
BPMC	Biased Probability Monte Carlo
CD	Circular dichroism
ES*	Covalent enzyme-substrate complex
Da	Dalton
^{o}C	Degree Celsius
DMF	Dimethylformamide
DMSO	Dimethylsulfoxide
ENZ	Enzyme
EDTA	Ethylenediaminetetraacetic acid
ESBL	Extended Spectrum Beta-Lactamase(s)
ESI-MS	Electrospray Ionization Mass Spectrometry
FRET	Forster Resonance Energy Transfer
h	hour
IPTG	Isopropyl-beta-$_{D}$-1-thiogalactopyranoside
IRT	Inhibitor-Resistant TEM

k	kilo (1×10^3)
m/z	mass-to-charge ratio
K_M	Michaelis constant
μ	micro (1×10^{-6})
m	mini (1×10^{-3})
min	minute(s)
M	Molarity
NAG	N-acetylglucosamine
NAM	N-acetylmuramic acid
n	nano (1×10^{-9})
Ω	Omega
PBP(s)	Penicillin-binding Protein(s)
PTA	Phosphotungstic acid
rpm	Revolution(s) per minute
SDS-PAGE	Sodium dodecyl sulfate polyacrylamide gel electrophoresis
s	second(s)
TIPP	Tetraiodophenolphthalein
TEM	Transmission Electron Microscopy
k_{cat}	turnover number

UV	Ultra-violet
VIS	Visible
V	Volt(s)
v/v	volume-to-volume

Chapter 1

Introduction

1.1 β-Lactam antibiotics

β-Lactam antibiotics are antibacterial agents which share a common structure of four-membered β-lactam ring. These drugs function by inhibiting the catalytic activity of peptidoglycan transpeptidase (also known as penicillin-binding protein, PBP), a bacterial enzyme responsible for cell wall synthesis. PBP catalyzes the cross-linking reaction (transpeptidation) of the glycine end and $_{D}$-alanyl-$_{D}$-alanine end of N-acetylmuramic acid (NAM)-N-acetylglucosamine (NAG) strands, thus forming a network of peptidoglycan (Figure 1.1). β-Lactam antibiotics can 'mimic' the $_{D}$-alanyl-$_{D}$-alanine group in peptidoglycan and bind to the active site of PBP to form a very stable enzyme-substrate complex (Figures 1.2 and 1.3). As a consequence, the active site of PBP is irreversibly blocked, making the protein unable to catalyze the cross-linking reaction in peptidoglycan.[1-3] The inhibitory activity of β-lactam antibiotics towards bacterial PBP is rather specific and is virtually harmless to humans (having no peptidoglycan) in general.[4]

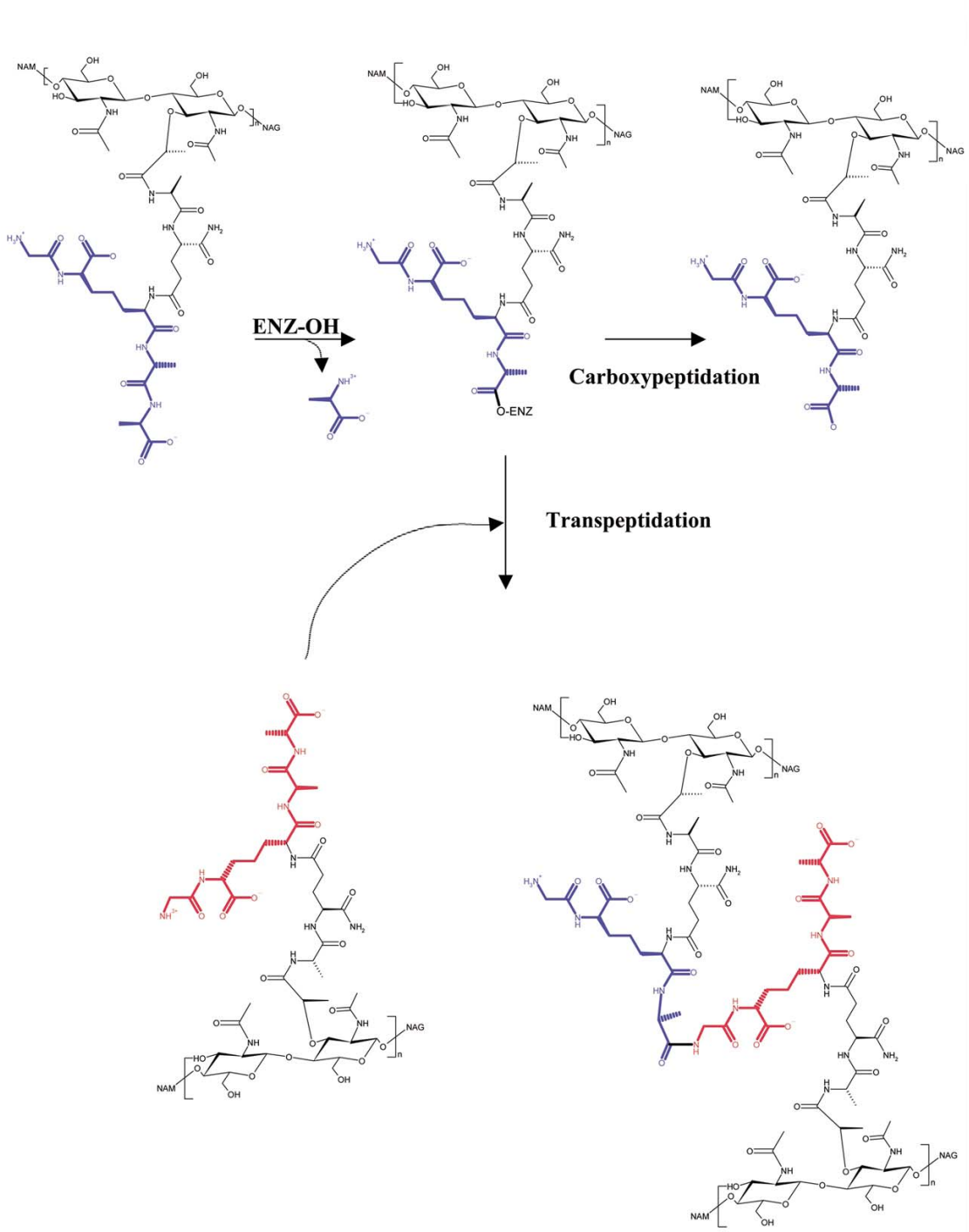

Figure 1.1 Transpeptidation of the peptidoglycans of *Streptomyces* sp. The $_{D}$-alanyl-$_{D}$-alanine end (blue) of a NAM-NAG strand (peptidoglycan) is covalently linked to the glycine end (red) of another NAM-NAG strand by penicillin-binding protein (ENZ-OH).[2]

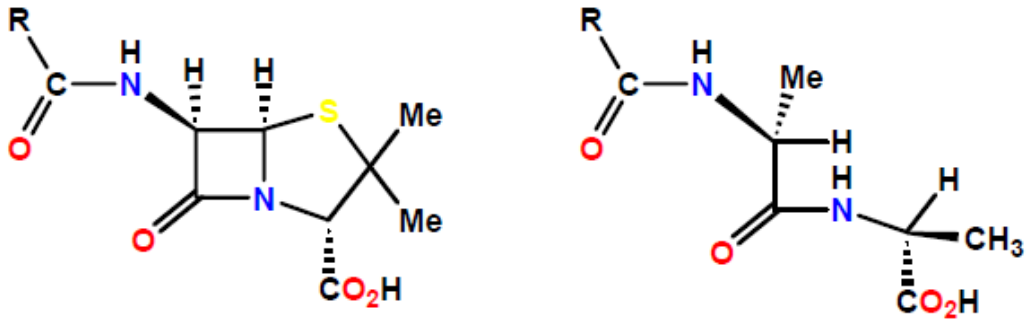

(a) (b)

Figure 1.2 Structures of a penicillin antibiotic (a) and D-alanyl-D-alanine (b).[1]

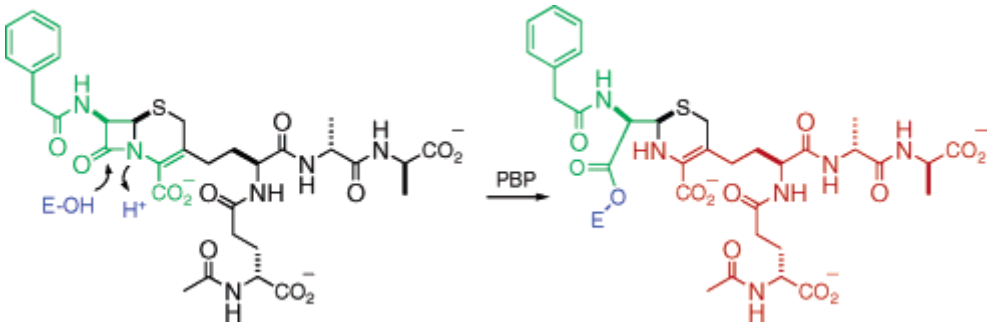

Figure 1.3 Irreversible inhibition of penicillin-binding protein by a β-lactam antibiotic.[5]

β-Lactam antibiotics are classified into 4 main categories: (i) penams, (ii) cephems, (iii) penems and (iv) monolactams. Penams have a tetracyclic β-lactam ring fused with a pentacyclic thiazolidine ring, which contains a sulfur atom and is fully saturated. A side chain (RCO-) is covalently linked to the amino group at the C-6 position on the β-lactam ring. The β-lactam ring is fused with the five-membered thiazolidine ring to form a 'bowl-type' structure (Figure 1.4). The cyclic β-lactam ring itself has structural strain, which can be released when it is hydrolyzed into carboxylic acid. Examples of penams include penicillin G and ampicillin.[1, 4]

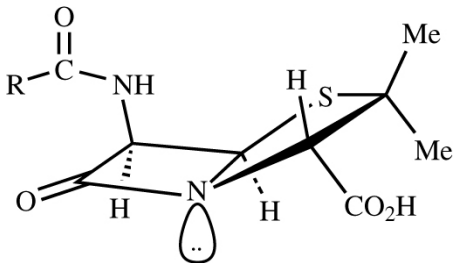

(a)

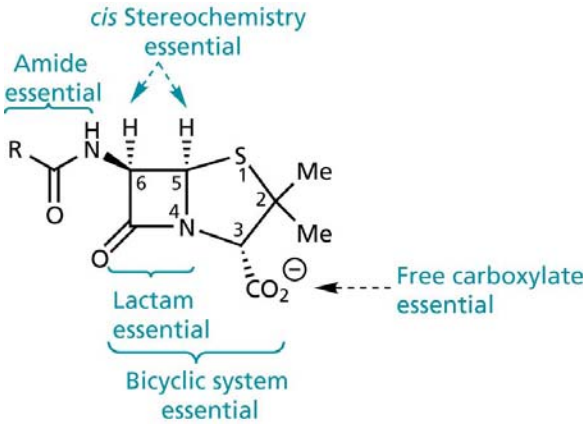

(b)

Figure 1.4 Typical structure of a penicillin-type antibiotic.[1]

Cephems are structurally similar to penams except that they have a hexacyclic ring fused with the β-lactam ring and a C=C double bond at the C-3 position (Figure 1.5). This class is further divided into cephalosporins (X = S), carbacephems (X = C) and oxa-1-cephems (X = O). Cephalosporins and penicillins are the 2 major classes of antibiotic that have been widely used in clinical treatment.[1, 4]

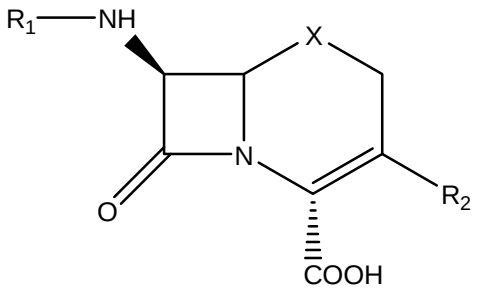

Figure 1.5 Typical structure of cephems.

The first cephalosporin antibiotic was discovered from *Cephalosporium acreminium* in which its mutant produces cephalosporin C antibiotic. The side chain at the C-3 position of the six-membered ring can be detached upon β-lactam hydrolysis. This antibiotic is effective in inhibiting the catalytic activity of PBP (Figure 1.6a). Cephalothin is a member of the first-generation cephalosporin and has broad spectrum activity against different bacteria. This antibiotic has been widely used to kill bacteria that are resistant to penicillins (Figure 1.6b). The second-generation cephalosporins, which contain a methoxy substituent at the C-7 position, are called cephamycins.

Cefoxitin is an example which has greater resistance against β-lactamase activity (Figure 1.6c).[6-8] Some oximinocephalosporins (e.g. cefuroxime) are also classified as the second-generation cephalosporins. It has an iminomethoxy group at the α-position of the acyl side chain which gives stronger resistance against β-lactamases and esterases (Figure 1.6d). Replacing the furan ring at the side chain of oximinocephalosporins with an aminothiazole ring gives the third-generation cephalosporins, including ceftazidime and cefotaxime (Figures 1.6e,f). These antibiotics show higher penetration through the outer membrane in bacteria and have higher affinity for PBP (Figures 1.6e,f).[1, 4, 9, 10]

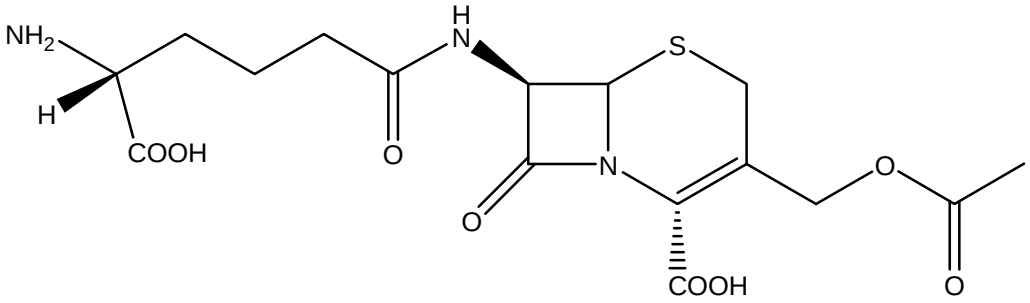
NH2
H
COOH
H
N
O
S
N
O
O
COOH
O

(a)

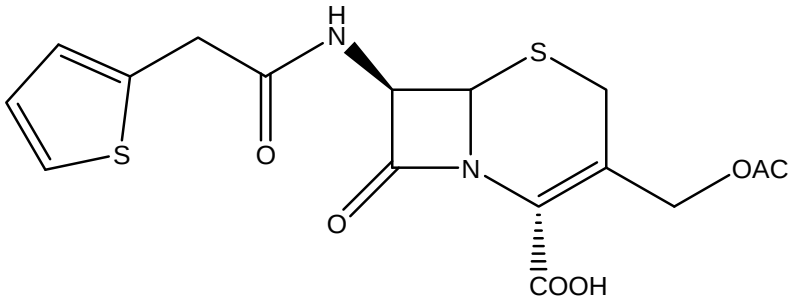
H
N
S
O
S
N
OAC
O
COOH

(b)

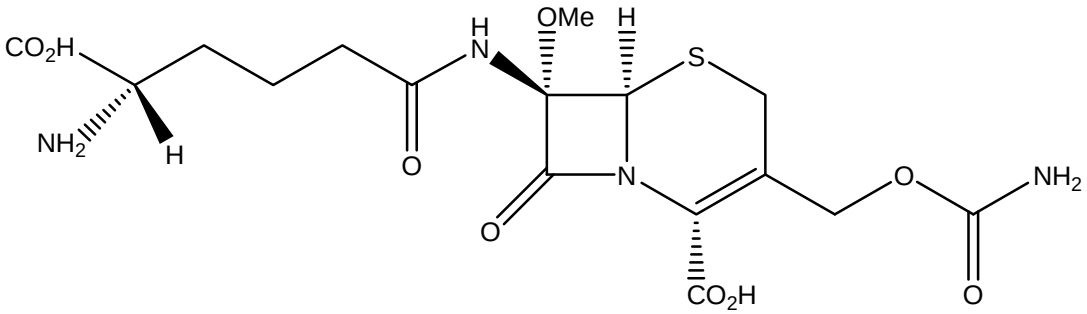
CO2H
NH2
H
H
N
O
OMe
H
S
N
O
O
NH2
CO2H
O

(c)

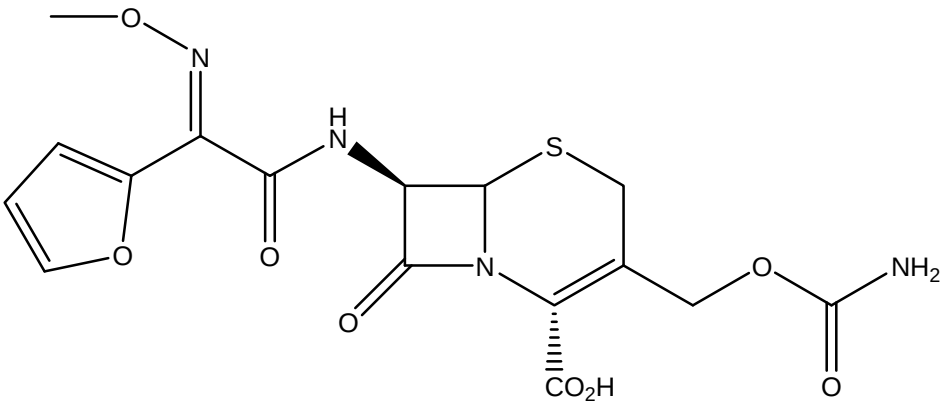
O
N
H
N
O
O
S
N
O
O
NH2
CO2H
O

(d)

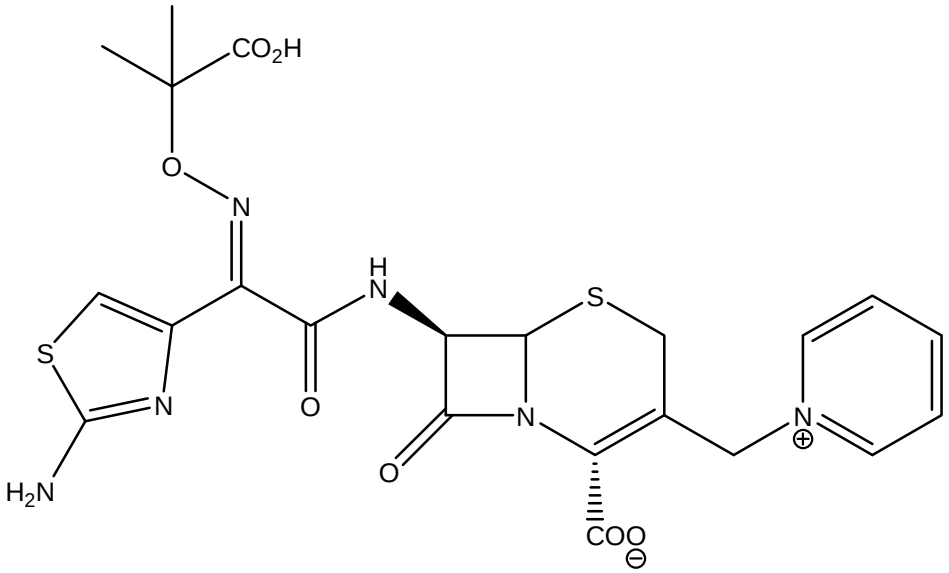

(e)

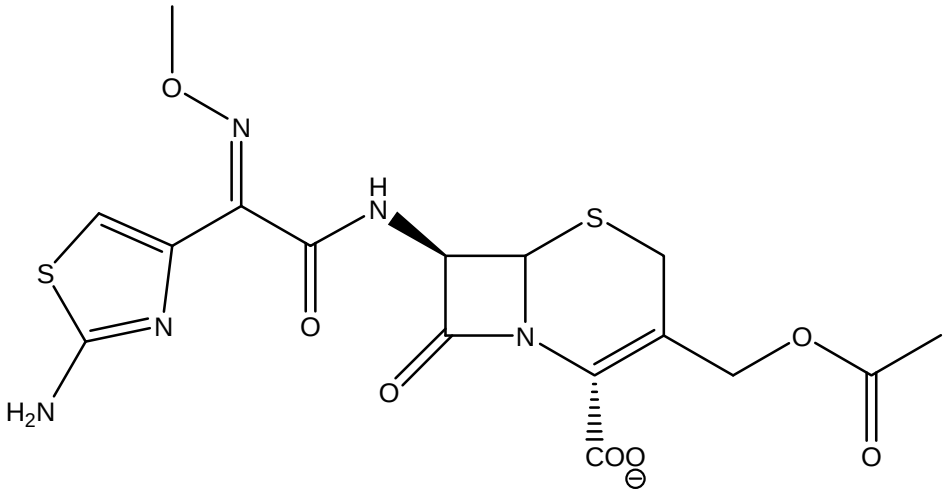

(f)

Figure 1.6 Structures of cephalosporin C (a), cephalothin (b), cefoxitin (c), cefuroxime (d), ceftazidime (e), and cefotaxime (f).

Penems are structurally similar to penams except that there is a C=C double bond at the C-2 position of the five-membered ring, which is fused with the β-lactam ring. A hydroxyl group is linked to the carbon connected to the C-6 on the β-lactam ring. The stereochemistry of the side chain at the C-6 is opposite to those of penicillins and cephalosporins. Antibiotics in this class have stronger resistance to various β-lactamases, including those that can hydrolyze ceftazidime and cefotaxime. Traditional penems contain a sulphur atom at position 1. For oxa-1-penems, an oxygen atom is at position 1, whereas a carbon atom is found at position 1 in carbapenems. Although carbapenems show broader spectrum activity compared to other β-lactam antibiotics, they are chemically unstable and have poor oral absorption.[11, 12] Thienamycin is the first carbapenem isolated from *Streptomyces cattleya*. Imipenem is one of its analogues used clinically (Figure 1.7).[1, 4]

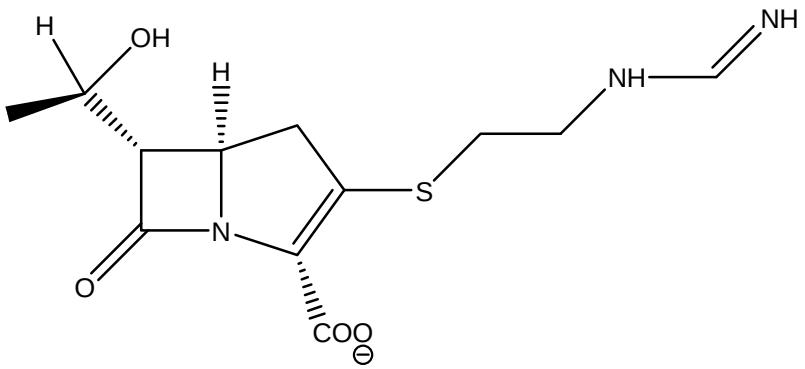

Figure 1.7 Structure of imipenem.

Monolactams consist of a single β-lactam ring only. This structure is different from other β-lactam antibiotics which usually contain a secondary fused ring next to the β-lactam ring. Monolactams are inactive against Gram-positive bacteria. Aztreonam is an example of monolactam (Figure 1.8).[1, 4, 13]

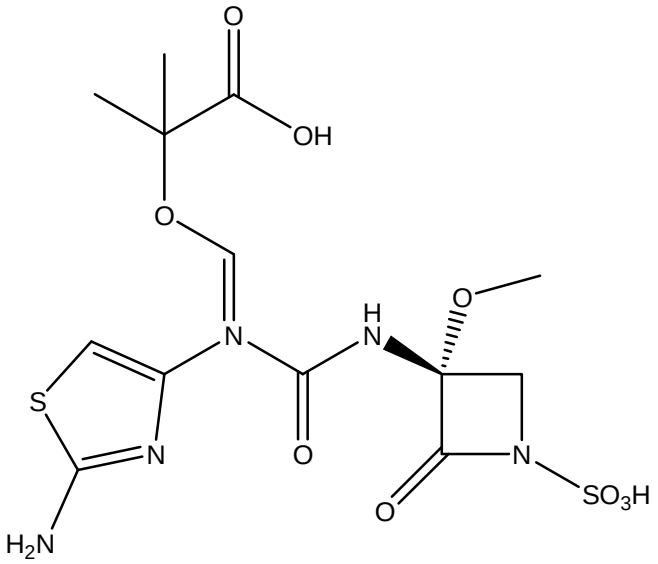

Figure 1.8 Structure of aztreonam.

Apart from β-lactam antibiotics, there is an important class of β-lactam drugs that target β-lactamases. There are 3 clinically important β-lactamase inhibitors: clavulanic acid, sulbactam and tazobactam (Figure 1.9). These inhibitors act as suicide substrates and can covalently bind to the –OH group of the catalytic serine residue in the active site with their β-lactam carbonyl group to form stable acyl-enzyme complexes. As a result of this irreversible binding, the enzyme's active site is permanently blocked, and the enzyme is no longer able to bind antibiotics. β-Lactamase inhibitors are often used in combination with β-lactam antibiotics in clinical treatment, such that the former can inactivate β-lactamases whereas the latter can target at the PBP in bacteria.[4, 8, 12, 14-17]

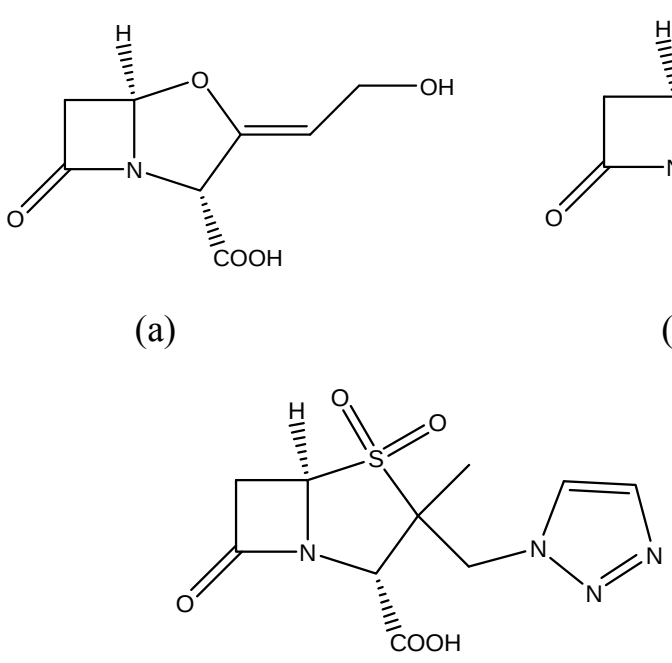

Figure 1.9 Structures of clavulanic acid (a), sulbactam (b) and tazobactam (c).

1.2 β-Lactamases

The extensive use of β-lactam antibiotics has led to a worrying clinical problem worldwide. To combat the antibacterial activity of β-lactam antibiotics, many bacteria have developed an effective mechanism for defense which involves the production of β-lactamases. These bacterial enzymes can efficiently hydrolyze the β-lactam ring in antibiotics into clinically inactive carboxylic acid, thus making the hydrolyzed antibiotics unable to bind to PBP. As a consequence, the bacteria can continue to produce cell walls and grow.[3, 5, 18-23] β-Lactamase genes can be spread among different bacteria through the transfer of plasmids.[24] To date, more than 400 β-lactamases with various substrate and catalytic profiles have been identified.[25] β-Lactamases can be classified by different ways (Richmond and Sykes, 1973; Mitsuhashi and Inoue, 1981; Bush et al, 1995[26]),[4] and the most common classification is based on the Ambler's method, which categorizes β-lactamases into classes A – D according to their primary sequences.[27]

Members in classes A, C and D are classified as serine-type β-lactamases. The general catalytic mechanism for these enzymes involves the use of serine (Figure 1.10). The hydroxyl group of the serine residue is first activated by a base to form Ser-O^-. The negatively charged oxide group on the serine then attacks the carbonyl

carbon in the β-lactam ring to form a covalent linkage, leading to the cleavage of the ring (acylation). A water molecule activated by another base attacks the carbonyl carbon to cleave the covalent linkage between the serine and the β-lactam substrate (deacylation), thus converting the substrate into carboxylic acid and regenerating the active enzyme (Figure. 1.10).[3, 20]

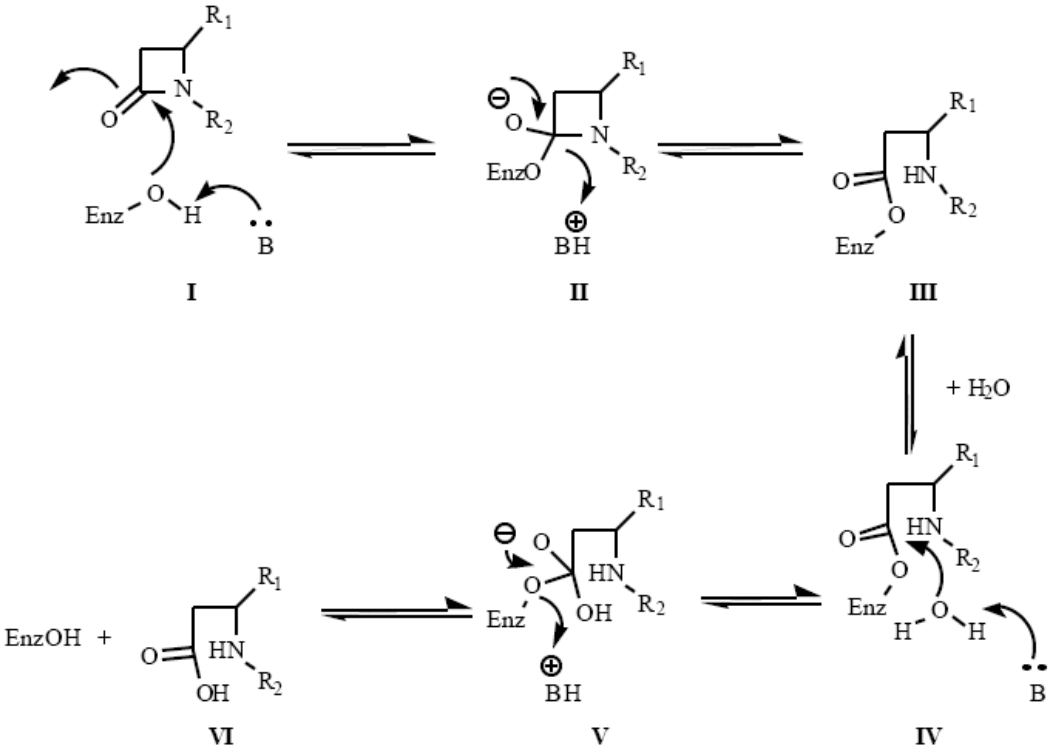

Figure 1.10 General mechanism for the hydrolysis of β-lactam by serine-type β-lactamases.[20]

Class A β-lactamases are the most prevalent enzymes which are often encountered in clinical cases. Members in class A contain four catalytically important residues: Ser70, Lys73, Ser130, and Glu166. These enzymes can hydrolyze penicillins with high efficiency as well as some cephalosporins and carbapenems. Ser70 is the catalytic residue involved in the acylation step, while Glu166 acts as the base to activate Ser70 via a water bridge (Figure 1.11). Examples of class A include TEM-, SHV- and CTX-M type β-lactamases.[3, 5, 28-38]

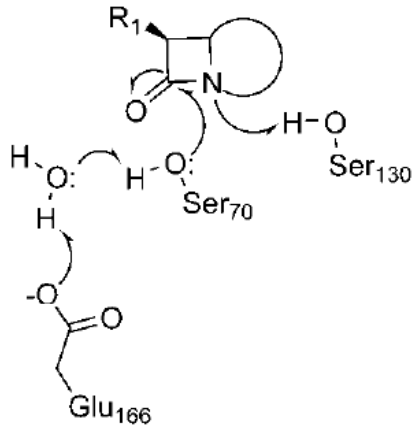

Figure 1.11 Mechanism of the acylation step for class A β-lactamases.[32]

Class B β-lactamases are metalloenzymes which make use of Zn^{2+} in the active site to hydrolyze β-lactam antibiotics and inhibitors (including clavulanic acid). These enzymes can hydrolyze a wide range of β-lactam antibiotics. The zinc ion appears to facilitate the hydrolytic process by binding to the β-lactam carbonyl group (Figure 1.12). Compounds capable of trapping the metal ion in the active site (e.g. EDTA) can inactivate class B enzymes.[3, 5, 20, 39, 40]

Class C β-lactamases share a similar catalytic mechanism to class A enzymes. The catalytic residues are Ser64, Lys67, Lys315 and Tyr150. Ser64 plays the same role as Ser70 in class A enzymes (for acylation), whereas Tyr150 acts as the base to activate Ser64. Class C β-lactamases can hydrolyze a wide range of antibiotics, including penicillins (e.g. ampicillin), cephalothin, and the third-generation cephalosporins. Inhibitors for class A β-lactamases (e.g. clavulanic acid) are, in general, inactive to class C β-lactamases.[3, 5, 41-44]

Class D β-lactamases are also serine-type enzymes. These enzymes are more efficient than classes A and C enzymes in hydrolyzing the third-generation cephalosporins and carbapenems. Examples of class D include OVA-type β-lactamases. Little is known about the structures and catalytic mechanism of class D

β-lactamases. It appears that the Lys70-carbamate moiety plays an important role in the acylation step.[3, 5]

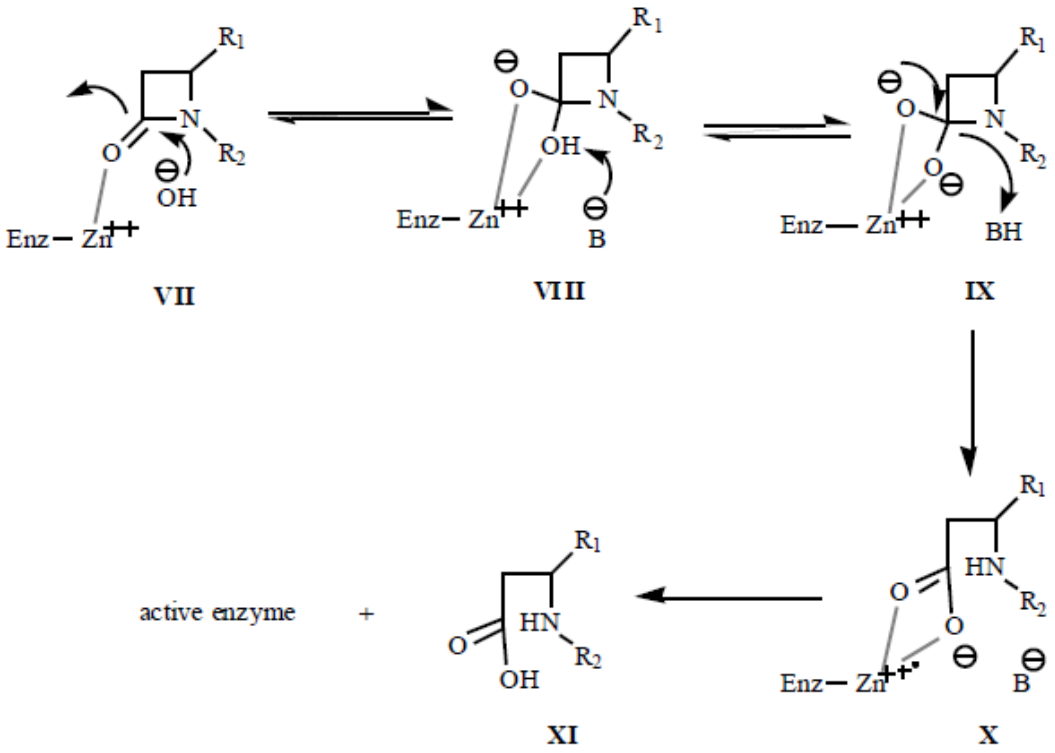

Figure 1.12 Catalytic mechanism of metallo β-lactamases (class B).[20]

1.3 Drug development

The increasing emergence of β-lactamases with different substrate and catalytic profiles has compromised the clinical utility of many existing antibiotics. One of the possible approaches to resolve this problem is to develop new-generation antibiotics with stronger resistance to β-lactamase activity.[45-53] In addition, extensive efforts have been directed to the discovery of new non-β-lactam inhibitors against β-lactamases.[3, 54-56] This development has been greatly facilitated by the advent of computational drug screening, which can search for potential drug candidates from chemical libraries in a high-throughput manner. This *in silico* drug screening approach involves the docking of compounds into the active site of the protein of interest. The docking process predicts the binding geometry and ranks the 'binding affinity' for each compound in terms of scoring. Compounds capable of fitting the binding site in the protein can be identified from non-binding compounds. Moreover, compounds with top scores (i.e. higher binding affinity) can be further selected for *in vitro* drug testing or drug development through structural modifications.[49, 57-61] Common docking programs include DOCK, FlexX, AutoDock, GOLD and ICM.[62, 63]

Although the use of computational drug screening can facilitate the discovery of new drugs against β-lactamases, drug candidates identified *in silico* may not behave

as predicted by docking (i.e. specific binding to the binding site of the protein target). Recent studies have shown that some compounds identified *in silico* may form aggregates in aqueous solution. Such aggregates can inhibit the activity of proteins through protein absorption/adsorption.[64-69] These non-specific mechanisms may cause the bound protein to undergo partial unfolding, thus losing its natural structure and hence activity (Figure 1.13).[70] Recent studies have shown that 95% of drug compounds identified *in silico* tend to form aggregates in aqueous solution.[71] Drug aggregates can also inhibit the activity of β-lactamase *in vitro*.[72] The non-specific inhibitory activity of drug aggregates (false positive) may mislead drug development teams in the selection of drug candidates, thus resulting in a huge waste of capital and resources.

Drug aggregates can be detected by transmission electron microscopy, control protein assays and dynamic light scattering. Recent studies have shown that the non-ionic surfactant triton X-100 can suppress the formation of aggregates by molecules in aqueous solution.[63, 73, 74] This approach, however, may not be applicable to all compounds, since some compounds identified *in silico* for the class C P99 β-lactamase can still form aggregates *in vitro* even in the presence of triton X-100 (unpublished results). Thus, in the development of new drugs for β-lactamases, the

identification of true-positive compounds (capable of specifically blocking the active site rather than forming aggregates) must be addressed. As such, it is highly desirable to develop a reliable drug screening tool that can identify active-site-binding compounds from non-binding compounds and aggregates *in vitro*.

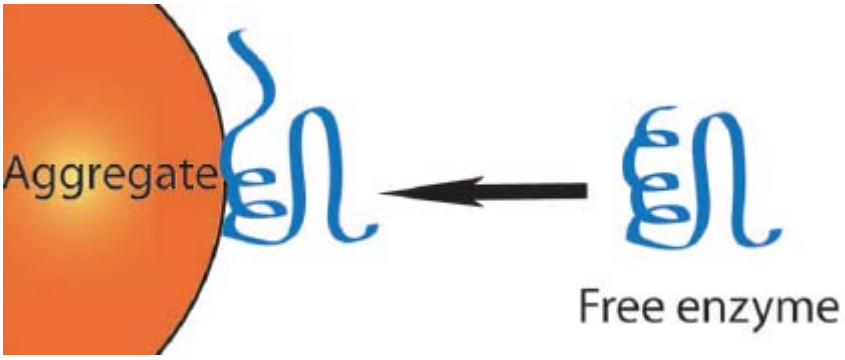

Figure 1.13 Non-specific inhibition of enzymes by aggregates formed by rottlerin. Enzymes are likely to undergo partial unfolding upon interacting with 'drug aggregates'.[70]

1.4 Methods for detection of β-lactamase activity

In the development of new drugs against β-lactamases, the potency of the drug candidates must be assessed by examining the catalytic activity of the enzymes *in vitro*. In this regard, compounds that can specifically bind to the active site and inhibit the activity of the enzyme can be potential drug candidates. Thus, monitoring β-lactamase activity is an essential task in the drug development against β-lactamases.[75]

Bacteria susceptibility test is the most common approach for assessing the potency of new drugs. Bacteria encoded with a β-lactamase expressing gene are able to produce the corresponding β-lactamase enzyme. In the presence of potent drugs (e.g. resistant antibiotics), the growth of the bacteria will be suppressed, thus leading to a large reduction in the bacterial population.[5, 76, 77] This approach is, however, less specific in the assessment of the potency of drugs against β-lactamases because the growth of bacteria can also be influenced by other resistant mechanisms in bacteria, such as porin channel mutations and active efflux pumps. These mechanisms can also help bacteria protect themselves against antibacterial agents. Thus, bacteria susceptibility test is not a direct method that can reveal the potency of drugs against β-lactamase targets.

The conventional spectrophotometric method has been routinely used to monitor the catalytic activity of β-lactamases. The chromogenic substrate nitrocefin is widely used as a reporter to examine the inhibitory effects of new drugs against β-lactamases. Nitrocefin is a yellow cephalosporin substrate which is highly reactive towards the hydrolytic action of β-lactamases. Upon hydrolysis, its visible absorption peak shifts from 386 nm to 482 nm, and the absorbance at 482 nm increases as a function of time (Figure 1.14). In the presence of drugs capable of binding to the enzyme's active site, the drugs will compete with nitrocefin for the enzyme's active site and therefore the catalytic activity of the β-lactamase enzyme towards nitrocefin will be reduced. Thus, the reduction in enzyme kinetics acts as an indicator of the inhibitory activity of the drug compound.[78, 79] This conventional approach is, however, unable to distinguish 'drug aggregates' from true-positive drugs; in both cases, a reduction in β-lactamase activity is resulted, although 'drug aggregates' exert their inhibitory effects through non-specific protein absorption/adsorption *in vitro*. The use of the spectrophotometric method may, therefore, give rise to the risk of selecting false-positive drugs (which tend to form aggregates *in vitro*).

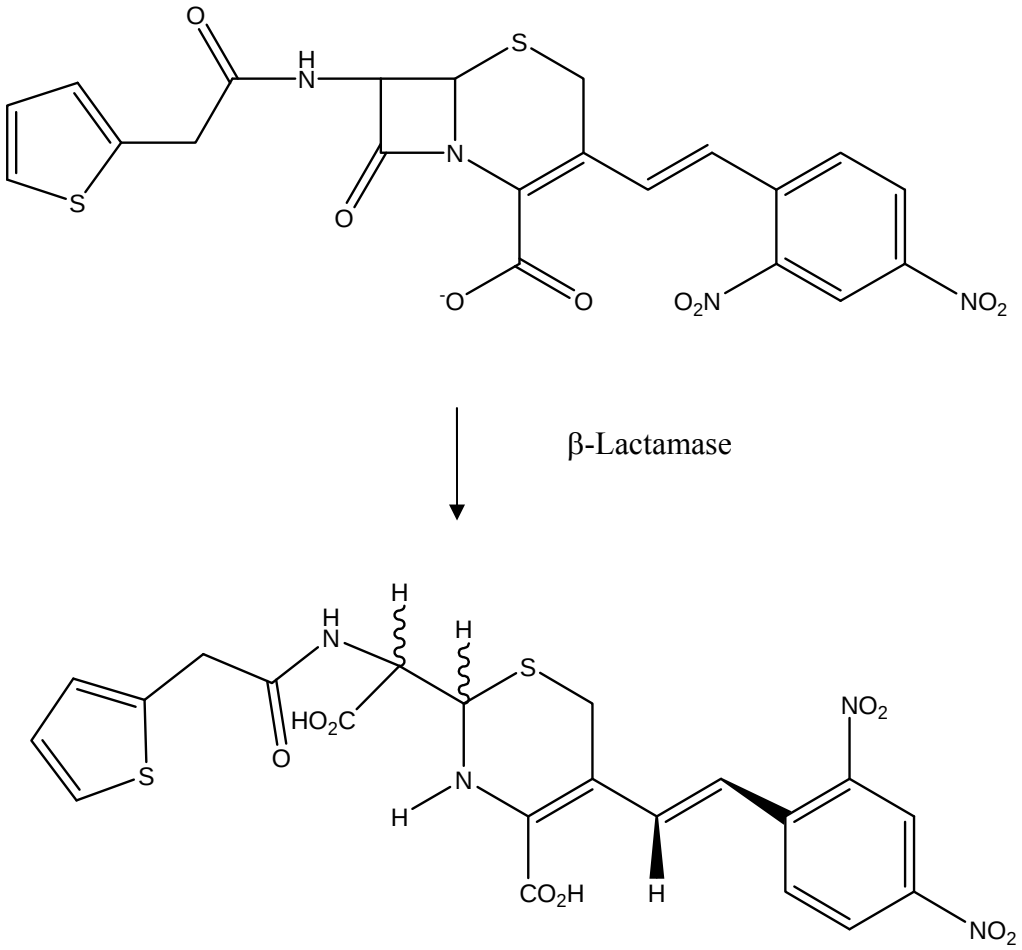

Figure 1.14 Hydrolysis of nitrocefin by β-lactamase. The absorption peak of nitrocefin shifts from 386 nm to 482 nm accompanied with an increase in the absorbance at 482 nm upon enzymatic hydrolysis.[79]

Recently, Puckett et al have developed a pH-dependent sensor for detection of β-lactamae activity. A pH-sensitive fluorogenic enzyme is added to a reaction mixture of β-lactamase and the β-lactam antibiotic. Hydrolysis of the β-lactam antibiotic results in a decrease in pH, thus giving a fluorescence change (Figure 1.15). The change in fluorescence is consistent with the rate of β-lactam hydrolysis. [80]

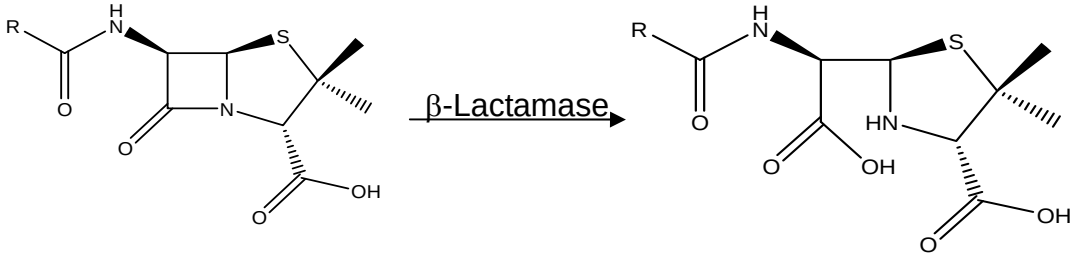

Figure 1.15 Hydrolysis of penicillin by β-lactamase. The pH of the sample is reduced as a result of the production of the hydrolyzed product (carboxylic acid).[80]

Jiang et al have developed a colorimetric assay for detecting β-lactamase activity.[81] This assay involves the use of gold nanoparticles and a cephalosporin antibiotic covalently linked to a thiol linker. In the presence of β-lactamase, the cephalosporin antibiotic is hydrolyzed and releases the attached thiol linker. The thiol linker then adsorb on nanoparticles, causing them to form blue aggregates in solution. In the presence of an inhibitor, the hydrolysis of cephalosporin antibiotic by β-lactamase is suppressed, and the thiol linker remains covalently attached to the antibiotic. As a result, the nanoparticles are unable to aggregate and produce a red solution.

Forster resonance energy transfer (FRET) has also been used to detect β-lactamase activity. A cephalosporin antibiotic is covalently linked to a fluorescence donor and a fluorescence acceptor. In the absence of β-lactamase, the antibiotic remains intact, and the fluorescence acceptor gives its characteristic emission upon excitation of the fluorescence donor due to their close proximity. Upon hydrolysis by β-lactamase, the fluorescence acceptor is detached from the antibiotic, rendering FRET impossible to occur. Thus, there will be a reduction in the fluorescence of the acceptor.

1.5 Objectives

The advent of computational drug screening has advanced the development of new drugs against β-lactamases. Despite this exciting development, the *in vitro* world is different from the *in silico* world. *In vitro* drug screening is equally important in drug development because of the possible formation of aggregates by compounds in aqueous solution, which inhibit β-lactamase activity through non-specific protein adsorption/absorption and hence give false-positive testing results. Thus, the success of drug development for β-lactamases requires (a) the identification of compounds capable of specifically binding to the active site *in vitro* and (b) the differentiation of these true-positive compounds from non-binding compounds and aggregates *in vitro*. The conventional and newly developed methods appear to be unable to fulfill these two important tasks. As such, it is highly desirable to develop a reliable *in vitro* drug screening tool which can fulfill the aforementioned purposes.

In this project, we are interested to develop an *in vitro* fluorescent drug screening tool from the clinically significant TEM-1 β-lactamase. This bacterial enzyme can confer ampicillin resistance on bacteria and is regarded as the ancestor from which a variety of TEM variants are derived. The fluorescent drug screening tool is constructed by engineering the wild-type TEM-1 enzyme into a cysteine-containing

mutant and subsequently attaching a fluorophore close to the active site.[82, 83] The fluorescently labeled mutant is constructed in such a way that its catalytic activity remains similar to that of the wild-type TEM-1 enzyme, while it can selectively respond to compounds capable of binding to its active site by giving fluorescence changes.[84, 85] These properties allow the fluorescently labeled mutant to act as the 'natural' drug target TEM-1 (due to having wild-type activity) to screen for drug compounds *in vitro*.

In Chapter 2 are presented the details of the experimental work involved in this project. The strategy for constructing fluorescent drug screening tools from TEM-1 and their characterization are discussed in Chapter 3. The fundamental studies of the fluorescent drug screening tool (including fluorescence, mass spectrometric and molecular modeling studies) are described in detail in Chapter 4.

Chapter 2

Materials and Methods

2.1 Chemicals

Penicillin G, ampicillin, cephalothin, cefoxitin, potassium clavulanate, N-benozyl-L-arginine ethyl ester hydrochloride, kanamycin, congo red, 3',3",5',5"-tetraiodophenolphthalein (TIPP), aspirin, glucose and hen egg white lysozyme were purchased from Sigma. Sodium chloride, potassium chloride, potassium hydroxide, potassium phosphate, imidazole, Tris-HCl, IPTG were obtained from USB. Yeast extract, tryptone, agar were purchased from Oxoid. Dimethylformamide (DMF) and dimethyl sulfoxide (DMSO) were obtained from Acros. Fluorescein-5-maleimide was purchased from Invitrogen.

2.2 Instruments

Fluorescence experiments were performed on a Perkin Elmer LS-50B spectrofluorimeter. Perkin Elmer Lambda 35 UV/VIS spectrophotometer was used for enzyme kinetic studies. ESI-MS experiments were conducted using a micromass Q-Tof-2^{TM} spectrometer. Circular dichroism (CD) measurements were performed on a Jasco J-810 spectropolarimeter. TEM measurements were done using a DEOL JEM-2010 electron microscope.

2.3 Preparation of the wild-type and mutant forms of the TEM-1 β-lactamase

E. coil BL21 DE-3 was used as the bacterial strain to produce the wild-type and mutant forms (N170C and V216C) of the TEM-1 β-lactamase. The enzymes were $(His)_6$-tagged at their C-terminus. 2xTY medium was prepared by dissolving 10 g of yeast extract, 16 g of tryptone and 5 g of NaCl into 1 L of H_2O and then sterilized with an autoclave. Pre-culture was prepared by inoculating a few frozen bacterial strains into 5 mL of sterile 2xTY medium containing 50 μg/mL kanamycin and then shaked at 280 rpm overnight at 37°C. A 2 mL portion of the pre-culture was then added to 200 mL of 2xTY medium with 50 μg/mL kanamycin at 37°C. When the optical density at 600 nm reached 0.8, a 400 μL portion of IPTG (200 mg/mL) was added to the bacterial culture to induce protein expression, and the culture was further incubated at 25 °C with shaking (280 rpm) for 20 h. After incubation, the culture was then centrifuged at 7000 rpm for 20 min at 4 °C, and the supernatant was discarded. The cell pellets were collected and resuspended in 20 mL of solubilization buffer (50 mM Tris, 0.1 M NaCl, pH 7.4). The sample was then added with 150 μL of hen lysozyme (10 mg/mL) and then incubated at 30 °C for 30 min, followed by sonication for 4 min (30-s on and off cycles). The solution fraction was collected by centrifugation at 13,000 rpm for 1 h at 4 °C and then filtered with a 0.22-μm membrane. The enzymes were purified by Ni^{2+}-affinity chromatography with a linear

gradient elution of 0-0.5 M imidazole in 20 mM sodium phosphate buffer (pH 7.0). The purified enzymes were dialyzed against H_2O at 4 ^oC, freeze-dried and then stored at -20 ^oC. The purity of the enzymes was examined by SDS-PAGE (Figures 2.1 - 2.3).

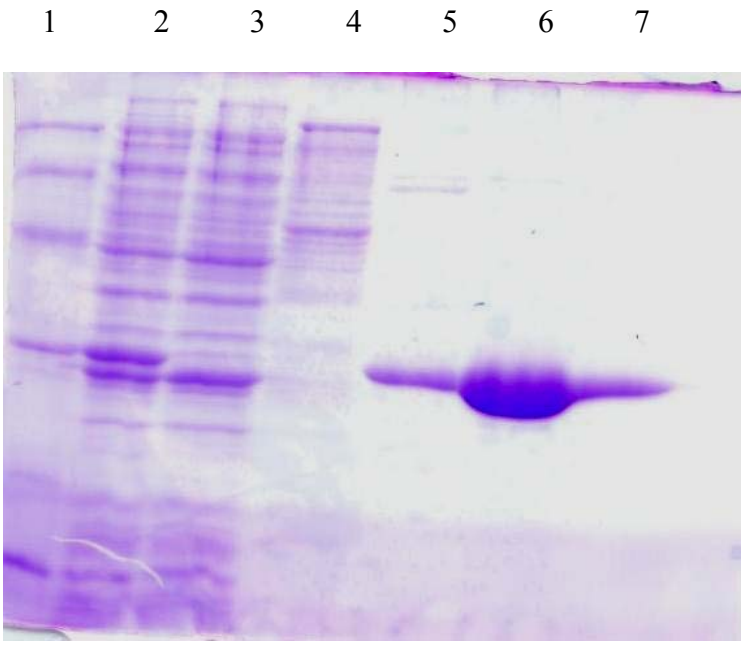

Figure 2.1 SDS-PAGE analysis of the wild-type TEM-1 β-lactamase. Lane 1, low range molecular marker: rabbit muscle phsophorylase b (97,400 Da), BSA (66,200 Da), hen egg white ovalbumin (45,000 Da), bovine carbonic anhydrolase (31,000 Da), soybean trypsin inhibitor (21,500 Da), hen egg white lysozyme (14,400 Da); lane 2: culture supernatant before loading onto the column; lane 3: flow-through supernatant (eluted at 0% imidazole); lane 4: protein sample eluted at 10% imidazole; lanes 5-7: protein sample eluted at 30% imidazole.

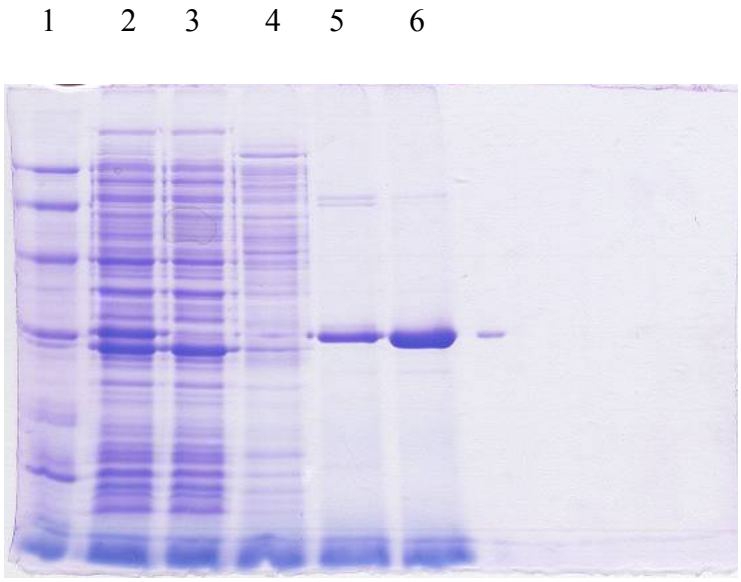

Figure 2.2 SDS-PAGE analysis of the N170C mutant of the TEM-1 β-lactamase. Lane 1, low range molecular marker: rabbit muscle phsophorylase b (97,400 Da), BSA (66,200 Da), hen egg white ovalbumin (45,000 Da), bovine carbonic anhydrolase (31,000 Da), soybean trypsin inhibitor (21,500 Da), hen egg white lysozyme (14,400 Da); lane 2: culture supernatant before loading onto the column; lane 3: flow-through supernatant (eluted at 0% imidazole); lane 4: protein sample eluted at 10% imidazole; lanes 5-6: protein sample eluted at 30% imidazole.

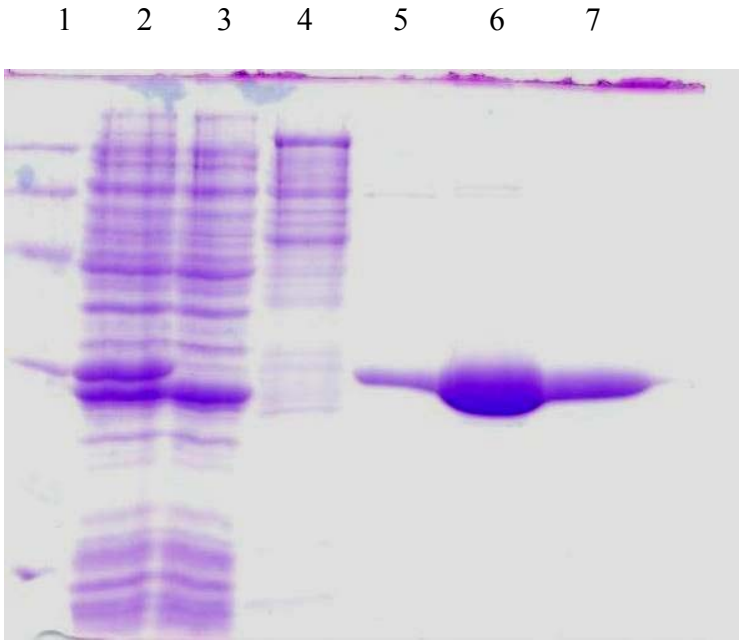

Figure 2.3 SDS-PAGE analysis of the V216C mutant of the TEM-1 β-lactamase. Lane 1, low range molecular marker: rabbit muscle phsophorylase b (97,400 Da), BSA (66,200 Da), hen egg white ovalbumin (45,000 Da), bovine carbonic anhydrolase (31,000 Da), soybean trypsin inhibitor (21,500 Da), hen egg white lysozyme (14,400 Da); lane 2: culture supernatant before loading onto the column; lane 3: flow-through supernatant (eluted at 0% imidazole); lane 4: protein sample eluted at 10% imidazole; lanes 5-7: protein sample eluted at 30% imidazole.

2.4 Protein labeling

The N170C and V216C mutants were labeled with fluorescein-5-maleimide. This thiol-reactive fluorophore can be covalently linked to the –SH group of cysteine (Scheme 2.1). The protein was first dissolved in 6 mL of potassium phosphate buffer (pH 7.0). A 5-fold molar excess of fluorescein-5-maleimide (20 mM, dissolved in dimethylformamide) was then added to the protein solution, and the protein solution was stirred in dark at 25 ^{o}C for 30 min. After labeling, the protein solution was dialyzed against deionized H_2O at 4 ^{o}C to remove excess dye and then freeze-dried.

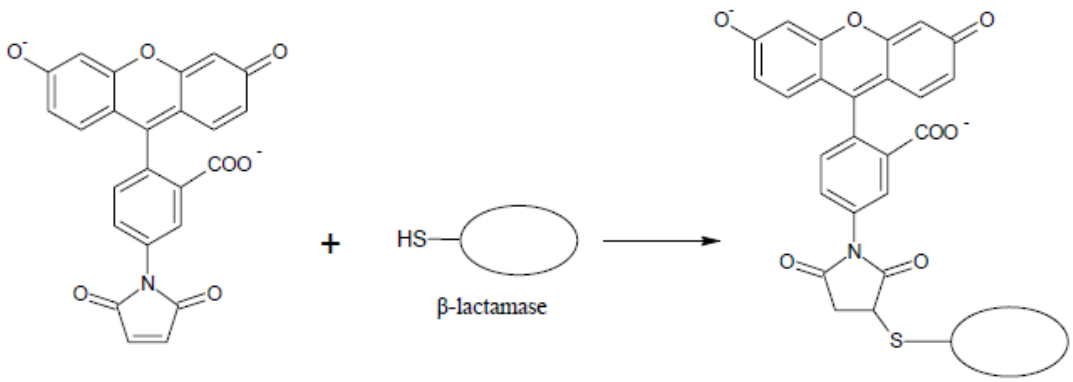

Scheme 2.1 Conjugation of fluorescein-5-maleimide with the cysteine residue of the TEM-1 β-lactamase mutant (N170C and V216C).

2.5 Electrospray ionization mass spectrometric studies

Determination of protein molecular mass

The molecular masses of the wild-type enzyme and the mutants (labeled and unlabeled N170C and V216C) were determined by electrospray ionization mass spectrometry (ESI-MS). Each of the proteins was dissolved in 150 μL of 20 mM ammonium acetate buffer (pH 7.0) to a final concentration of 5-10 μM. The protein solution was centrifuged to remove insoluble materials. ESI-MS measurements were performed on a Micromass Q-Tof-2^{TM} spectrometer. Concentrated protein samples were mixed with acetonitrile (1:1 v/v) and injected into the electrospray source by a syringe pump (Harvard Apparatus, model 22) at a flow rate of 5 μL/min. The mass spectrometer was scanned over a range of 700–1600 m/z and the multiply-charged protein ion peaks were detected. The capillary and cone voltage were set at 3kV and 30V, respectively. Nitrogen was used as the desolvation, cone and nebulizing gas. The nebulizing gas was fully opened. The flow rates of the desolvation gas and cone gas were set at 400 and 50 L/h, respectively. The m/z axis was calibrated externally with 10 μM horse heart myoglobin (M_α = 16950.5 Da). The raw multiply charged spectra were deconvoluted by a MassLynx 4.1 Transform Program.

Detection of enzyme-substrate complexes

The formation of covalent enzyme-substrate complex during the course of hydrolytic reaction was probed by ESI-MS. A 200 μL portion of the labeled mutant (50 μM and 2 μM in the case of cefoxitin and clavulanate, respectively) was added to 200 μL of substrates (100 mM cefoxitin and 100 μM clavulanate), and the mixture was made up to 2000 μL with 20 mM ammonium acetate solution (pH 7.0). At different time intervals, a 400 μL portion of the reaction mixture was pipetted to 400 μL of 20 mM ammonium acetate with 2% formic acid (v/v) to quench the hydrolytic reaction. The mixture was then concentrated and buffer-exchanged (20 mM ammonium acetate with 2% formic acid (v/v)) 1 - 2 times by means of Amicron® Ultra-15 (NMWL = 10000) centrifugal filter devices (Millipore, Billerica, USA) to a final volume of about 150 μL. ESI-MS measurements were then performed on a Micromass Q-Tof-2™ spectrometer. Concentrated protein samples were mixed with acetonitrile (1:1 v/v) and injected into the electrospray source by a syringe pump (Harvard Apparatus, model 22) at a flow rate of 5 μL/min. The mass spectrometer was scanned over a range of 700–1600 m/z and the multiply-charged protein ion peaks were detected. The capillary and cone voltage were set to 3 kV and 30 V, respectively. Nitrogen was used as the desolvation, cone and nebulizing gas. The nebulizing gas was fully opened. The flow rates of the desolvation gas and cone gas were set at 400 and 50 L/h, respectively.

The m/z axis was calibrated externally with 10 μM horse heart myoglobin (M_α = 16950.5 Da). The raw multiply charged spectra were deconvoluted by a MassLynx 4.1 Transform Program.

2.6 Circular dichroism measurements

Circular dichroism (CD) measurements were performed on a JASCO J-810 spectropolarimeter. The instrument was purged with nitrogen for 30 min before CD measurements. Quartz cuvettes of 0.1-cm and 1-cm path length were used for far UV (190–250 nm) and near UV (250–350 nm) CD measurements, respectively. The wild-type enzyme and the mutants (labeled and unlabeled N170C and V216C) were dissolved in 50 mM potassium phosphate buffer (pH 7.0) to a concentration of 5 and 10 μM for far UV and near UV CD measurements, respectively. The CD spectra were recorded in triplicate with a scan rate of 100 nm/min.

2.7 Fluorescence studies

The fluorescence of the labeled mutant (20 nM) in the absence and presence of drug compounds in potassium phosphate buffer (pH 7.0) was monitored using a Perkin Elmer LS-50B spectrofluorimeter. The samples were placed in a quartz cuvette of 1 cm path length. The scan rate was 100 nm/min, and the excitation and emission slit

widths were 5 nm. For single-wavelength fluorescence measurements, the fluorescence signal of the labeled mutant was recorded at 515 nm with excitation at 494 nm.

2.8 Enzyme kinetic studies

The catalytic activities of the wild-type enzyme and the mutants (labeled and unlabeled N170C and V216C) were studied by the spectrophotometric method.[86] The kinetics assays were performed with enzymes (10 nM for wild-type enzyme, unlabeled and labeled V216C mutants; 100 nM for unlabeled N170C mutant and 200 nM for labeled N170C mutant) and substrates (10–1000 μM penicillin G and ampicillin) in 50 mM potassium phosphate buffer (pH 7.0) at 20 °C. The hydrolytic reaction was initiated by mixing the enzymes with the substrates in a quartz cuvette of 1 cm path length. The UV absorbance of penicillin G and ampicillin were then monitored at 233 and 235 nm (respectively) at each substrate concentration as a function of time (Table 2.1). The initial rate for each substrate concentration was determined in duplicate by analyzing the absorbance over the first 15 s, using the corresponding molar extinction coefficient (Table 2.1). The initial rates were then fitted to the Hanes-Woolf equation to determine the k_{cat} and K_m values using Prism 3.0 Software.

Hane-Woolf equation:

$$\frac{[S]}{v} = [S]\frac{1}{V_{max}} + \frac{K_M}{V_{max}}$$

where v is the initial rate of reaction; V_{max} is the maximum rate of reaction; [S] is the substrate concentration, and K_M is the Michaelis constant.

Table 2.1 The UV absorption wavelengths (for the β-lactam amide bond) and molar extinction coefficients of common β-lactam antibiotics.[87]

β-Lactam antibiotic	λ (nm)	Δε ($l \cdot mm^{-1} \cdot cm^{-1}$)
Cephaloridine	260	10.2
Cefazolin	263	7.71
Cephalothin	262	7.66
Cephalexin	262.5	6.88
Cefotiam	276	8.82
Cefamandole	274	10.3
Cefoperazone	273	9.00
Cefuroxime	262	8.54
Cefotaxime	264	7.25
Ceftizoxime (FK-749)	250	7.03
Cefoxitin	265	7.38
Cefmetazole	275	8.38
Moxalactam (6059S)	275	7.96
Penicillin G	233	1.14
Ampicillin	235	0.90
Carbenicillin	235	0.83

2.9 Transmission electron microscopic studies

Transmission electron microscopy (TEM) was used to examine the formation of drug aggregates by small molecules under aqueous conditions. Solutions of 10 μM of congo red (dissolved in deionized water) and TIPP (dissolved in 0.5% DMSO) were incubated with TEM-1 mutant (10 nM). A drop of the solution mixture (10 μL) was then applied onto a carbon grid (400 mesh), stained with 0.5% phosphotungstic acid (PTA) and then dried overnight. TEM pictures were obtained with a 200 kV DEOL JEM-2010 electron microscope equipped with a Gatan MSC 794 CCD camera.

2.10 Molecular modeling

Molecular modeling of TEM-1 N170C, V216C and fluorescein-labeled V216C mutants was performed using ICM-Pro 3.4-8a (Molsoft). The wild-type TEM-1 structure was obtained from Protein Data Bank (1FQG).[88] Biased Probability Monte Carlo (BPMC) minimization was used for energy minimization.

Chapter 3

Characterization of the Labeled TEM-1 N170C and V216C Mutants

3.1 Introduction

The TEM-1 β-lactamase is regarded as the ancestor of the TEM family from which various clinically significant TEM variants (with different substrate and activity profiles) have been derived through mutation (e.g. extended spectrum β-lactamases (ESBL) and inhibitor-resistant TEM (IRT) β-lactamases).[22, 89] The TEM-1 β-lactamase and its variants share a similar overall structure, and therefore TEM-1 represents a good protein model in the development of protein-based drug screening tools for TEM-type β-lactamases. In this regard, the protein-based drug screening tool should be able to 'mimic' the catalytic activity of the wild-type enzyme, such that it can accurately reflect the potency of drug candidates against the drug target.[90] This is particularly important in the development of new-generation antibiotics because it is important to investigate whether the drugs can resist the hydrolytic action of β-lactamase.

In this project, we are interested to construct a fluorescent drug screening tool from the TEM-1 β-lactamase. To this end, we constructed two fluorescently labeled mutants from TEM-1 and studied their catalytic properties so as to find out a suitable candidate with wild-type activity for *in vitro* drug screening. The two mutants were constructed by replacing the Asn170 and Val216 residues of TEM-1 with a cysteine

(to give the N170C and V216C mutants) and then labeling them with an environment-sensitive fluorophore.[82, 91] These amino acids were chosen because both residues lie close to the enzyme's active site; the N170 residue is located at the flexible Ω-loop at the bottom of the enzyme's active site, whereas the V216 residue resides at the upper cleft of the active site (Figure 3.1). Moreover, both residues are not directly involved in the catalytic process. The resulting N170C and V216C mutants were then labeled with the thiol-reactive fluorophore fluorescein-5-maleimide. The physical properties of the labeled N170C and V216C mutants were then characterized. The molecular masses of the unlabeled and labeled mutants as well as the wild-type TEM-1 enzyme were examined by ESI-MS. The labeling efficiency and structural properties of the mutants were also investigated by ESI-MS and circular dichroism spectropolarimetry, respectively. Moreover, we also studied the catalytic activities of the wild-type enzyme and the labeled and unlabeled mutants by the spectrophotometric method. The details and the results of these studies are described in this chapter.

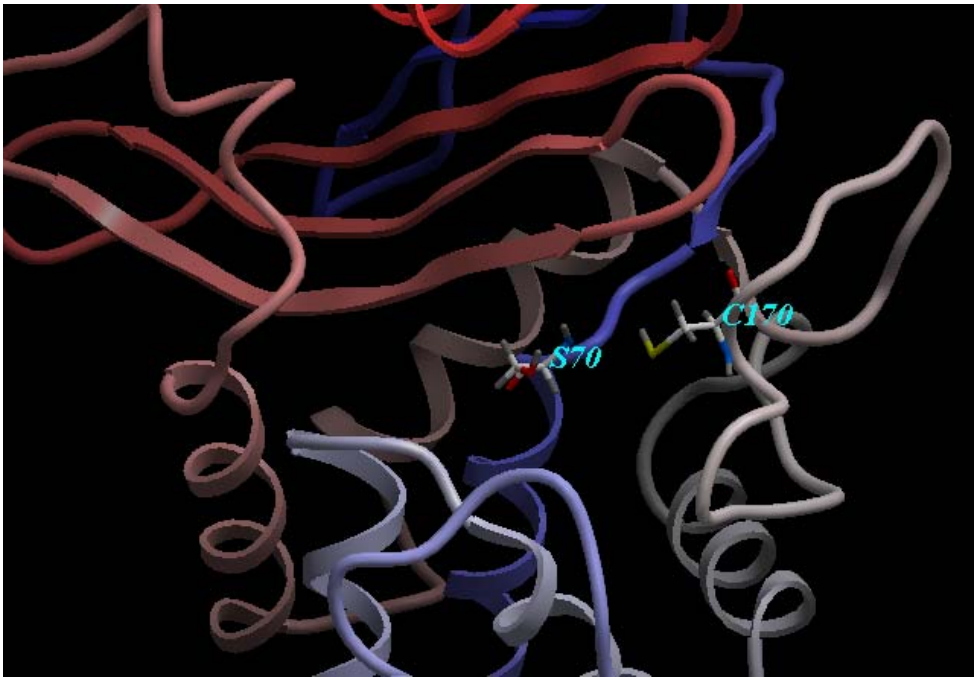

(a)

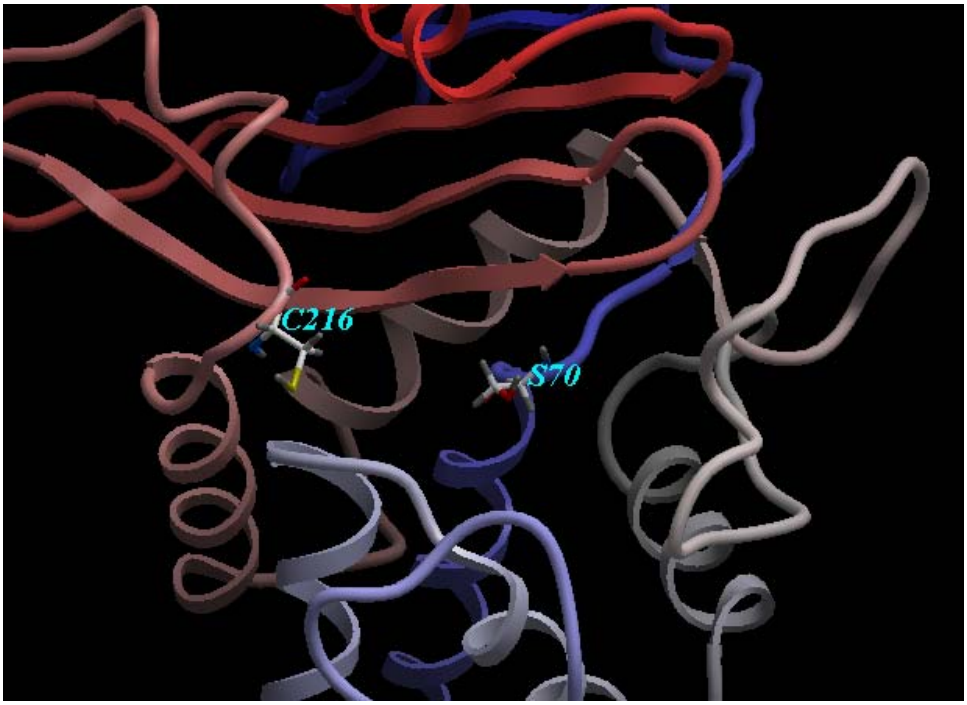

(b)

Figure 3.1 Structures of the TEM-1 N170C (a) and V216C (b) mutants. Cys170 and Cys216 lie close to the active site which contains the catalytic residue Ser70.

3.2 Results

3.2.1 SDS-PAGE and UV-Visble spectrophotometric studies

The labeling reaction of the N170C and V216C mutants with the thiol-reactive fluorophore fluroescein-5-maleimide was monitored by SDS-PAGE. The wild-type enzyme, the N170C and V216C mutants were incubated with fluorescein-5-maleimide and then purified by dialysis to remove excess dye. The protein samples were then loaded onto a SDS-PAGE gel for analysis. Figure 3.2 shows the proteins bands for the wild-type enzyme, the labeled and unlabeled N170C and V216C mutants. For the wild-type enzyme (containing no free cysteine), no observable fluorescent band appears after fluorophore labeling (Lane 2, Figure 3.2). In contrast, the labeled V216C mutant gives a strong fluorescent band upon illumination with a UV lamp (Lane 4, Figure 3.2). Similarly, the labeled N170C mutant also exhibits a fluorescent band after fluorophore labeling (Lane 6, Figure 3.2). These observations indicate that fluorescein-5-maleimide is attached to the free cysteine residues (Cys170 and Cys216) in the mutants. In order to verify that the maleimide of the fluorophore is covalently bound to the free cysteine residues in the proteins, control experiments were performed in which both unlabeled N170C and V216C mutants were incubated with fluorescein (without maleimide) and analyzed by SDS-PAGE. In such cases, the N170C and V216C mutants do not show fluorescence

(Lanes 3 and 5, Figure 3.2). These observations imply that fluorescein is covalently linked to the cysteine residues in the mutant proteins with a thioether as the linker.

The labeled N170C and V216C mutants were further analyzed by UV-Visible spectrophotometry. Figures 3.3 and 3.4 show the UV-Visible spectra of the labeled N170C and V216C mutants, respectively. In both cases, the labeled mutants exhibit a visible absorption peak at 280 nm, which arises from the UV light absorption by aromatic amino acids (e.g. tryptophan and tyrosine). In addition, both labeled mutants also show a strong absorption peak at 494 nm, which corresponds to the visible light absorption by fluorescein. These results are consistent with the observations that the N170C and V216C mutants are linked to fluorescein after fluorophore labeling (Figure 3.2).

1 2 3 4 5 6

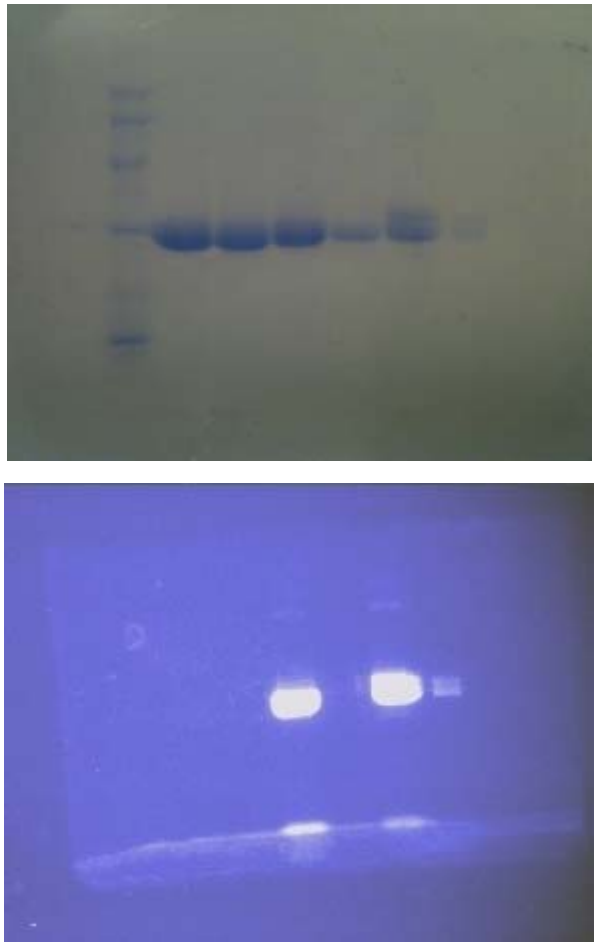

Figure 3.2 SDS-PAGE analysis of the wild type and mutant forms of the TEM-1 β-lactamase. Lane 1 (low range marker): rabbit muscle phosphorylase b (97,400 Da), BSA (66,200 Da), hen egg white ovalbumin (45,000 Da), bovine carbonic anhydrolase (31,000 Da), soybean trypsin inhibitor (21,500 Da), hen egg white lysozyme (14,400 Da); lane 2: wild-type TEM-1; lane 3: unlabeled V216C; lane 4: labeled V216C; lane 5: unlabeled N170C; lane 6: labeled N170C. The fluorescent image (lower picture) was obtained by illuminating the protein gel (upper picture) with a UV lamp.

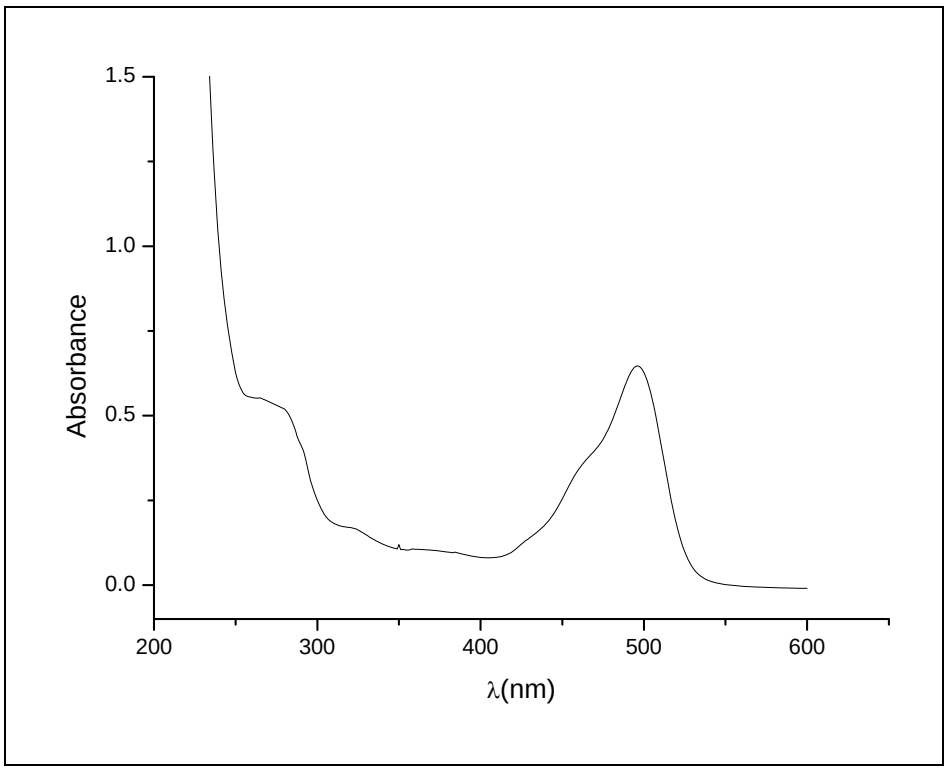

Figure 3.3 UV/Visible absorption spectrum of the labeled N170C mutant (10 μM) in 50 mM potassium phosphate buffer (pH 7.0).

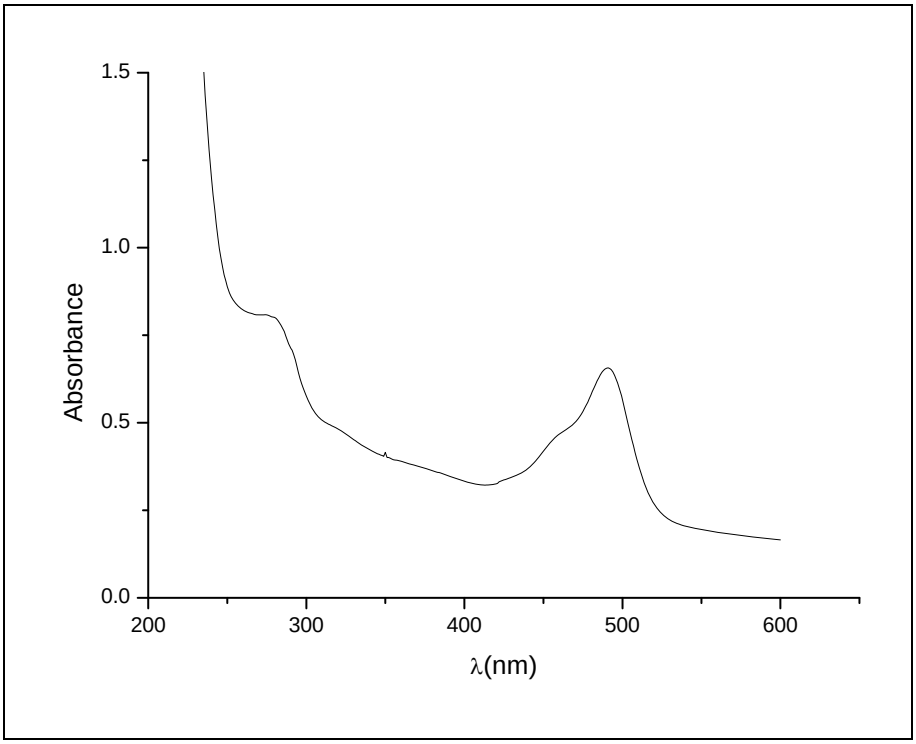

Figure 3.4 UV/Visible absorption spectrum of the labeled V216C mutant (10 μM) in 50 mM potassium phosphate buffer (pH 7.0).

3.2.2 Electrospray ionization mass spectrometric studies

ESI-MS has been widely used to determine the molecular masses of biomolecules such as proteins and peptides. This instrumental technique can distinguish different molecules according to their different mass values.[92] In our studies, we used ESI-MS to determine the molecular mass values of the N170C and V216C mutants in both labeled and unlabeled forms. Such studies allowed us to get an insight into the labeling efficiency of the mutants with the thiol-reactive fluorophore fluorescein-5-maleimide.

The labeled and unlabeled N170C and V216C mutants were dissolved in 20 mM ammonium acetate buffer (pH 7.0) and analyzed by ESI-MS. Figures 3.5–3.8 show the ESI mass spectra for the unlabeled and labeled N170C and V216C mutants. The measured mass values are shown in Table 3.1. The unlabeled N170C mutant shows a mass peak at 29890 Da (Figure 3.5). After labeling with fluorescein-5-maleimide, the N170C mutant shows a new peak at 30336 Da in the mass spectrum (Figure 3.6). The mass difference between the labeled and unlabeled mutants was found to be 445 Da, which is consistent with the molecular mass of fluorescein-5-maleimide plus a water molecule adduct (427 + 18 Da), indicating that the fluorophore is attached to the N170C mutant (Table 3.1). In the mass spectrum of the labeled N170C mutant, no

significant peak at 29890 Da (corresponding to the unlabeled N170C mutant) appears (Figure 3.6). This observation indicates that the N170C mutant is completely labeled with fluorescein-5-maleimide.

Similar ESI-MS experiments were performed with the labeled and unlabeled V216C mutant. The resulting ESI mass spectra for the unlabeled V216C mutant and the labeled one are shown in Figures 3.7 and 3.8, respectively. The mass difference between the labeled and unlabeled mutants gives 427 Da, which corresponds to the molecular mass of fluorescein-5-maleimide (Table 3.1). This observation implies that fluorescein-5-maleimide is covalently linked to the V216C mutant. Similarly, no significant mass peak at 29898 Da (corresponding to the unlabeled V216C mutant) appears in the mass spectrum of the labeled V216C mutant, indicating that the fluorophore labeling for the V216C mutant is virtually complete (Figure 3.8).

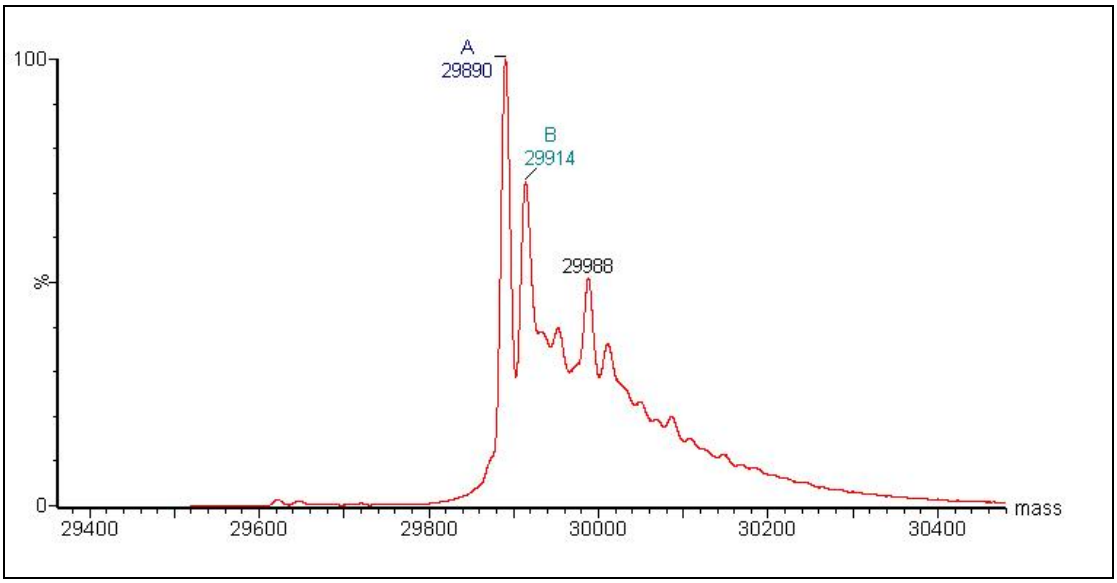

Figure 3.5 ESI-MS spectrum of the unlabeled N170C mutant.

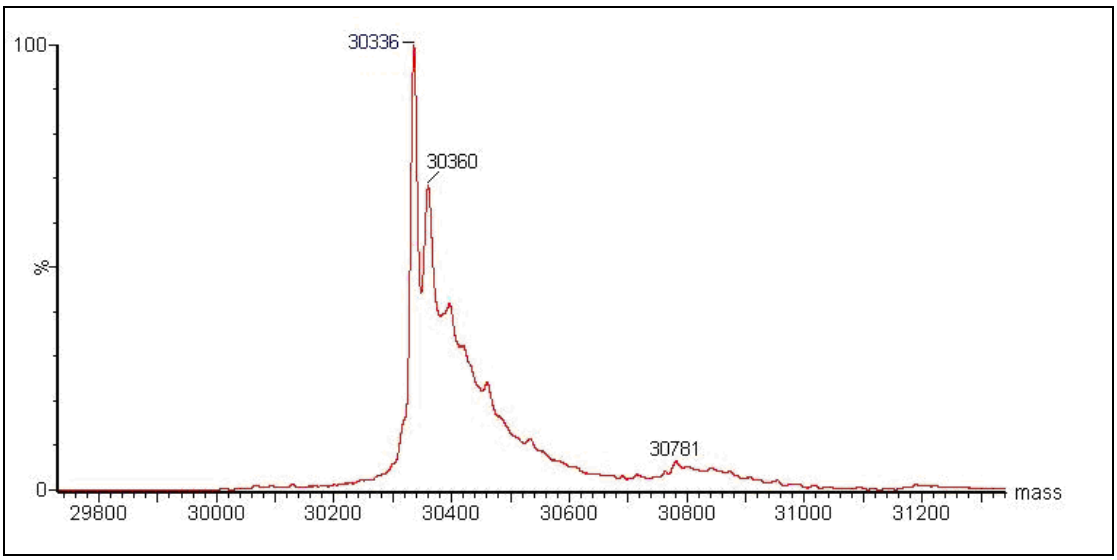

Figure 3.6 ESI-MS spectrum of the labeled N170C mutant.

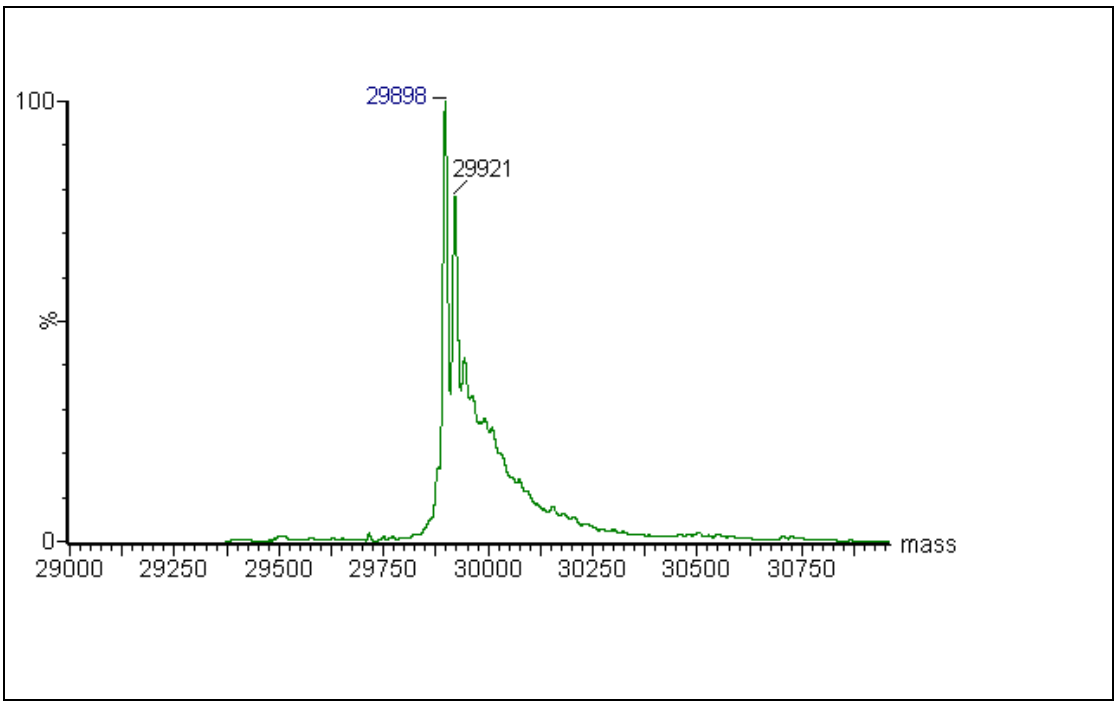

Figure 3.7 ESI-MS spectrum of the unlabeled V216C mutant.

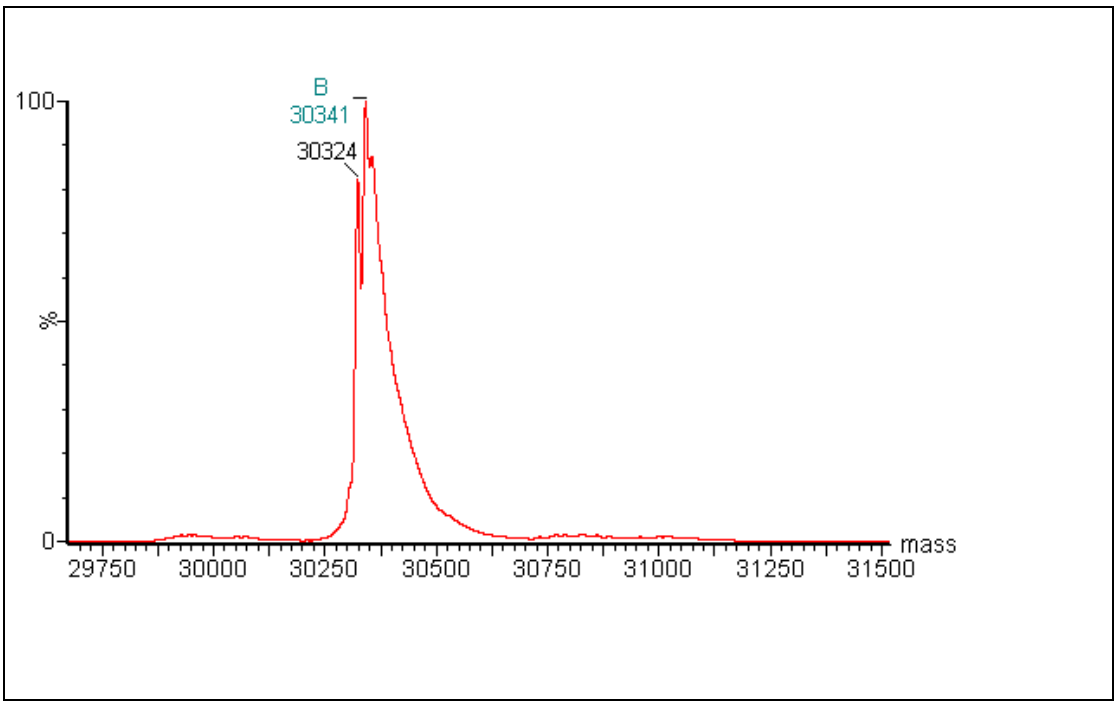

Figure 3.8 ESI-MS spectrum of the labeled V216C mutant.

Table 3.1 Molecular mass values of the unlabeled and labeled V216C and V216Cf mutants determined by ESI-MS

Mutant	Measured Mass (Da)
N170C	29890.47 ± 0.44
Labeled N170C	30336.14 ± 1.01
Mass difference	445.67 ± 1.45

Mutant	Measured Mass (Da)
V216C	29897.53 ± 0.48
Labeled V216C	30324.51 ± 2.65
Mass difference	426.98 ± 3.13

3.2.3 Enzyme kinetic studies

TEM-type β-lactamases catalyze the hydrolysis of β-lactam antibiotics according to the three-step model:[93-95]

Scheme 3.1: Catalytic pathway of TEM-type β-lactamases

$$E + S \underset{k_{-1}}{\overset{k_{+1}}{\Leftrightarrow}} ES \overset{k_2}{\rightarrow} ES^* \overset{k_3}{\rightarrow} E + P$$

where *E* is the free enzyme, *S* is the substrate, *ES* is a non-covalent enzyme-substrate complex, *ES** is a covalent enzyme-substrate complex, and *P* is the product.

The kinetics of TEM-type β-lactamases follows the Michaelis-Menten model.

Equation 3.1

$$v = \frac{V_{\max}[S]}{K_M + [S]}$$

where *v* is the initial rate of reaction; V_{max} is the maximum rate of reaction; *[S]* is the substrate concentration, and K_M is the Michaelis constant.

The equation can be rearranged to give the Hanes-Woolf equation (equation 3.2):

Equation 3.2

$$\frac{[S]}{v} = [S]\frac{1}{V_{\max}} + \frac{K_M}{V_{\max}}$$

By plotting $\frac{[S]}{v}$ against *[S]*, V_{max} and K_M can be determined from the slope and the y-intercept of the plot, respectively. The k_{cat} value can be determined from V_{max} / *[E]*, where *[E]* refers to the concentration of enzyme. Turnover number (k_{cat}) refers to as the number of molecules of substrate converted into the product per active site per unit time (s^{-1}). K_M is the Michaelis constant which measures the affinity of an enzyme for its substrate. K_M refers to as the substrate concentration at half of V_{max}.[96]

Figures 3.9 and 3.10 show the Hanes-Woolf plots for the wild-type TEM-1 enzyme, the unlabeled and labeled mutants (N170C and V216C) with penicillin G and ampicillin as substrates. In all cases, [S]/*v* follows a linear relationship with *[S]*. The catalytic parameters (k_{cat} and K_M) were then determined from the Hanes-Woolf plots. The k_{cat} and K_M values are tabulated in Table 3.2. With penicillin G as the substrate, the k_{cat} value for the labeled V216C mutant is close to that of the wild-type enzyme; the k_{cat} values are within the same order of magnitude (Table 3.2). Similar observation is also obtained with the unlabeled V216C mutant. These results indicate that the catalytic activity of the labeled V216C mutant is largely retained (with respect to the wild-type enzyme) after the V216C mutation and fluorophore labeling. For the labeled N170C mutant, the k_{cat} value is significantly lower than that of the wild-type enzyme (by about 1700-fold) with penicillin G as the substrate (Table 3.2). Similarly,

the unlabeled N170C mutant shows weaker catalytic activity compared to the wild-type enzyme; the k_{cat} value for the unlabeled N170C mutant is lower by about 180-fold with respect to that of the wild-type enzyme (Table 3.2). These observations imply that the N170C mutation and fluorophore labeling significantly weaken the catalytic activity of the enzyme.

Similar enzyme kinetics assays were also performed on the wild-type and the mutant enzymes with ampicillin as the substrate. The k_{cat} value for the unlabeled V216C mutant is similar to that of the wild-type enzyme, indicating that the V216C mutant has similar catalytic activity to the wild-type enzyme after mutation (Table 3.2). Interestingly, the labeled V216C mutant has similar catalytic activity to the wild-type enzyme (similar k_{cat}) even though the mutant is attached to the fluorophore close to its active site (Table 3.2). For the unlabeled N170C mutant, the k_{cat} value is significantly lower than that of the wild-type enzyme (about 25-fold lower), indicating that the N170C mutation weakens the catalytic activity of the enzyme (Table 3.2). The labeled N170C mutant has much lower catalytic activity relative to the wild-type enzyme; the k_{cat} value for the labeled N170C mutant is about 1400-fold lower than that of the wild-type enzyme (Table 3.2). This observation indicates that the attached fluorophore has a strong weakening effect on the catalytic activity of the enzyme.

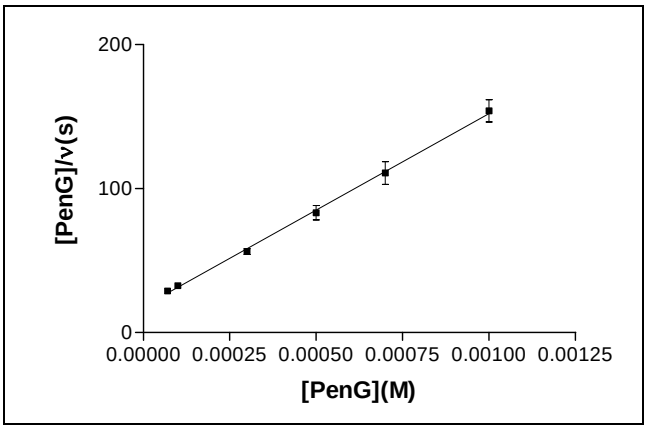
200
100
0
[PenG]/v(s)
0.00000 0.00025 0.00050 0.00075 0.00100 0.00125
[PenG](M)

(a)

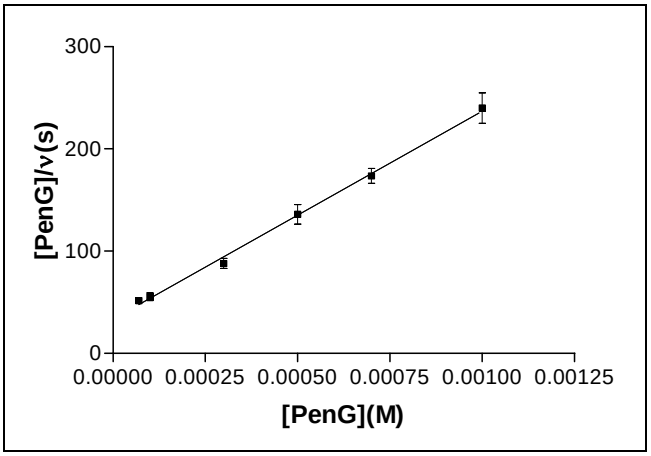
300
200
100
0
[PenG]/v(s)
0.00000 0.00025 0.00050 0.00075 0.00100 0.00125
[PenG](M)

(b)

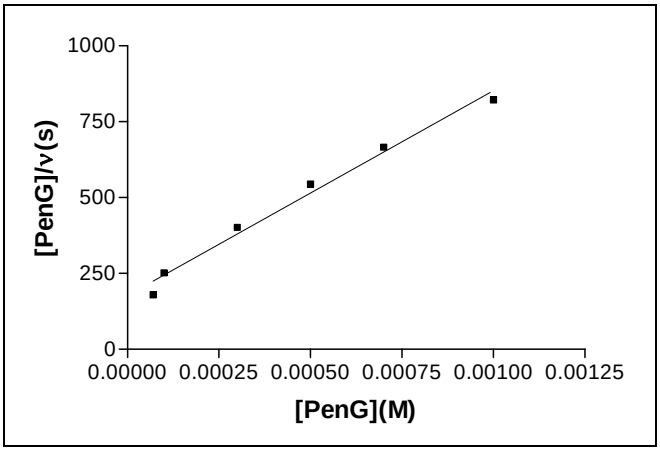
1000
750
500
250
0
[PenG]/v(s)
0.00000 0.00025 0.00050 0.00075 0.00100 0.00125
[PenG](M)

(c)

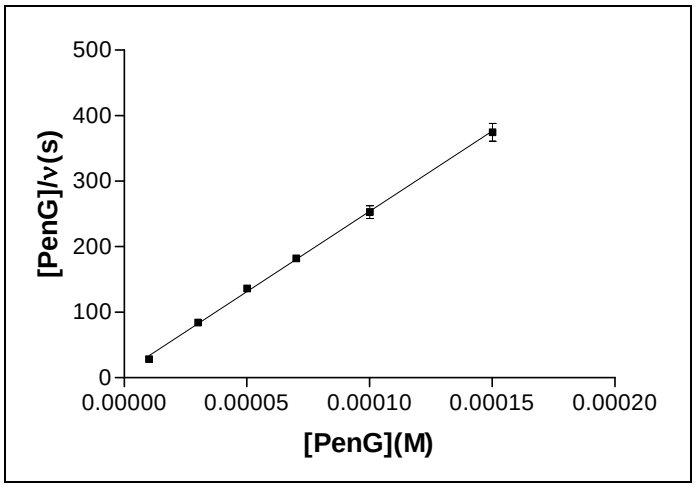

(d)

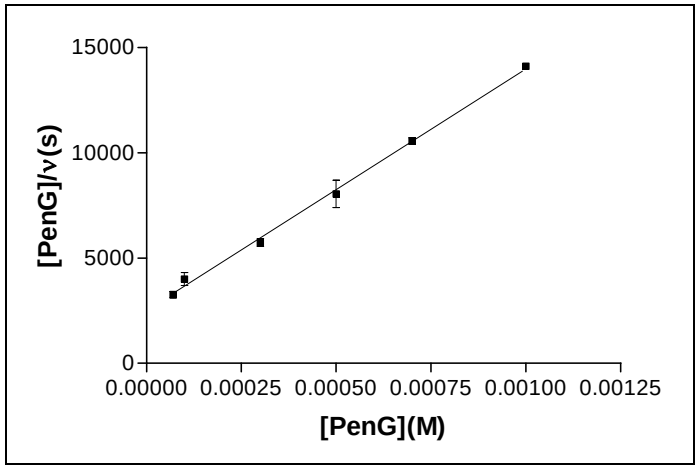

(e)

Figure 3.9 Hanes-Woolf plots of the wild-type and mutant forms of the TEM-1 β-lactamase. (a) Wild-type TEM-1, (b) unlabeled V216C; (c) labeled V216C; (d) unlabeled N170C; (e) labeled N170C with penicillin G as the substrate. The enzyme kinetics assays were preformed in 50 mM potassium phosphate solution (pH 7.0) at 20 ^{o}C.

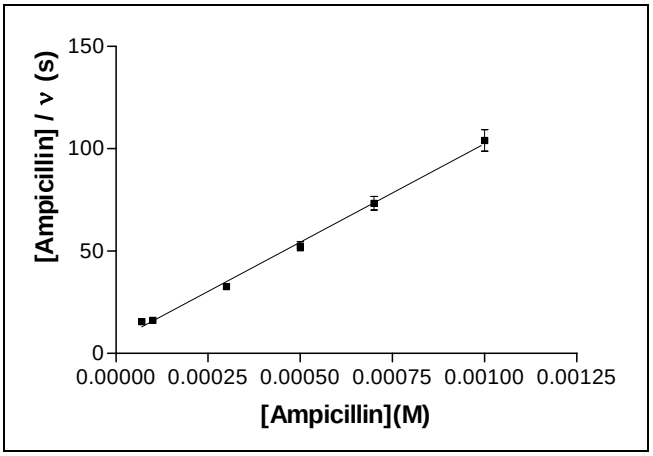
[Ampicillin] / v (s)
150
100
50
0
0.00000 0.00025 0.00050 0.00075 0.00100 0.00125
[Ampicillin](M)

(a)

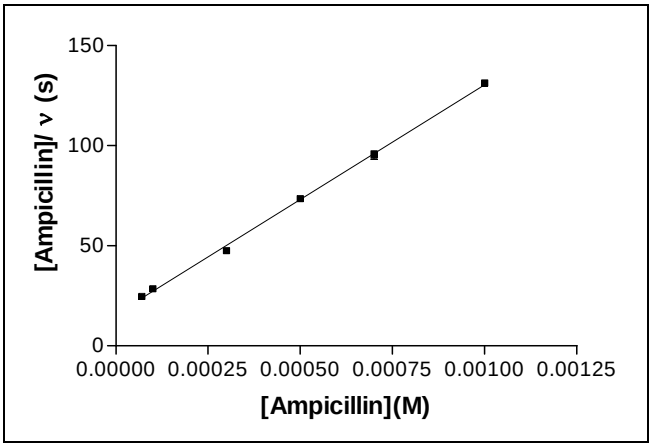
[Ampicillin]/ v (s)
150
100
50
0
0.00000 0.00025 0.00050 0.00075 0.00100 0.00125
[Ampicillin](M)

(b)

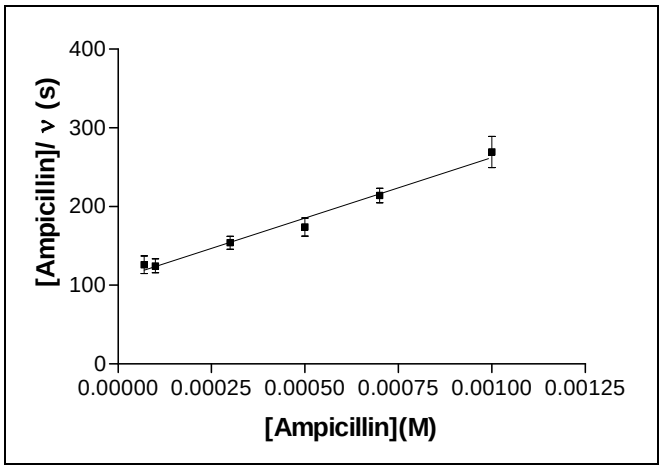
[Ampicillin]/ v (s)
400
300
200
100
0
0.00000 0.00025 0.00050 0.00075 0.00100 0.00125
[Ampicillin](M)

(c)

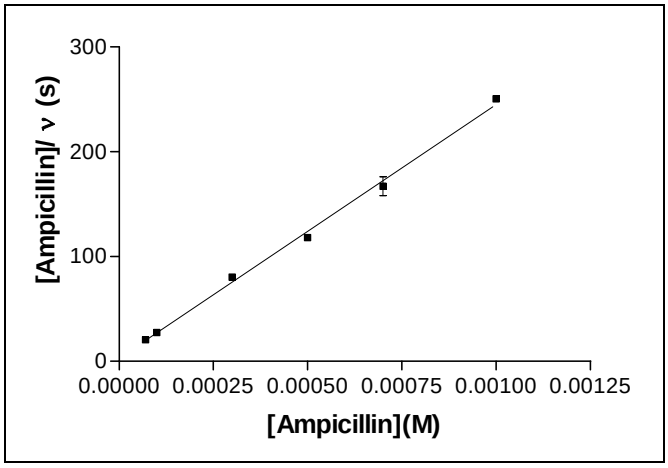

(d)

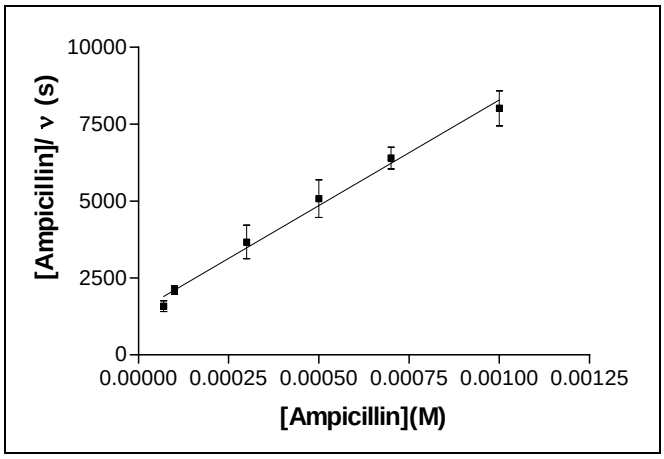

(e)

Figure 3.10 Hanes-Woolf plots of the wild-type and mutant forms of the TEM-1 β-lactamase. (a) Wild-type TEM-1, (b) unlabeled V216C; (c) labeled V216C; (d) unlabeled N170C; (e) labeled N170Cf with ampicillin as the substrate. The enzyme kinetics assays were preformed in 50 mM potassium phosphate buffer (pH 7.0) at 20^{o}C.

Table 3.2 Steady-state kinetic parameters for the wild-type TEM-1 β-lactamase, the labeled and unlabeled N170C and V216C mutants.

Penicillin G

	$k_{cat}(s^{-1})$	$K_M(M)$	k_{cat}/K_M $(s^{-1}M^{-1})$
Wild-type	746 ± 31	$(1.34 \pm 0.23) \times 10^{-4}$	$(5.56 \pm 1.2) \times 10^{6}$
V216C	491 ± 13	$(1.64 \pm 0.15) \times 10^{-4}$	$(2.99 \pm 0.35) \times 10^{6}$
Labeled V216C	148 ± 9	$(2.62 \pm 0.38) \times 10^{-4}$	$(5.64 \pm 1.2) \times 10^{5}$
N170C	4.1 ± 0.1	$(3.79 \pm 2.0) \times 10^{-6}$	$(1.08 \pm 0.6) \times 10^{6}$
Labeled N170C	0.44 ± 0.01	$(2.19 \pm 0.18) \times 10^{-4}$	$(1.99 \pm 0.23) \times 10^{3}$

Ampicillin

	$k_{cat}(s^{-1})$	$K_M(M)$	k_{cat}/K_M $(s^{-1}M^{-1})$
Wild-type	1040 ± 34	$(6.49 \pm 1.9) \times 10^{-5}$	$(1.60 \pm 0.52) \times 10^{7}$
V216C	873 ± 13	$(1.38 \pm 0.0051) \times 10^{-4}$	$(6.32 \pm 0.12) \times 10^{6}$
Labeled V216C	650 ± 58	$(7.05 \pm 0.8) \times 10^{-4}$	$(9.22 \pm 1.9) \times 10^{5}$
N170C	41 ± 1	$(1.19 \pm 0.028) \times 10^{-5}$	$(3.46 \pm 0.16) \times 10^{6}$
Labeled N170C	0.730 ± 0.05	$(2.07 \pm 0.41) \times 10^{-4}$	$(3.53 \pm 0.94) \times 10^{3}$

3.2.4 Circular dichroism studies

Circular dichroism (CD) spectropolarimetry is an instrumental technique widely used to analyze protein structures.[97] The secondary structures of proteins give characteristic signals in the far-UV region (190 – 250 nm); α-helix gives strong double peaks at around 210 and 222 nm, whereas β-sheet shows a broad single peak at 215 nm.[98] The tertiary structure of proteins can be monitored in the near-UV CD region (250 – 350 nm). CD signals in this optical region are contributed by aromatic amino acids (e.g. tryptophan, tyrosine and phenylalanine) and are sensitive to conformational changes of proteins.[99]

Far-UV CD measurements were performed with the wild-type TEM-1 enzyme and the unlabeled and labeled V216C mutants. Figure 3.11(a) shows the resulting far-UV CD spectra. The CD signal for the labeled V216C mutant is very similar to those of the unlabeled V216C mutant and the wild-type enzyme, indicating that the secondary structure of the labeled V216C mutant is virtually similar to those of the unlabeled mutant and the wild-type enzyme. Similar far-UV CD measurements were also carried out with the wild-type enzyme and the labeled and unlabeled N170C mutants. In all cases, the CD spectra show strong peaks at 210 and 220 nm and are very similar to each other (Figure 3.11(b)). These observations imply that the

secondary structures of the wild-type enzyme, the labeled and unlabeled N170C mutants are very similar.

Near-UV CD measurements were also performed with the wild-type TEM-1 enzyme as well as the unlabeled and labeled V216C mutants. The near-UV CD signals for the wild-type enzyme and the unlabeled V216C mutant are very similar; a strong peak at about 275 nm appears in both cases (Figure 3.12(a)). For the labeled V216C mutant, an additional peak appears at around 280 nm, which is likely to be contributed by the attached fluorescein (Figure 3.12(a)). Similar near-UV CD measurements were also conducted with the wild-type TEM-1 enzyme and the unlabeled and labeled N170C mutants. The wild-type enzyme shows a well-defined peak at around 275 nm, whereas the unlabeled N170C mutant gives a rather broad peak from 250 to 300 nm (Figure 3.12(b)). These observations imply that the unlabeled N170C mutant might have a conformational change with respect to the wild-type enzyme as a result of the N170C mutation. For the labeled N170C mutant, this protein also shows a broad peak from 250 to 300 nm, as similar to the case of the unlabeled N170C mutant (Figure 3.12(b)). This observation reveals that the labeled N170C mutant is likely to have a conformation change in its structure compared to the wild-type enzyme.

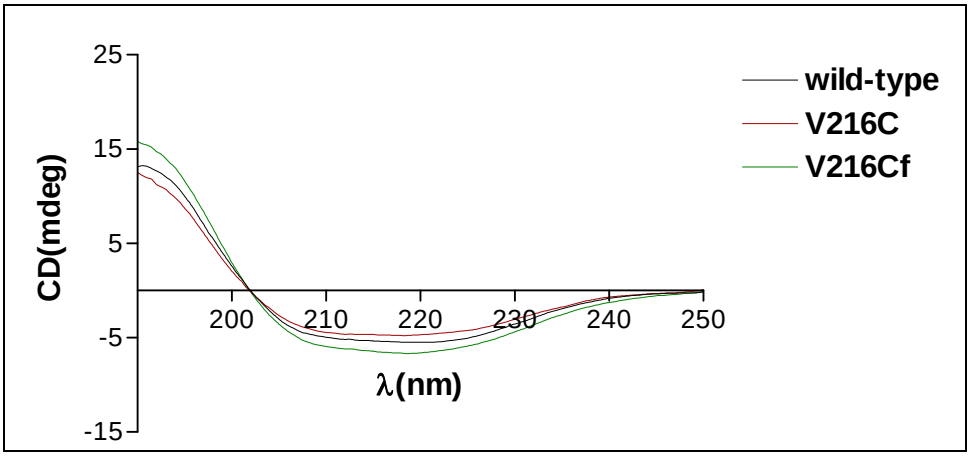

(a)

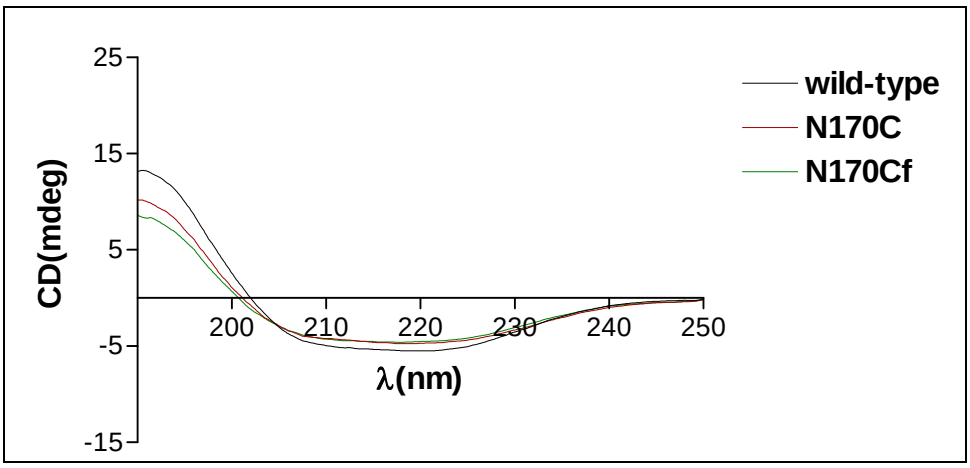

(b)

Figure 3.11 Far-UV CD measurements of the wild-type and mutant forms of the TEM-1 β-lactamase. (a) Far-UV CD signals of wild-type TEM-1 enzyme (black line), unlabeled V216C (red line), and labeled V216C (green line). (b) Far-UV CD signals of the wild-type TEM-1 enzyme (black line), unlabeled N170C (red line), and labeled N170C (green line). The proteins were dissolved in 50 mM potassium phosphate buffer (pH 7.0).

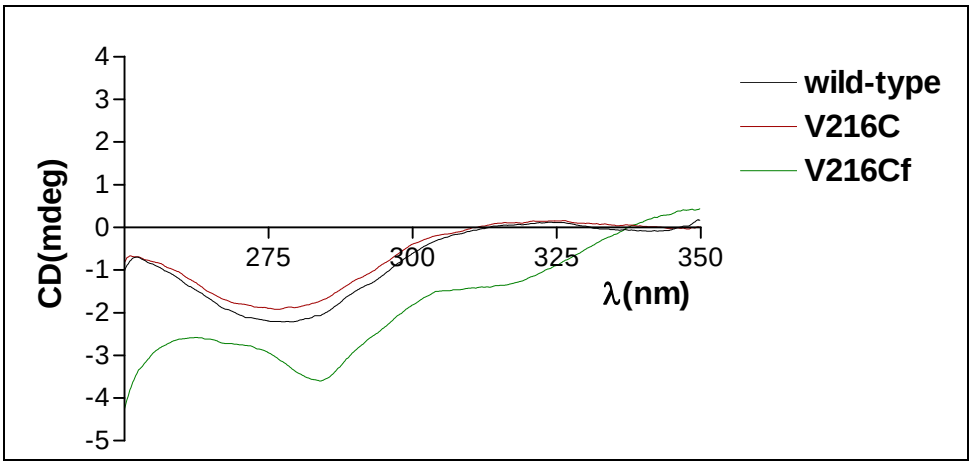

(a)

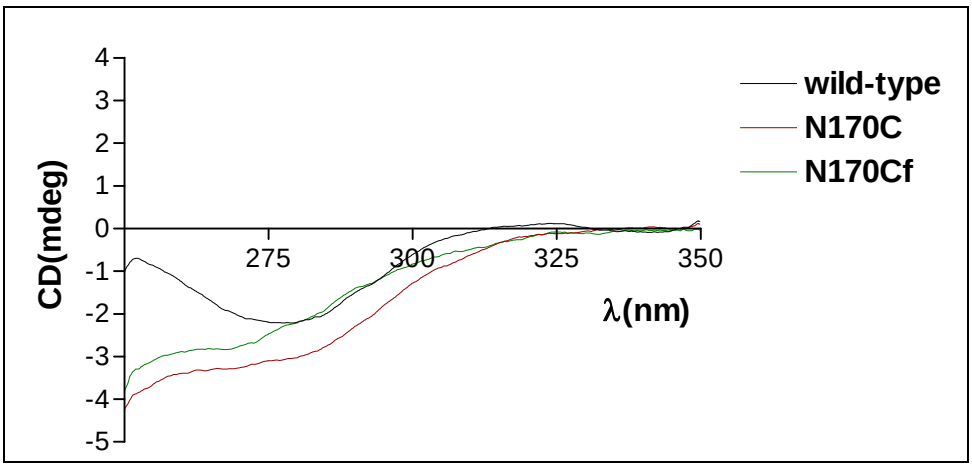

(b)

Figure 3.12 Near-UV CD measurements of the wild-type and mutant forms of the TEM-1 β-lactamase. (a) Near-UV CD signals of the wild-type TEM-1 enzyme (black line), unlabeled V216C (red line), and labeled V216C (green line). (b) Near-UV CD signals of the wild-type TEM-1 enzyme (black line), unlabeled N170C (red line), and labeled N170C (green line). The proteins were dissolved in 50 mM potassium phosphate buffer (pH 7.0).

3.3 Discussions

Proteins are perfectly tailored biomolecules which can recognize their targets (e.g. ligands, substrates and proteins) with high specificity and affinity. These advantageous properties render proteins great potential in the development of biosensors, bioassays and drug screening tools. To this end, an environment-sensitive fluorophore is often attached close to the binding site of a protein for sensing purposes. This approach can be accomplished by incorporating a cysteine into the protein structure (usually close to the binding site) through site-directed mutagenesis and then labeling the cysteine residue with a thiol-reactive fluorophore.[82, 83] The attached fluorophore can then sensitively detect the local environmental change induced by ligand/substrate binding.[84, 85]

In this project, we developed a fluorescent drug screening tool from the TEM-1 β-lactamase with the strategy as described. The Asn170 and Val216 residues, located close to the active site of the TEM-1 enzyme, were each replaced with a cysteine to construct the single mutants N170C and V216C (Figure 3.1). These cysteine-containing mutants were then labeled with fluorescein-5-maleimide. The fluorophore is specifically bound to the Cys170 and Cys216 residues in the mutants. This site-specific labeling is revealed by the fact that after fluorophore labeling, both

N170C and V216C mutants exhibit strong fluorescence, whereas the wild-type enzyme (containing no free cysteine) remains non-fluorescent upon illumination with the UV light on the SDS-PAGE gel (Figure 3.2). The protein-fluorophore conjugation is further evidenced by the fact that after fluorophore labeling, the N170C and V216C mutants also show a strong visible absorption peak at 494 nm (by fluorescein) in addition to the UV absorption peak at 280 nm (by the aromatic amino acids of the proteins) (Figure 3.3 and 3.4). The labeling reaction is so efficient that the N170C and V216C mutants are completely labeled with fluorescein-5-maleimide. This phenomenon is clearly revealed by the observation that the labeling reaction leads to the appearance of new mass peaks for the fluorophore-labeled N170C and V216C mutants accompanied with the disappearance of the mass peaks for the mutants (Figure 3.5–3.8).

In order to act as reliable drug screening tools, the fluorescently labeled mutants should be able to ‘mimic’ the natural catalytic function of the wild-type TEM-1 enzyme as produced by pathogenic bacteria. In this regard, the catalytic activity of the labeled mutants should be similar to that of the wild-type enzyme. This property is particularly important when new-generation antibiotics are developed because the resistance of the antibiotic to β-lactamase activity must be carefully assessed. To

accomplish this task, the fluorescently labeled mutant should be therefore catalytically similar to the wild-type enzyme. The catalytic activity of the labeled N170C mutant is significantly lower than that of the wild-type TEM-1 enzyme; the k_{cat} values for the labeled N170C mutant are lower than those of the wild-type enzyme by more than 1000-fold with penicillin G and ampicillin as substrates (Table 3.2). These results imply that the N170C mutation and fluorophore labeling are likely to cause weakening effects on the catalytic activity of the enzyme. The Asn170 residue is located at the Ω-loop at the bottom of the active site (Figure 3.1) and participates in the hydrogen bonding network with Glu166 and Lys73 in the active site. This hydrogen bonding network appears to be important for keeping the Ω-loop close to the catalytic residue Ser70, such that Glu166 (also located at the Ω-loop) can activate Ser70 through a water bridge to hydrolyze the β-lactam ring in the active site. The replacement of the Asn170 residue with a cysteine is likely to disrupt the hydrogen bonding network and hence the conformation of the Ω-loop. As a result of this conformational change, the Glu166 residue is likely to lose at least in part its activating function, thus causing the catalytic activity (k_{cat}) of the N170C mutant to drop significantly compared to that of the wild-type enzyme (Table 3.2).[31, 32, 100-103] The conjugation of bulky fluorescein-5-maleimide to the Cys170 residue at the Ω-loop in the labeled N170C mutant might further disrupt the conformation of the

loop and hence interfere with the activating function of Glu166. As a consequence, the labeled N170C mutant has even much lower catalytic activity (k_{cat}) compared to the unlabeled N170C mutant (Table 3.2).

In contrast to the case of the labeled N170C mutant, the catalytic activity (k_{cat}) of the labeled V216C mutant is largely retained after the V216C mutation and fluorophore labeling (Table 3.2). The Val216 residue lies at the upper part of the active site (Figure 3.1). This residue is relatively far from the catalytic residues Ser70 and Glu166 and is not directly involved in the catalytic process. The replacement of Val216 with a cysteine in the V216C mutant appears not to significantly interfere with the catalytic action of the enzyme. Thus, the V216C mutant remains catalytically active compared to the wild-type TEM-1 enzyme (similar k_{cat}) (Table 3.2). Interestingly, the conjugation of fluorescein-5-maleimide to the Cys216 residue in the V216C mutant does not cause a strong weakening effect on the catalytic activity of the enzyme; the k_{cat} values of the wild-type enzyme and the labeled V216C mutant are virtually within the same order of magnitude (Table 3.2). This observation is presumably due to the fact that the fluorophore lies relatively far from the catalytic residues Ser70 and Glu166 and does not interfere with the catalytic process significantly.

3.4 Conclusions

We have successfully constructed two single mutants of the TEM-1 β-lactamase in which the Asn170 and Val216 residues are replaced with a cysteine. The N170C and V216C mutants are fluorescently labeled with fluorescein-5-maleimide at the desired sites (Cys170 and Cys216), which are close to the active site. The catalytic activity of the labeled N170C mutant is significantly lower than that of the wild-type TEM-1 enzyme, presumably due to the interfering effects of the N170C mutation and the conjugation of the bulky fluorophore. In contrast, the labeled V216C mutant has similar catalytic activity to the wild-type TEM-1 enzyme despite the V216C mutation and the fluorophore conjugation. This high catalytic similarity enables the labeled V216C mutant to fulfill the role as *in vitro* drug screening tool. In Chapter 4, we will further investigate the ability of the labeled V216C mutant to screen drugs. The fluorescence response of the labeled V216C mutant to drug binding and the mechanism of drug screening will be discussed in Chapter 4.

Chapter 4

Studies of the Labeled TEM-1 V216C Mutant

4.1 Introduction

In Chapter 3, we have shown that the catalytic activity of the labeled V216C mutant remains similar to that of the wild-type TEM-1 enzyme despite the V216C mutation and fluorophore labeling. This catalytically active mutant can potentially act as an *in vitro* drug screening tool. In order to fulfill this function, the labeled V216C mutant should be able to fluorescently respond to drugs that can bind to the enzyme's active site. Fluorescence is used as the sensing approach because the attached fluorophore can detect local environmental changes at the active site caused by drug binding, thus allowing binding and non-binding compounds to be distinguished *in vitro*.[91] Moreover, the attached fluorophore can also reduce the chance of identifying 'drug aggregates' as positive compounds because such bulky materials are unlikely to bind to the enzyme's active site. The 'selective' fluorescence response of the labeled V216C mutant to positive compounds can reduce the possibility of wasting resources and capital in drug discovery due to identification of 'false-positive' compounds.

In this chapter, we study the fluorescence response of the labeled V216C mutant to different antibiotics and inhibitors. The ability of the labeled V216C mutant to differentiate between binding and non-binding compounds is also examined. The origin of the fluorescence response of the labeled V216C mutant to drug binding is

also studied by ESI-MS and molecular modeling. The details of these studies are discussed in this chapter.

4.2 Results

4.2.1 Fluorescence studies

The ability of the labeled V216C mutant to detect drug binding was investigated by fluorescence spectroscopy. To this end, we examined the fluorescence response of the labeled V216C mutant with cefoxitin. Cefoxitin is a cephalosporin antibiotic which is resistant to the hydrolytic activity of class A TEM-type β-lactamases. Figure 4.1 shows the fluorescence signals of the labeled V216C mutant at different time intervals with different concentrations of cefoxitin. In the absence of cefoxitin, the labeled V216C mutant gives a relatively weak fluorescence peak at 515 nm, and no significant fluorescence changes are observed over the time course (Figure 4.1). Upon addition of cefoxitin, the fluorescence signal of the labeled V216C mutant increases as a function of time and then becomes sustained (Figure 4.1). The fluorescence enhancement increases as a function of the concentration of cefoxitin (0.01 – 1 mM) (Figure 4.1).

The fluorescence response of the labeled V216C mutant with less-resistant β-lactam antibiotics was also studied. Figure 4.2 shows the fluorescence signals of the labeled V216C mutant with penicillin G at different time intervals. Without penicillin G, the labeled V216C mutant does not show steady fluorescence signals over the time

course (Figure 4.2). In the presence of penicillin G (1 mM), the fluorescence signal increases instantaneously and then declines (Figure 4.2). With lower concentration of penicillin G (0.1 mM), the fluorescence signal also increases instantaneously (but to a lower extent) and then decreases gradually (Figure 4.2). Similar fluorescence measurements were also performed on the labeled V216C mutant with other less-resistant antibiotics (e.g. ampicillin and cephalothin). As similar to the case of penicillin G, the fluorescence signals of the labeled V216C mutant increase rapidly at the early stage and then decline (Figures 4.3 and 4.4).

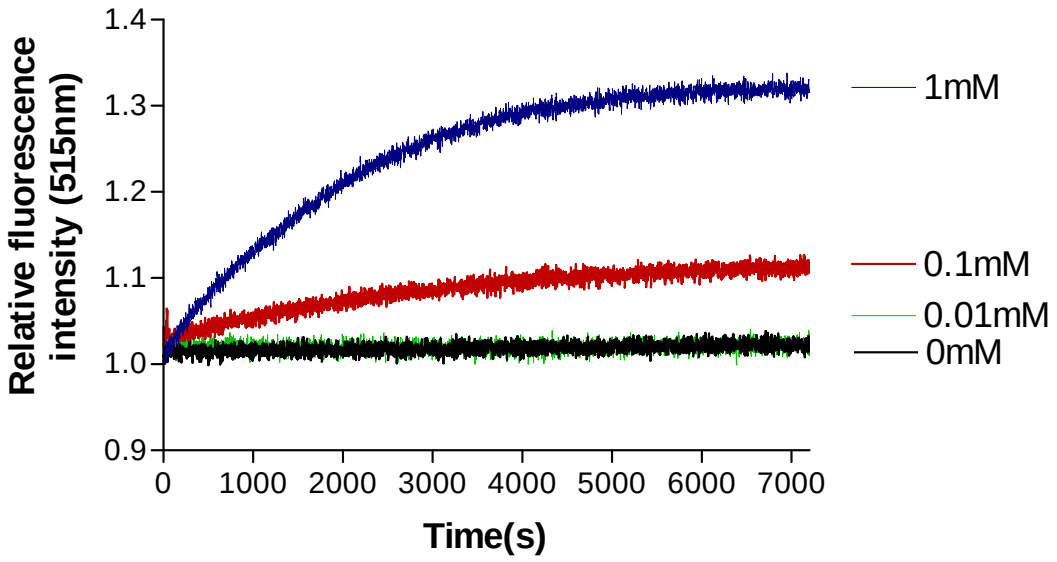

Figure 4.1 Time-course fluorescence measurements of the labeled V216C mutant (20nM) with different concentrations of cefoxitin. Fluorescence profiles obtained without cefoxitin (black line), with 0.01 mM cefoxitin (green line), 0.1 mM cefoxitin (red line), and 1 mM cefoxitin (blue line). The labeled V216C mutant (20 nM) was dissolved in 50 mM potassium phosphate buffer (pH 7.0) at 20^{o}C.

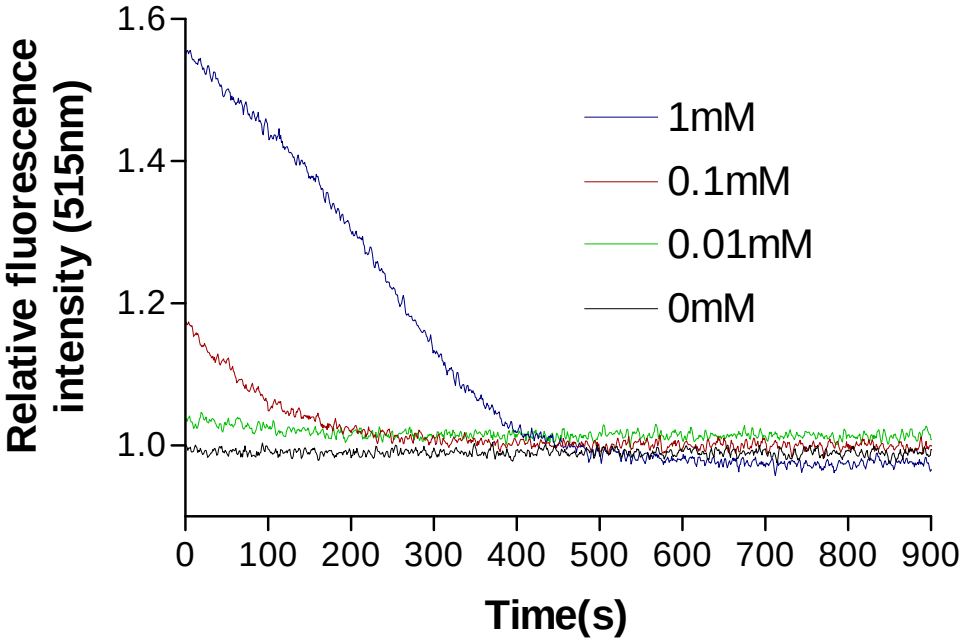

Figure 4.2 Time-course fluorescence measurements of the labeled V216C mutant with different concentrations of penicillin G. Fluorescence profiles obtained without penicillin G (black line), with 0.01 mM penicillin G (green line), 0.1 mM penicillin G (red line), and 1 mM penicillin G (blue line). The labeled V216C mutant (20 nM) was dissolved in 50 mM potassium phosphate buffer (pH 7.0) at 20^{o}C.

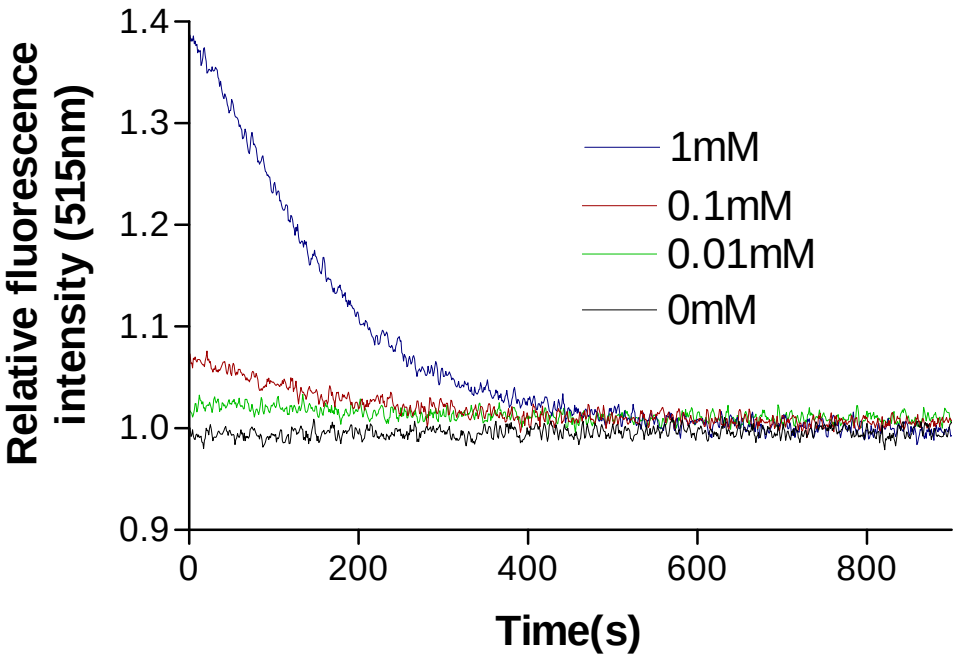

Figure 4.3 Time-course fluorescence measurements of the labeled V216C mutant with different concentrations of ampicillin. Fluorescence profiles obtained without ampicillin (black line), with 0.01 mM ampicillin (green line), 0.1 mM ampicillin (red line), and 1 mM ampicillin (blue line). The labeled V216C mutant (20 nM) was dissolved in 50 mM potassium phosphate buffer (pH 7.0) at 20^{o}C.

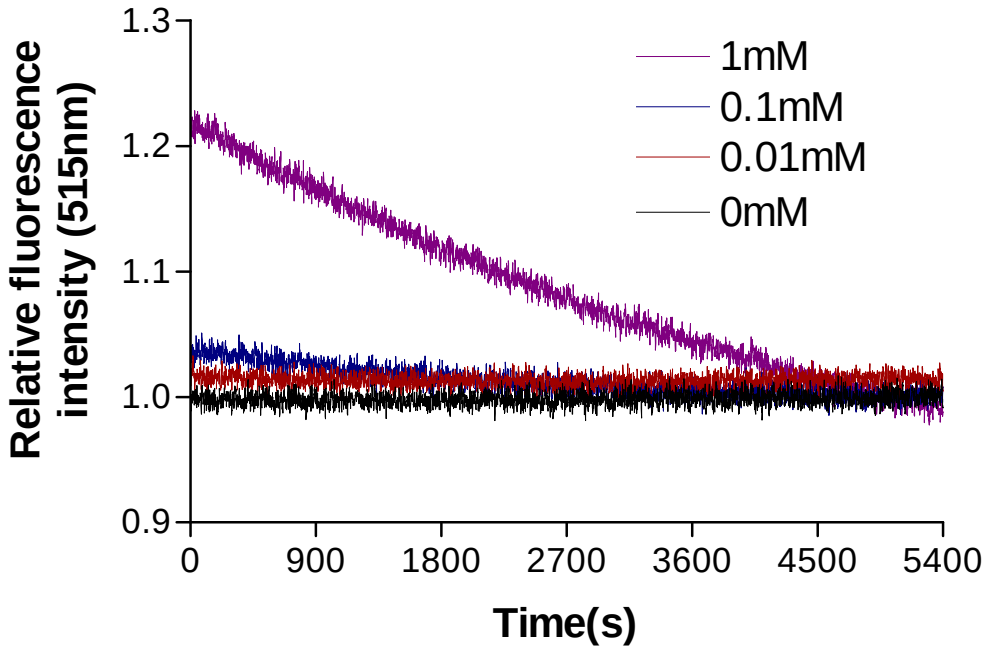

Figure 4.4 Time-course fluorescence measurements of the labeled V216C mutant with different concentrations of cephalothin. Fluorescence profiles obtained without cephalothin (black line), with 0.01 mM cephalothin (red line), 0.1 mM cephalothin (blue line), and 1 mM cephalothin (purple line). The labeled V216C mutant (20 nM) was dissolved in 50 mM potassium phosphate buffer (pH 7.0) at 20^{o}C.

The fluorescence response of the labeled V216C mutant towards clavulanate was also investigated. Clavulanate is a β-lactamase inhibitor for class A β-lactamases (including TEM-type β-lactamases). This inhibitor can irreversibly bind to the enzyme's active site to form a stable covalent complex, thus leading to the suppression of the catalytic function of the enzyme.[8, 15, 17] The fluorescence signals of the labeled V216C mutant in the presence of different concentrations of clavulanate are shown in Figure 4.5. In the absence of clavulanate, the labeled V216C mutant does not show significant fluorescence changes over the time course (Figure 4.5). Upon addition of clavulanate (0.01 mM), the fluorescence signal of the labeled V216C mutant increases gradually as a function of time and then levels off (Figure 4.5). The fluorescence signals of the labeled V216C mutant become stronger in the presence of higher concentrations of clavulanate (0.1 and 1 mM) (Figure 4.5).

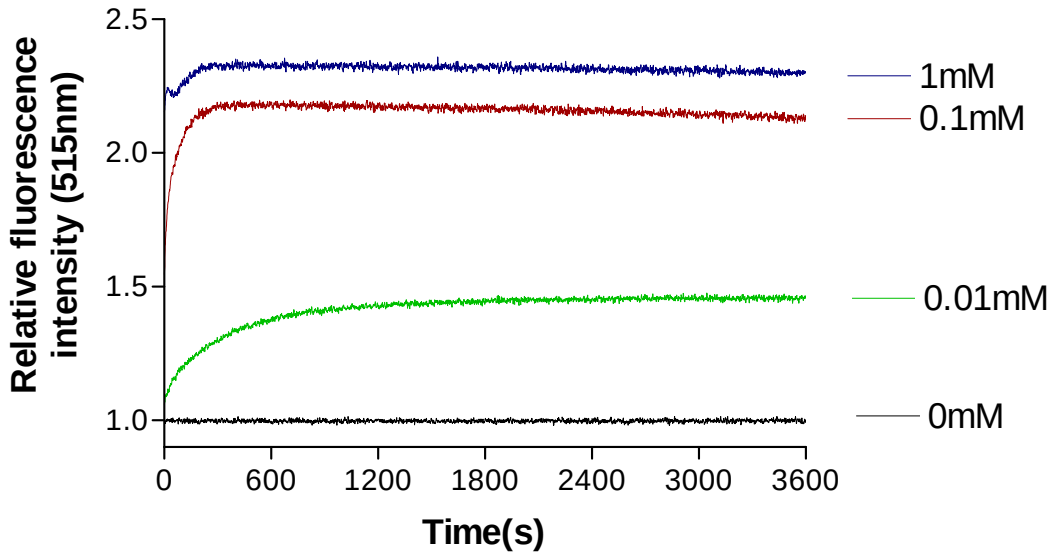

Figure 4.5 Time-course fluorescence measurements of the labeled V216C mutant with different concentrations of clavulanate (β-lactamase inhibitor). Fluorescence profiles obtained without clavulanate (black line), with 0.01 mM clavulanate (green line), 0.1 mM clavulanate (red line), and 1 mM clavulanate (blue line). The labeled V216C mutant (20 nM) was dissolved in 50 mM potassium phosphate buffer (pH 7.0) at 20^{o}C.

The specificity of the labeled V216C mutant was then examined. To this end, the fluorescence response of the labeled V216C mutant with non-binding compounds (e.g. aspirin and $_{n}$-benozyl-$_{L}$-arginine ethyl ester) was monitored. As shown in Figure 4.6, the fluorescence signals of the labeled V216C mutant remain virtually unchanged over the time course. For comparison, the fluorescence response of the labeled V216C mutant with cefoxitin (which is known to bind to TEM-type β-lactamases) was also monitored. With cefoxitin, the fluorescence signal of the labeled mutant increases gradually over the time course under similar experimental conditions (Figure 4.6). These observations indicate the labeled V216C mutant can specifically recognize compounds capable of binding to the active site.

The ability of the labeled V216C mutant to distinguish binding compounds from drug aggregates was also studied. It is known that congo red itself can form aggregates in aqueous solution[69]. Instead of binding to the enzyme's active site, such aggregates inhibit β-lactamase activity *in vitro* through non-specific mechanisms (e.g. protein adsorption/absorption). Thus, in *in vitro* drug screening, drug aggregates must be eliminated in order to reduce the possibility of hitting false-positive drug candidates. The effects of drug aggregates (formed by congo red and tetraiodophenolphthalein TIPP, respectively) on the fluorescence of the labeled

V216C mutant were examined. Transmission electron microscopic measurements indicated that congo red and TIPP each form aggregates in water (Figure 4.7). In the presence of congo red aggregates, the labeled V216C mutant does not show significant fluorescence changes (Figure 4.8a). A similar observation was also obtained with the labeled V216C mutant in the presence of TIPP aggregates (Figure 4.8b). In contrast, with binding compounds (e.g. cefoxitin), the labeled V216C mutant gives a characteristic fluorescence profile (Figure 4.8c). These observations highlight the ability of the labeled V216C mutant to differentiate active-site-binding compounds from aggregates formed by molecules *in vitro*.

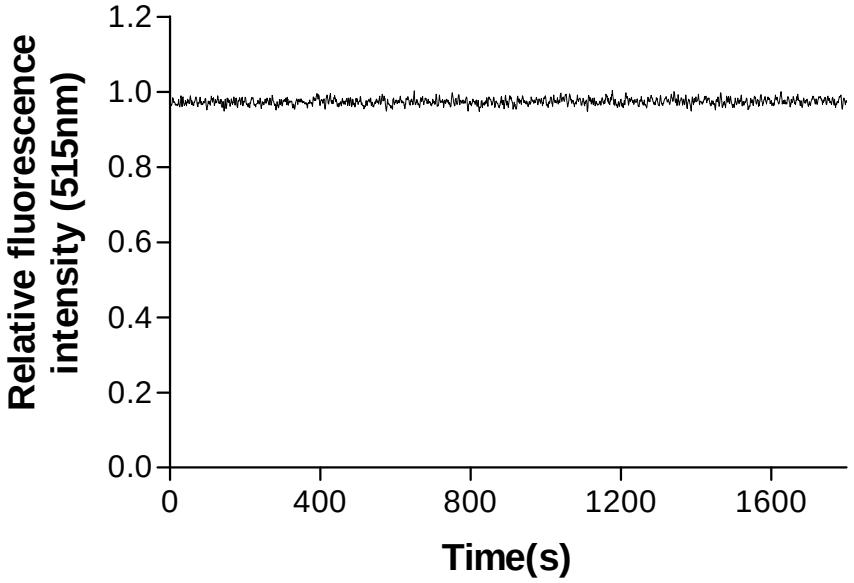
Relative fluorescence intensity (515nm)
1.2
1.0
0.8
0.6
0.4
0.2
0.0
0
400
800
1200
1600
Time(s)

(a)

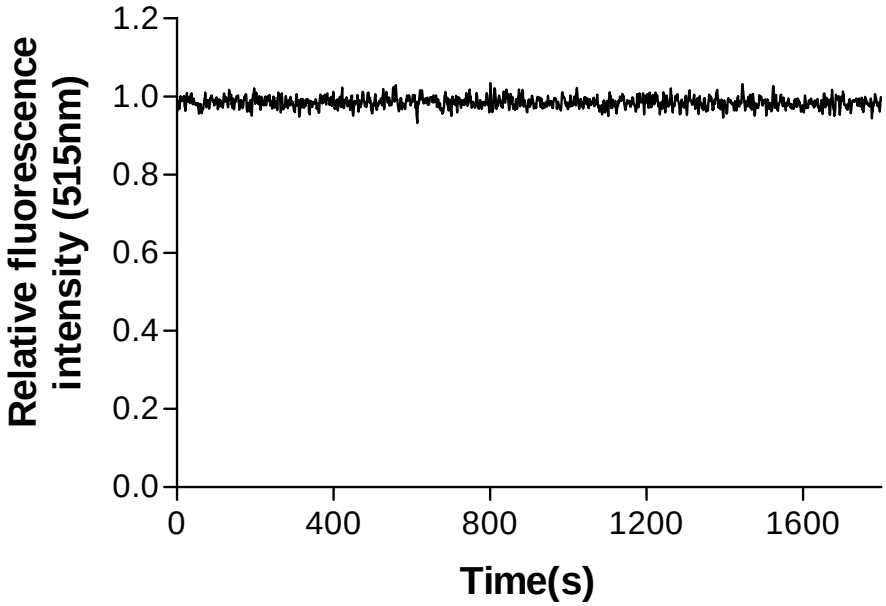
Relative fluorescence intensity (515nm)
1.2
1.0
0.8
0.6
0.4
0.2
0.0
0
400
800
1200
1600
Time(s)

(b)

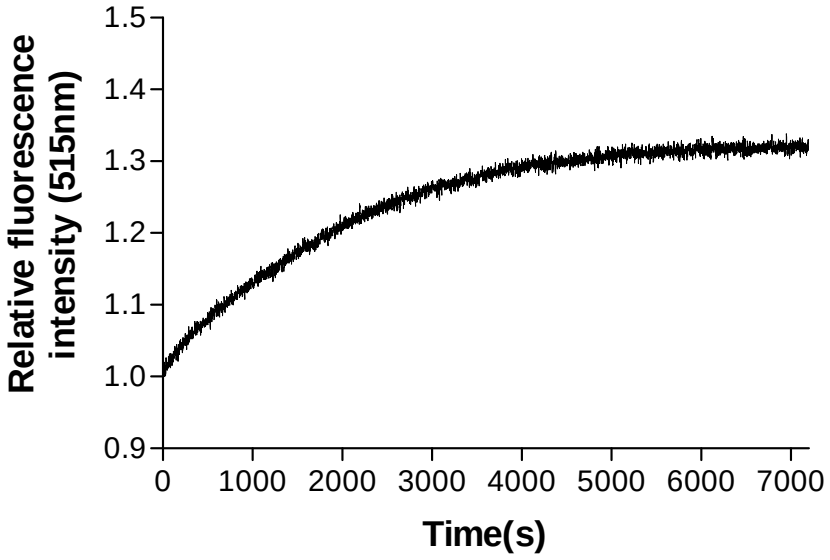

(c)

Figure 4.6 Time-course fluorescence measurements of the labeled V216C mutant. Fluorescence signals from the labeled V216C mutant (20 nM) with 1 mM aspirin (a), 1 mM $_{n}$-benozyl-$_{L}$-arginine ethyl ester (b), and 1 mM cefoxitin (c). Buffer: 50 mM potassium phosphate (pH 7.0) at 20^{o}C.

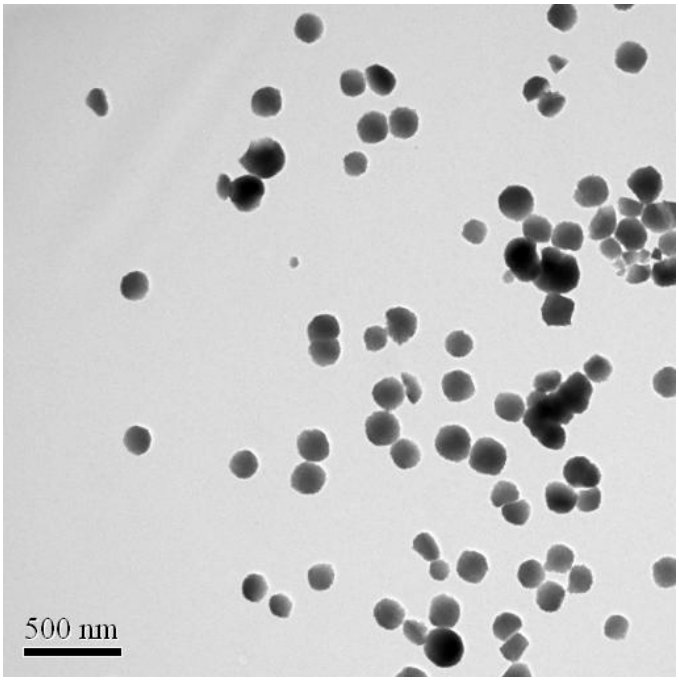

(a)

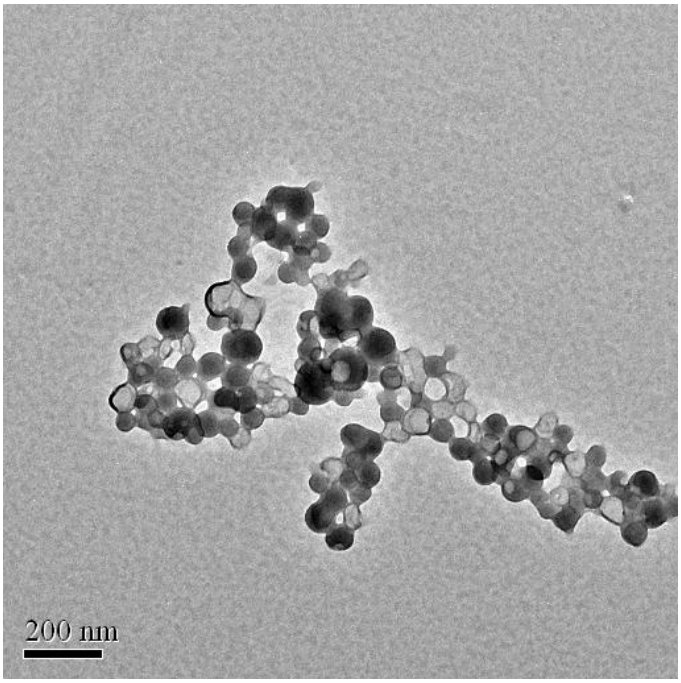

(b)

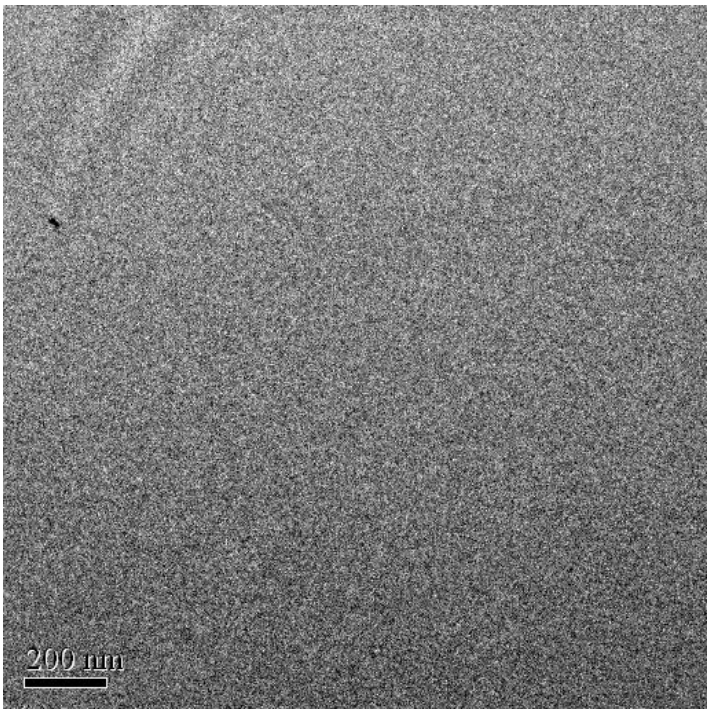

(c)

Figure 4.7 Transmission electron microscopic images of congo red and tetraiodophenolphthalein aggregates. Aggregates formed by congo red and 3',3",5',5"-tetraiodophenolphthalein (TIPP) are shown in (a) and (b), respectively. No aggregates are formed by cefoxitin in aqueous solution (c). The labeled V216C mutant (20 nM) was present in the solutions. Congo red aggregates were prepared by dissolving the molecule (10 μM) in deionized water. TIPP aggregates were prepared by dissolving the molecule (10 μM) in deionized water containing 0.5% DMSO. Cefoxitin sample was prepared by dissolving the molecule (1 mM) in deionized water.

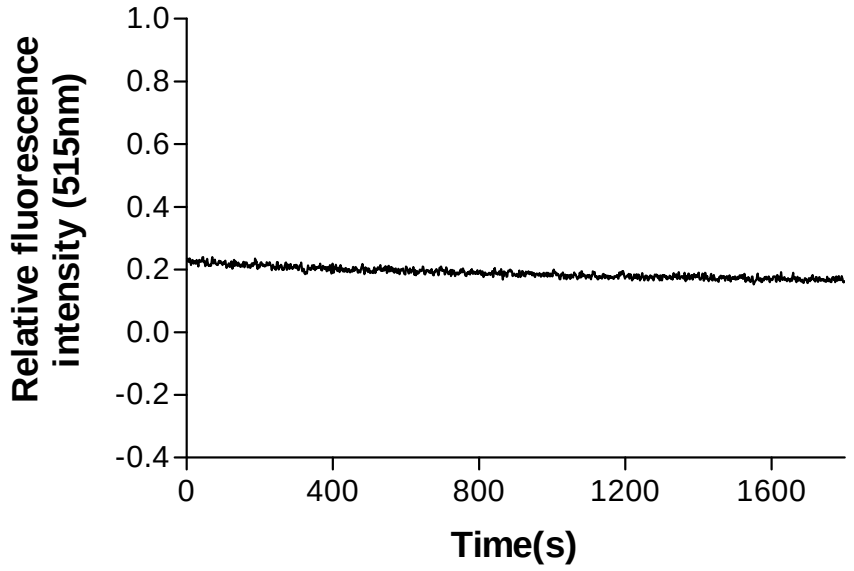
Relative fluorescence intensity (515nm)
1.0
0.8
0.6
0.4
0.2
0.0
-0.2
-0.4
0
400
800
1200
1600
Time(s)

(a)

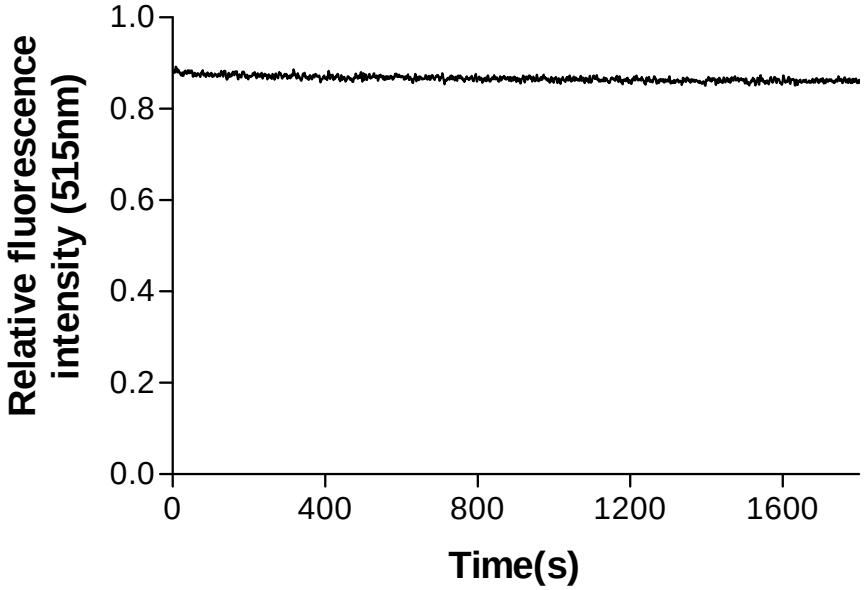
Relative fluorescence intensity (515nm)
1.0
0.8
0.6
0.4
0.2
0.0
0
400
800
1200
1600
Time(s)

(b)

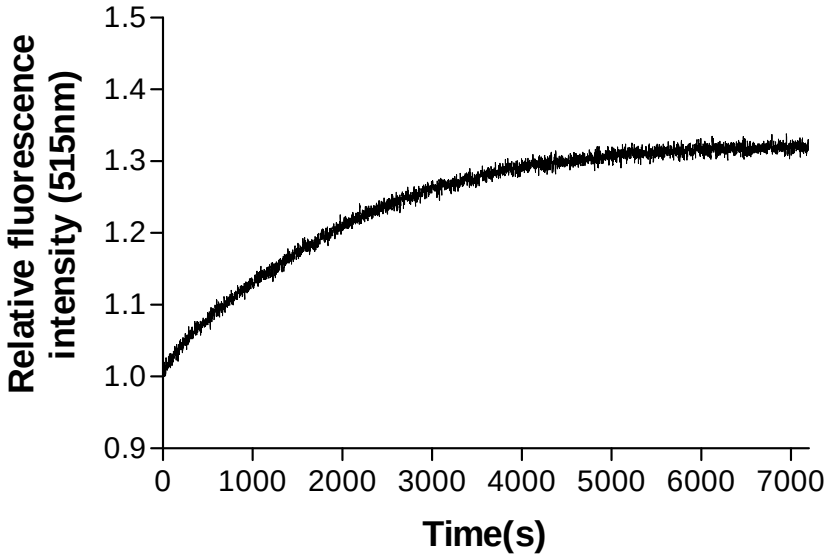

(c)

Figure 4.8 Time-course fluorescence measurements of the labeled V216C mutant. Fluorescence signals from the labeled V216C mutant (20 nM) in the presence of 10 μM congo red (a), 10 μM 3',3",5',5"-tetraiodophenolphthalein (TIPP) (with 0.5 % (v/v) DMSO) (b) and 1 mM cefoxitin (c). Congo red and TIPP form aggregates, whereas cefoxitin does not form aggregates under aqueous conditions (Figure 4.7).

4.2.2 Enzyme-substrate binding studies

To investigate the origin of the fluorescence changes of the labeled V216C mutant, the catalytic reaction of the labeled V216C mutant with cefoxitin was analyzed by ESI-MS. Cefoxitin was chosen because it is resistant to the hydrolytic action of class A β-lactamases (including TEM-type β-lactamases) and can form a stable covalent enzyme-substrate complex in which the hydroxyl group of Ser70 in the enzyme is covalently linked to the β-lactam carbonyl carbon with the aid of the activating residue Glu166.[8, 104] The resulting enzyme-substrate complexes are long-lived and therefore can be easily probed by ESI-MS.

Figure 4.9 shows the ESI mass spectra of the labeled V216C mutant with cefoxitin obtained at different time intervals. The mass peaks (A and B) correspond to the free labeled V216C mutant (*E*) and the covalent enzyme-substrate complex (ES^*), respectively. The relative population of ES^* ($[ES^*] / [E] + [ES^*]$) at each time interval was then determined. The relative ES^* population increases as a function of time, indicating that the covalent enzyme-substrate complex accumulates over the time course (Figure 4.9). The relationship of the population of ES^* with the fluorescence change of the labeled mutant was then studied. To this end, the fluorescence of the labeled V216C mutant with cefoxitin was monitored at different time intervals under

the solution conditions for the ESI-MS measurements ([labeled V216C] = 5 μM; [cefoxitin] = 10 mM; 20 mM ammonium acetate, pH 7.0). The fluorescence signal of the labeled V216C mutant was found to increase as a function of time (Figure 4.9). Interestingly, the increasing fluorescence profile of the labeled V216C mutant is consistent with the increasing MS profile for ES^*, indicating that the fluorescence enhancement is likely to arise from the formation of covalent enzyme-substrate complex (Figure 4.9).

Similar ESI-MS measurements were also performed on the labeled V216C mutant with clavulanate. Figure 4.10 shows the ESI-MS mass spectra of the labeled V216C mutant with clavulanate at different time intervals. The mass peaks A and B correspond to the E and ES^* state of the labeled V216C mutant, respectively. As similar to the case of cefoxitin, the relative ES^* population also increases as a function of time (Figure 4.10). Fluorescence measurements were also performed on the labeled V216C mutant with clavulanate under the solution conditions for the ESI-MS experiments ([labeled V216C] = 0.2 μM; [clavulanate] = 10 μM; 20 mM ammonium acetate, pH 7.0). The fluorescence profile of the labeled V216C mutant is very consistent with the MS profile, indicating that the formation of ES^* enhances the fluorescence of the labeled V216C mutant (Figure 4.10).

We tried to probe the covalent enzyme-substrate complexes of the labeled V216C mutant with penicillin G and ampicillin by ESI-MS. However, the reaction was so fast under the solution conditions for the ESI-MS experiments that the ES^* complexes could not be traced. In order to unravel the origin of the fluorescence enhancement obtained with penicillin G and ampicillin, we performed spectrophotometric measurements on the labeled V216C mutant with these substrates and then compared the UV absorption signals with the fluorescence data. For penicillin G, the UV absorbance at 233 nm decreases as a function of time due to the hydrolysis of the β-lactam amide bond (Figure 4.11). The hydrolytic reaction is virtually complete after 500 s. Interestingly, the fluorescence signal of the labeled V216C mutant is enhanced instantaneously upon addition of penicillin G and then declines gradually over a similar time interval (~500 s). Similar spectrophotometric and fluorescence measurements were also performed on the labeled V216C mutant with ampicillin. The fluorescence and absorbance signals decrease over a similar time interval (~300 s) (Figure 4.12). These observations indicate that the fluorescence of the labeled V216C mutant is enhanced when penicillin G and ampicillin bind to the enzyme's active site. The hydrolysis of the antibiotic and the subsequent release of the acid product then restore the weak fluorescence of the labeled V216C mutant.

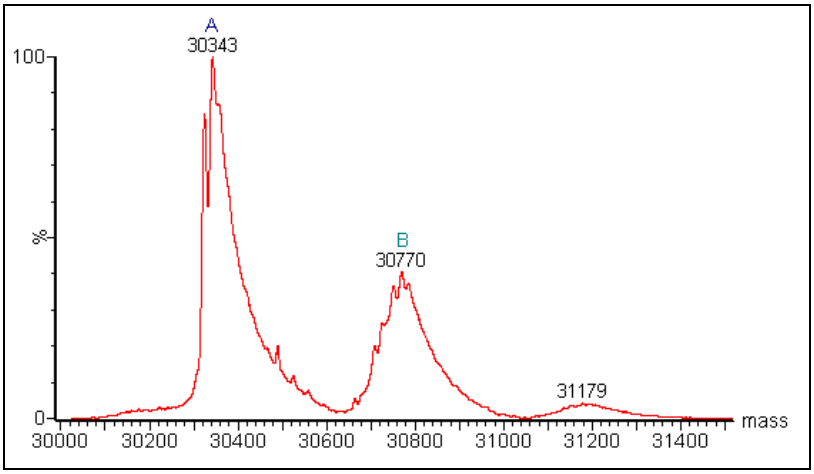
A
30343
B
30770
31179
100
%
0
30000
30200
30400
30600
30800
31000
31200
31400
mass

(a)

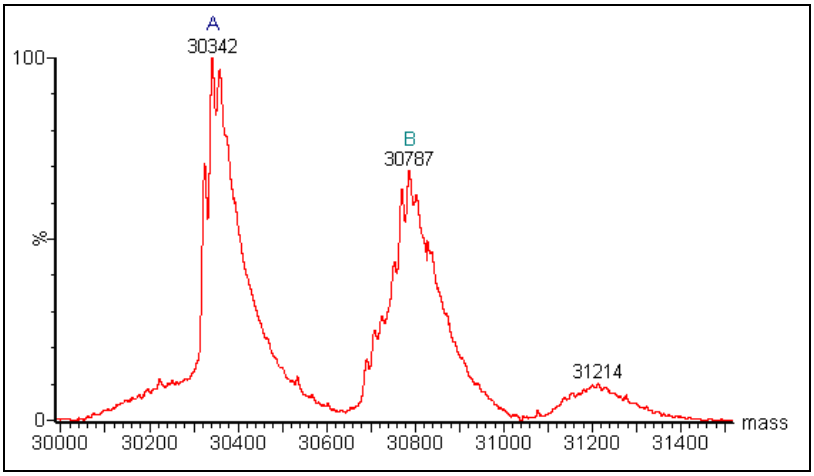
A
30342
B
30787
31214
100
%
0
30000
30200
30400
30600
30800
31000
31200
31400
mass

(b)

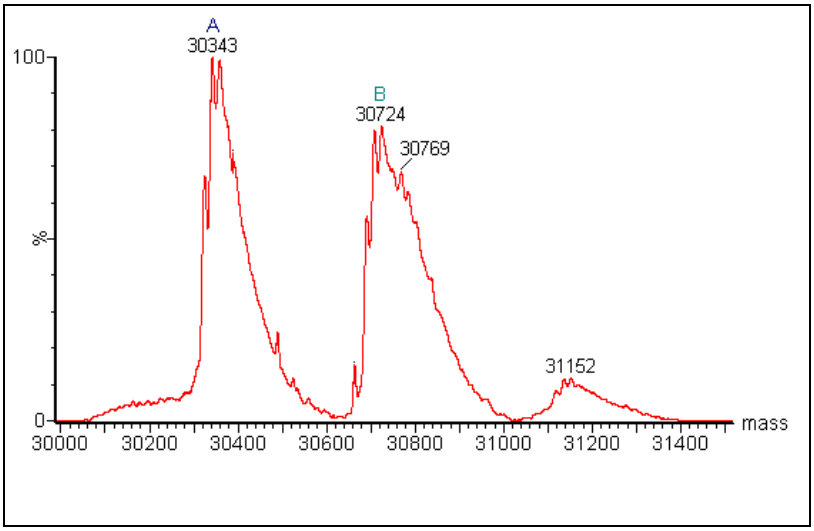
A
30343
B
30724
30769
31152
100
%
0
30000
30200
30400
30600
30800
31000
31200
31400
mass

(c)

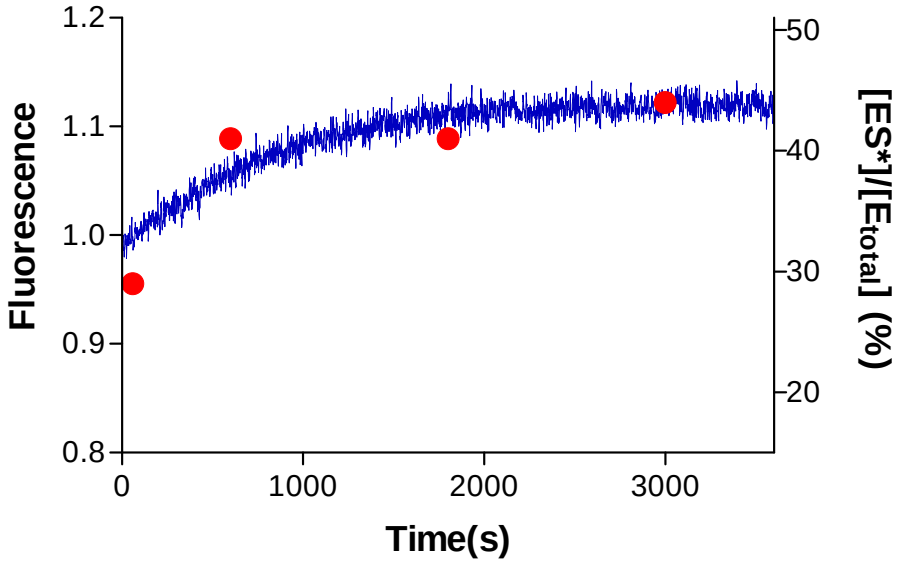

(d)

Figure 4.9 ESI-MS spectra of the labeled V216C mutant (5 μM) with cefoxitin (10 mM) at t = 1 min (a), t = 10 min (b), and t = 50 min (c). Time-course ESI-MS and fluorescence measurements for the binding of the labeled V216C mutant (5 μM) with cefoxitin (10 mM) are shown in (d). The blue line represents the fluorescence signal, and the red circles represent the [*ES**] / [E_{total}] value of the labeled V216C–cefoxitin complex measured by ESI-MS. The reaction of the labeled V216C mutant with cefoxitin took place in 20 mM ammonium acetate solution (pH 7.0) at 20°C.

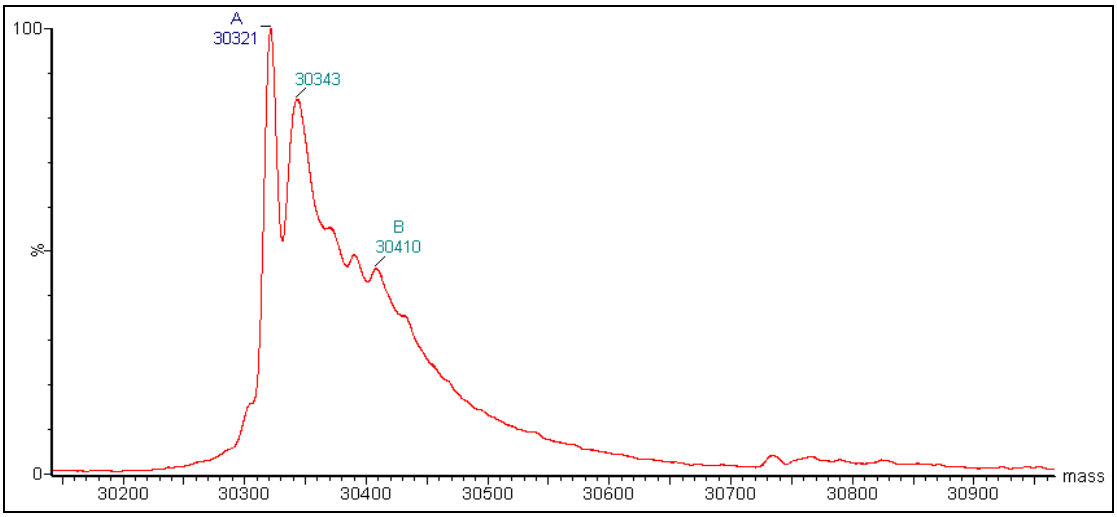
A
30321
30343
B
30410
100
%
0
30200
30300
30400
30500
30600
30700
30800
30900
mass

(a)

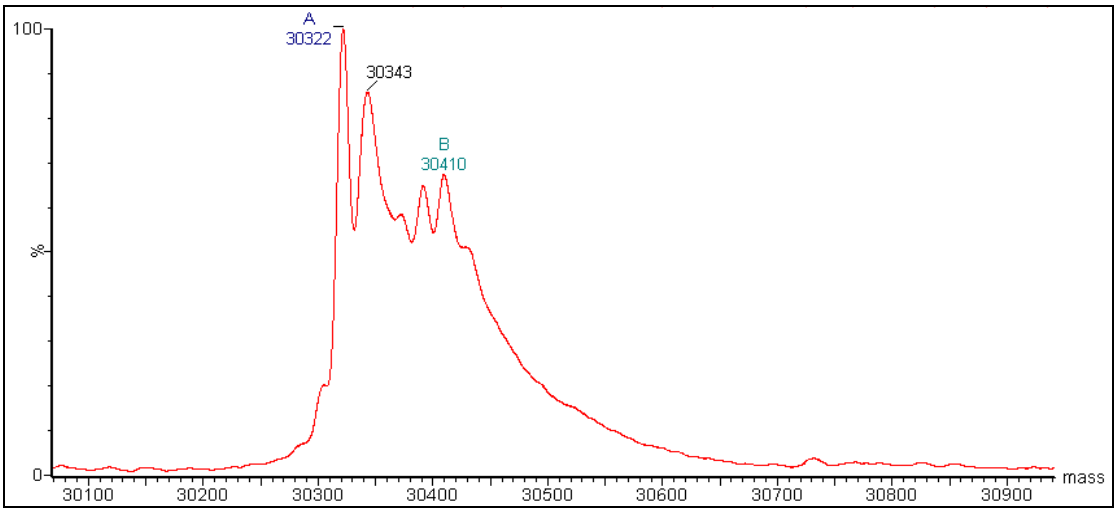
A
30322
30343
B
30410
100
%
0
30100
30200
30300
30400
30500
30600
30700
30800
30900
mass

(b)

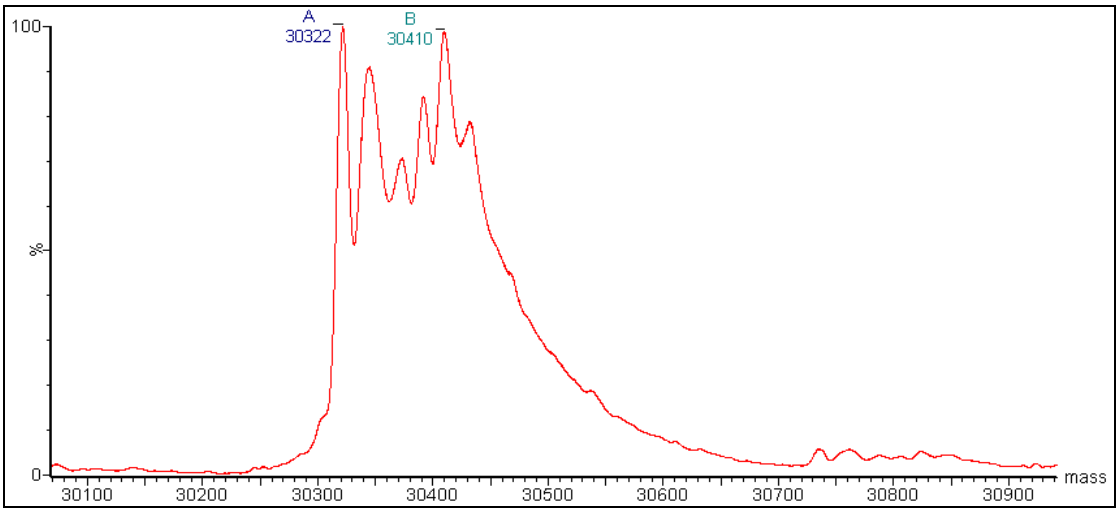
A
30322
B
30410
100
%
0
30100
30200
30300
30400
30500
30600
30700
30800
30900
mass

(c)

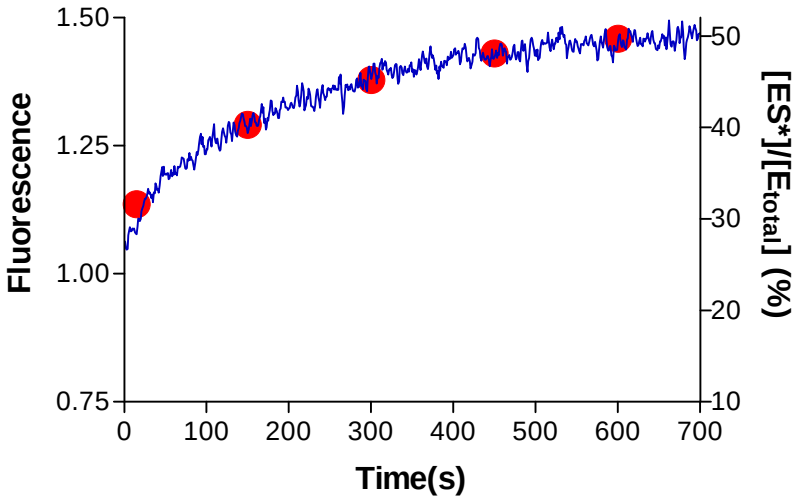

(d)

Figure 4.10 ESI-MS spectra of the labeled V216C mutant (0.2 μM) with clavulanate (10 μM) at t = 0.25 min (a), t = 2.5 min (b), and t = 10 min (c). Time-course ESI-MS and fluorescence measurements for the binding of the labeled V216C mutant (0.2 μM) with clavulanate (10 μM) are shown in (d). The blue line represents the fluorescence signal, and the red circles represent the [*ES**] / [E_{total}] value of the labeled V216C–clavulanate complex measured by ESI-MS. The reaction of the labeled V216Cf mutant with clavulanate took place in 20 mM ammonium acetate solution (pH 7.0) at 20°C.

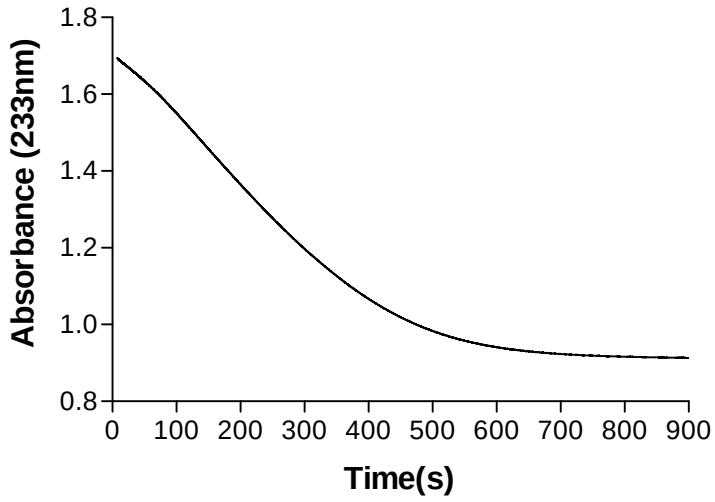

(a)

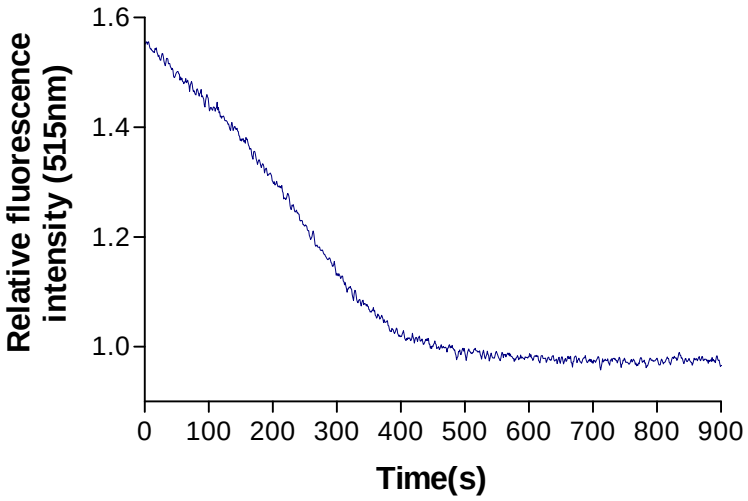

(b)

Figure 4.11 Time-course fluorescence and UV absorption measurements of the labeled V216C mutant with penicillin G. Signals obtained from UV absorption measurements (a) and fluorescence measurements (b). The concentration of the labeled V216C mutant was 20 nM. [Penicillin G] = 1 mM; buffer: 50 mM potassium phosphate buffer (pH 7.0) at 20^{o}C.

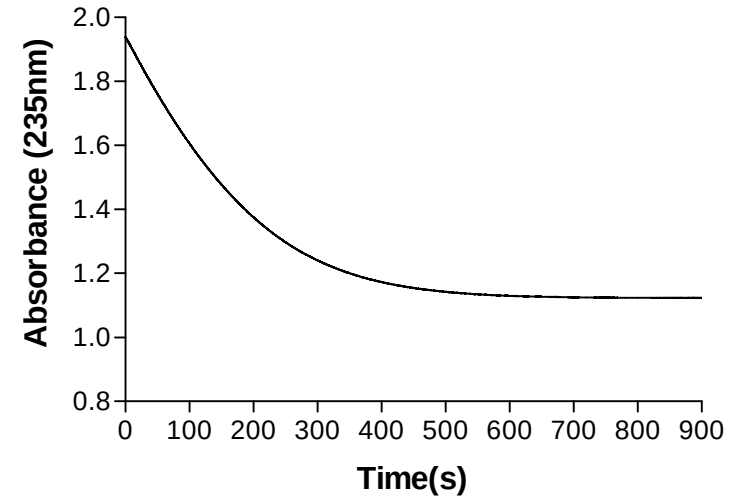

(a)

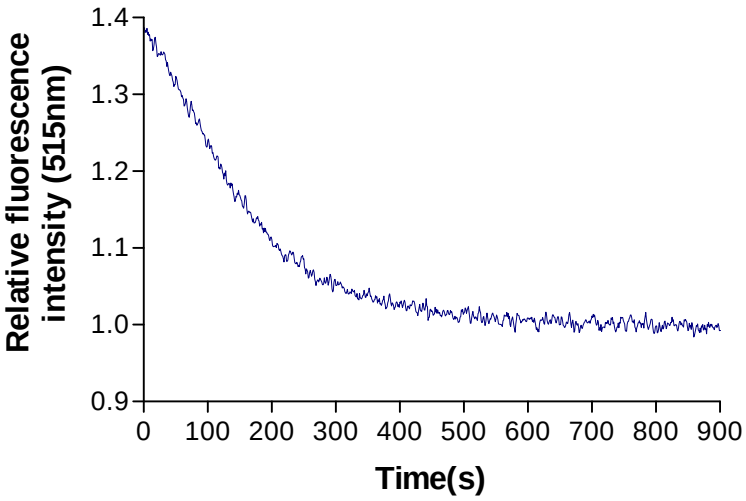

(b)

Figure 4.12 Time-course fluorescence and UV absorption measurements of the labeled V216C mutant with ampicillin. Signals obtained from UV absorption measurements (a) and fluorescence measurements (b). The concentration of the labeled V216C mutant was 20 nM. [Ampicillin] = 1 mM; buffer: 50 mM potassium phosphate buffer (pH 7.0) at 20^{o}C.

4.2.3 Molecular modeling

In order to investigate the effect of drug binding on the conformation of the attached fluorophore, molecular modeling studies were performed on the labeled V216C mutant before and after binding of a substrate. Figure 4.13 shows the structures of the substrate-free and substrate-bound states of the labeled V216C mutant. Without a substrate, the fluorescein label is buried inside the enzyme's active site (Figure 4.13a). After binding to penicillin G, the fluorescein label moves away from the active site (Figure 4.13b). This subtle movement is likely to be caused by the spatial clash between the bound substrate and the attached fluorescein label.

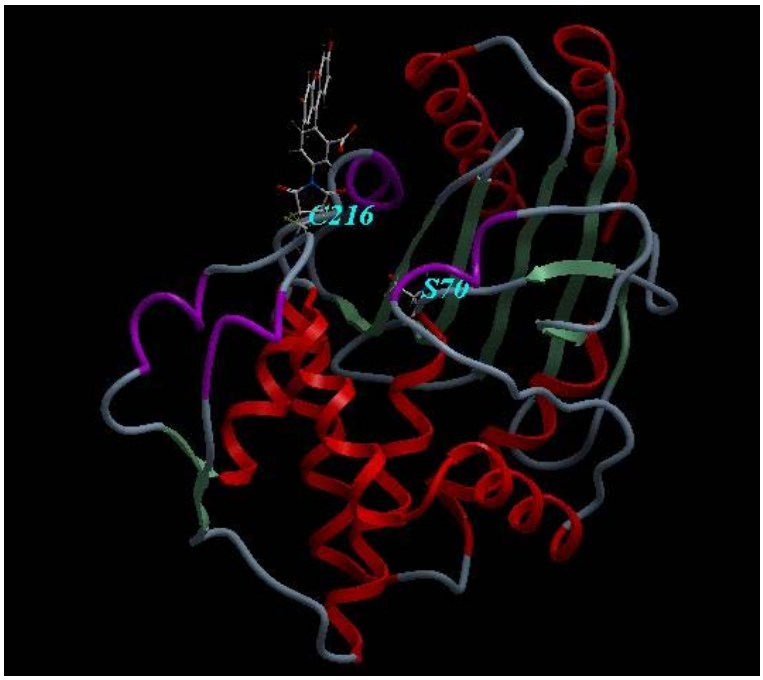

(a)

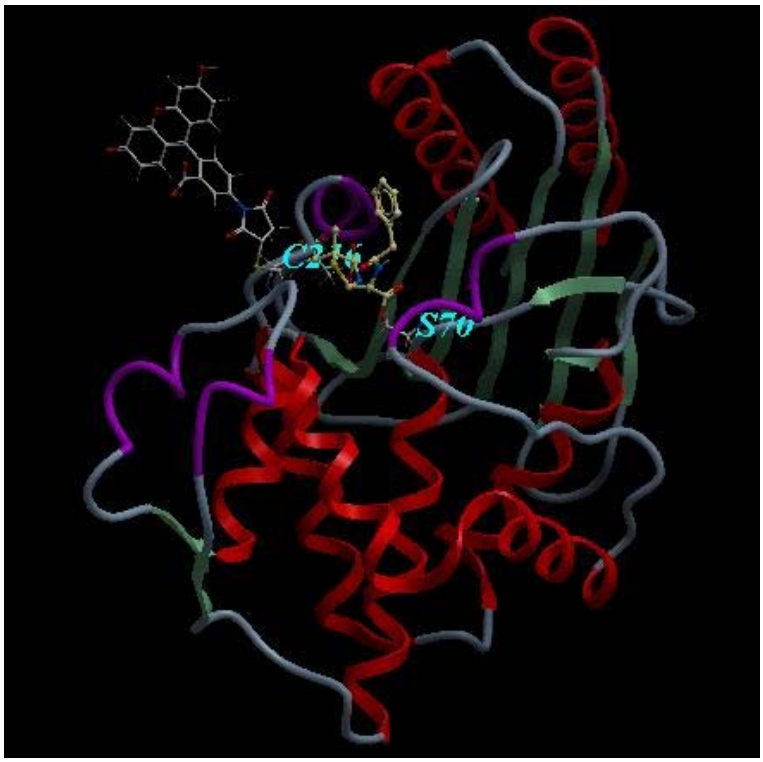

(b)

Figure 4.13 Molecular models of the free labeled V216C mutant (a) and the labeled V216C mutant bound to penicillin G (b). The fluorescein label (grey) is attached to

the Cys216 of the protein and is buried in the active site in the free enzyme state (a) After binding to penicillin G (yellow), the fluorescein label is expelled from the active site (b).

4.3 Discussion

In the discovery of new drugs, it is important to ensure that drug candidates bind to their target with high specificity. In the case of enzymes such as β-lactamase, drug candidates should be able to bind to the active site and hence inhibit the catalytic activity of the enzyme. This protein-drug binding interaction can be probed by fluorescence spectroscopy because this sensitive technique can detect the local environmental change in the enzyme's active site. With this specific detection, compounds capable of binding to the active site can be easily identified from non-binding compounds *in vitro*.

The fluorescence of the labeled V216C mutant is relatively weak in the substrate-free state, but is triggered when a molecule binds to the active site (Figures 4.1 and 4.5). For cefoxitin and clavulanate, these β-lactams are resistant to the hydrolytic activity of the TEM-1 enzyme and can covalently bind to the hydroxyl group of Ser70 in the active site with their β-lactam carbonyl group. This phenomenon is revealed by the persistent appearance of the mass peaks for the covalent enzyme-substrate complexes over the time course (Figures 4.9 and 4.10). The formation of enzyme-substrate complex causes the labeled V216C mutant to give stronger fluorescence, as revealed by the high similarity in the mass spectral and

fluorescence profiles (Figures 4.9 and 4.10). In the substrate-bound state, the fluoresein label is expelled from the active site (Figure 4.13). This subtle movement is likely to cause the fluorescein label to stay away from fluorescence-quenching amino acids such as methionine, tryptophan and tyrosine, which are present in the region around the active site (e.g. Met69, Tyr105 and Trp165). This outward movement causes the fluorescein label to experience weaker quenching and therefore give stronger fluorescence (Figures 4.1 and 4.5). In the case of penicillin G and ampicillin, these antibiotics can also bind to the active site of the labeled V216C mutant and trigger the fluorescence of the fluorescein label. These antibiotics are, however, readily hydrolyzed and leave the active site of the labeled V216C mutant. This fast hydrolytic reaction causes the labeled V216C mutant to return to the substrate-free state in which the fluorescein label stays close the quenching amino acids again, thus restoring its weak fluorescence (Figures 4.2 and 4.3).

The labeled V216C mutant is specific for compounds that can bind to the active site. In the presence of active-site-binding compounds, the labeled V216C mutant shows fluorescence changes. The labeled V216C mutant, however, does not show significant fluorescence changes with non-binding compounds (Figure 4.6) and aggregates formed by small molecules (Figure 4.8). These observations indicate that

the labeled V216C mutant is able to screen for drug compounds capable of binding to the enzyme's active site *in vitro*. The labeled V216C mutant can distinguish between β-lactamase-resistant and β-lactamase-unstable antibiotics by giving characteristic fluorescence profiles. In the case of resistant antibiotics, the labeled V216C mutant shows enhanced and sustained fluorescence profiles (Figures 4.1 and 4.5). For unstable antibiotics, the labeled V216C mutant exhibits declining fluorescence profiles (Figures 4.2–4.4). These observations highlight the value of the labeled V216C mutant as an *in vitro* drug screening tool in the development of new-generation antibiotics.

4.4 Conclusions

The labeled V216C mutant, which has wild-type activity, can detect compounds that can bind to its active site by giving fluorescence changes. For example, the labeled V216C mutant gives stronger fluorescence upon binding to drug compounds (e.g. β-lactam antibiotics). ESI-MS and fluorescence studies have shown that the fluorescence enhancement is likely to arise from the formation of enzyme-substrate complex. In this substrate-bound state, the fluorescein label attached close to the active site is likely to depart from amino acids (e.g. methionine, tryptophan and tyrosine) capable of quenching fluorescence, thus triggering its fluorescence.[105] In the substrate-free state, the fluorescein label is likely to return to the active site and stay close to the fluorescence quenching amino acids and hence restore its weak fluorescence. The labeled V216C mutant can distinguish between β-lactamase-resistant and β-lactamase-unstable antibiotics by giving different fluorescence profiles, highlighting its ability to act as an *in vitro* drug screening tool in the development of new antibiotics. Moreover, the labeled V216C mutant can differentiate active-site-binding compounds from non-binding compounds and aggregates formed by molecules *in vitro*. Taking these observations together, the labeled V216C mutant can serve as a reliable *in vitro* fluorescent drug screening tool in drug development.

Chapter 5

Conclusions

The increasing emergence of β-lactamases has led to a worrying clinical problem worldwide. These bacterial enzymes have different substrate and catalytic profiles and have compromised the clinical utility of a wide range of β-lactam antibiotics.[106-108] As such, extensive efforts have been directed to the development of new inhibitors and antibiotics against clinically relevant β-lactamases. This development has been greatly facilitated by the use of computational drug screening, which can rapidly identify potential drug compounds *in silico*. Despite this exciting development, many drug compounds selected *in silico* can form aggregates *in vitro* which inhibit β-lactamase activity by non-specific protein absorption/adsorption rather than blocking the enzyme's active site. Such compounds are regarded as 'false-positive' drugs and have no genuine potency. To reduce the possibility of selecting 'false-positive' drug candidates, it is highly desirable to develop a reliable drug screening tool that can identify active-site-binding compounds *in vitro*.

In this project, we are interested to develop a fluorescent drug screening tool from a TEM-type β-lactamase. TEM-type β-lactamases are often encountered in pathogenic bacteria, and many of them are derived from the clinically significant TEM-1 enzyme through mutations. Thus, the TEM-1 β-lactamase represents a good protein model in the development of *in vitro* drug screening tools. In our work, we

replaced the Asn170 and Val216 residues (close to the active site) with a cysteine to construct two single mutants (N170C and V216C). Both mutants were further labeled at their cysteine with the environment-sensitive fluorophore fluorescein-5-maleimide. Among these mutants, the labeled V216C mutant has similar catalytic activity to the wild-type TEM-1 enzyme and is therefore suitable for serving as the 'natural' drug target for *in vitro* drug screening. The fluorescence of the labeled V216C mutant is triggered when a drug binds to its active site, as revealed by the ESI-MS and fluorescence studies. This property enables the labeled V216C mutant to distinguish active-site binding compounds from non-binding compounds and 'drug aggregates'. Moreover, the labeled V216C mutant can differentiate between β-lactamase-resistant and β-lactamase-unstable antibiotics by giving different fluorescence profiles, highlighting its value in the development of new-generation antibiotics. With its useful *in vitro* drug screening function, the labeled V216C mutant will find its application in drug development. Moreover, the labeled V216C mutant also serves as a protein model for the development of fluorescent drug screening tools from other TEM-type β-lactamases.

High-throughput drug screening has become an indispensible task in drug development because of its ability to screen a large pool of drug candidates in a short

time. This task can be achieved by using fluorescence-based microtiter plate readers, which can simultaneously monitor up to 1536 samples. In this study, we have demonstrated that the labeled TEM-1 V216C mutant is able to perform *in vitro* drug screening. This labeled mutant also has the potential to be further developed as a high-throughput drug screening tool. For example, the labeled V216C mutant can be immobilized on the well of a microtiter plate by chemical modification (e.g. covalently linking the free amino group of the N-terminus of the labeled mutant to the amino-reactive chemical groups on the wells). With automatic sample injectors, different drug candidates can be injected to the immobilized labeled V216C mutant, and the fluorescence signals of the labeled mutant are monitored simultaneously. Such development can greatly facilitate the drug development for the β-lactamases in the TEM family.

References:

1. Patrick, G. L., *An Introduction to Medicinal Chemistry*. 4 ed.; Oxford University Press: 2009.

2. McDonough, M. A.; Anderson, J. W.; Silvaggi, N. R.; Pratt, R. F.; Knox, J. R.; Kelly, J. A., Structures of two kinetic intermediates reveal species specificity of penicillin-binding proteins. *Journal of Molecular Biology* **2002,** 322, (1), 111-122.

3. Matagne, A.; Dubus, A.; Galleni, M.; Frere, J. M., The beta-lactamase cycle: a tale of selective pressure and bacterial ingenuity. *Natural Product Reports* **1999,** 16, (1), 1-19.

4. Bryskier, A., *Antimicrobial Agents: Antibacterials and Antifungals*. ASM Press: 2005.

5. Fisher, J. F.; Meroueh, S. O.; Mobashery, S., Bacterial resistance to beta-lactam antibiotics: Compelling opportunism, compelling opportunity. *Chemical Reviews* **2005,** 105, (2), 395-424.

6. Minami, S.; Matsubara, N.; Yotsuji, A.; Araki, H.; Watanabe, Y.; Yasuda, T.; Saikawa, I.; Mitsuhashi, S., Inactivation of Cephamycins by Various Beta-Lactamases from Gram-Negative Bacteria. *Journal of Antibiotics* **1984,** 37, (5), 577-587.

7. Ayers, L. W.; Jones, R. N.; Barry, A. L.; Thornsberry, C.; Fuchs, P. C.; Gavan, T. L.; Gerlach, E. H.; Sommers, H. M., Cefotetan, a New Cephamycin - Comparison of

Invitro Antimicrobial Activity with Other Cephems, Beta-Lactamase Stability, and Preliminary Recommendations for Disk Diffusion Testing. *Antimicrobial Agents and Chemotherapy* **1982,** 22, (5), 859-877.

8. Sawai, T.; Tsukamoto, K., Cefoxitin, N-Formimidoyl Thienamycin, Clavulanic Acid, and Penicillanic Acid Sulfone as Suicide Inhibitors for Different Types of Beta-Lactamases Produced by Gram-Negative Bacteria. *Journal of Antibiotics* **1982,** 35, (11), 1594-1602.

9. Cantu, C.; Huang, W. Z.; Palzkill, T., Cephalosporin substrate specificity determinants of TEM-1 beta-lactamase. *Journal of Biological Chemistry* **1997,** 272, (46), 29144-29150.

10. Galante, D.; Esposito, S.; Barba, D.; Pennucci, C.; Limauro, D.; Scioli, C., Comparative Activity of Ceftazidime and 4 Other Cephalosporins against Gram-Negative Bacteria and Their Sensitivity to Beta-Lactamases. *Chemioterapia* **1984,** 3, (4), 250-254.

11. Kumagai, T.; Tamai, S.; Abe, T.; Hikida, M., Current Status of Oral Carbapenem Development. *Curr. Med. Chem. – Anti-Infective Agents* **2002,** 1, 1-14.

12. Livermore, D. M., beta-lactamase-mediated resistance and opportunities for its control. *Journal of Antimicrobial Chemotherapy* **1998,** 41, 25-41.

13. Bush, K.; Freudenberger, J. S.; Sykes, R. B., Interaction of Azthreonam and

Related Monobactams with Beta-Lactamases from Gram-Negative Bacteria. *Antimicrobial Agents and Chemotherapy* **1982,** 22, (3), 414-420.

14. Perilli, M.; Franceschini, N.; Bonfiglio, G.; Segatore, B.; Stefani, S.; Nicoletti, G.; Perez, M. D. T.; Bianchi, C.; Zollo, A.; Amicosante, G., A kinetic study on the interaction between tazobactam (a penicillanic acid sulphone derivative) and active-site serine beta-lactamases. *Journal of Enzyme Inhibition* **1999,** 15, (1), 1-10.

15. Imtiaz, U.; Billings, E.; Knox, J. R.; Manavathu, E. K.; Lerner, S. A.; Mobashery, S., Inactivation of Class-a Beta-Lactamases by Clavulanic Acid - the Role of Arginine-244 in a Proposed Nonconcerted Sequence of Events. *Journal of the American Chemical Society* **1993,** 115, (11), 4435-4442.

16. Bush, K.; Macalintal, C.; Rasmussen, B. A.; Lee, V. J.; Yang, Y. J., Kinetic Interactions of Tazobactam with Beta-Lactamases from All Major Structural Classes. *Antimicrobial Agents and Chemotherapy* **1993,** 37, (4), 851-858.

17. Reading, C.; Farmer, T., The Inhibition of Beta-Lactamases from Gram-Negative Bacteria by Clavulanic Acid. *Biochemical Journal* **1981,** 199, (3), 779-787.

18. Walsh, C.; Wright, G., Introduction: Antibiotic resistance. *Chemical Reviews* **2005,** 105, (2), 391-393.

19. Russell, A. D., Antibiotic and biocide resistance in bacteria: Introduction. *Journal of Applied Microbiology* **2002,** 92, 1S-3S.

20. Sandanayaka, V. P.; Prashad, A. S., Resistance to beta-lactam antibiotics: Structure and mechanism based design of beta-lactamase inhibitors. *Current Medicinal Chemistry* **2002,** 9, (12), 1145-1165.

21. Bush, K.; Miller, G. H., Bacterial enzymatic resistance: beta-lactamases and aminoglycoside-modifying enzymes. *Current Opinion in Microbiology* **1998,** 1, (5), 509-515.

22. Livermore, D. M., Beta-Lactamases in Laboratory and Clinical Resistance. *Clinical Microbiology Reviews* **1995,** 8, (4), 557-&.

23. Medeiros, A. A., Beta-Lactamases. *British Medical Bulletin* **1984,** 40, (1), 18-27.

24. Brook, I., Beta-lactamase-producing bacteria and their role in infection. *Reviews in Medical Microbiology* **2005,** 16, (3), 91-99.

25. Gupta, V., An update on newer beta-lactamases. *Indian Journal of Medical Research* **2007,** 126, (5), 417-427.

26. Bush, K.; Jacoby, G. A.; Medeiros, A. A., A Functional Classification Scheme for Beta-Lactamases and Its Correlation with Molecular-Structure. *Antimicrobial Agents and Chemotherapy* **1995,** 39, (6), 1211-1233.

27. Ambler, R. P., The Structure of Beta-Lactamases. *Philosophical Transactions of the Royal Society of London Series B-Biological Sciences* **1980,** 289, (1036), 321-331.

28. Paterson, D. L.; Bonomo, R. A., Extended-spectrum beta-lactamases: a clinical

update. *Clinical Microbiology Reviews* **2005,** 18, (4), 657-+.

29. Nukaga, M.; Mayama, K.; Hujer, A. M.; Bonomo, R. A.; Knox, J. R., Ultrahigh resolution structure of a class A beta-lactamase: On the mechanism and specificity of the extended-spectrum SHV-2 enzyme. *Journal of Molecular Biology* **2003,** 328, (1), 289-301.

30. Matagne, A.; Lamotte-Brasseur, J.; Frere, J. M., Catalytic properties of class A beta-lactamases: efficiency and diversity. *Biochemical Journal* **1998,** 330, 581-598.

31. Maveyraud, L.; Pratt, R. F.; Samama, J. P., Crystal structure of an acylation transition-state analog of the TEM-1 beta-lactamase. Mechanistic implications for class A beta-lactamases. *Biochemistry* **1998,** 37, (8), 2622-2628.

32. Minasov, G.; Wang, X. J.; Shoichet, B. K., An ultrahigh resolution structure of TEM-1 beta-lactamase suggests a role for Glu166 as the general base in acylation. *Journal of the American Chemical Society* **2002,** 124, (19), 5333-5340.

33. Saves, I.; Burletschiltz, O.; Maveyraud, L.; Samama, J. P.; Prome, J. C.; Masson, J. M., Mass-Spectral Kinetic-Study of Acylation and Deacylation during the Hydrolysis of Penicillins and Cefotaxime by Beta-Lactamase Tem-1 and the G238S Mutant. *Biochemistry* **1995,** 34, (37), 11660-11667.

34. Lamottebrasseur, J.; Dive, G.; Dideberg, O.; Charlier, P.; Frere, J. M.; Ghuysen, J. M., Mechanism of Acyl Transfer by the Class-a Serine Beta-Lactamase of

Streptomyces-Albus-G. *Biochemical Journal* **1991,** 279, 213-221.

35. Escobar, W. A.; Tan, A. K.; Fink, A. L., Site-Directed Mutagenesis of Beta-Lactamase Leading to Accumulation of a Catalytic Intermediate. *Biochemistry* **1991,** 30, (44), 10783-10787.

36. Adachi, H.; Ohta, T.; Matsuzawa, H., Site-Directed Mutants, at Position 166, of Rtem-1 Beta-Lactamase That Form a Stable Acyl-Enzyme Intermediate with Penicillin. *Journal of Biological Chemistry* **1991,** 266, (5), 3186-3191.

37. Ambler, R. P.; Coulson, A. F. W.; Frere, J. M.; Ghuysen, J. M.; Joris, B.; Forsman, M.; Levesque, R. C.; Tiraby, G.; Waley, S. G., A Standard Numbering Scheme for the Class-a Beta-Lactamases. *Biochemical Journal* **1991,** 276, 269-270.

38. Matagne, A.; Misselynbauduin, A. M.; Joris, B.; Erpicum, T.; Granier, B.; Frere, J. M., The Diversity of the Catalytic Properties of Class-a Beta-Lactamases. *Biochemical Journal* **1990,** 265, (1), 131-146.

39. Garau, G.; Garcia-Saez, I.; Bebrone, C.; Anne, C.; Mercuri, P.; Galleni, M.; Frere, J. M.; Dideberg, O., Update of the standard numbering scheme for class B beta-lactamases. *Antimicrobial Agents and Chemotherapy* **2004,** 48, (7), 2347-2349.

40. Galleni, M.; Lamotte-Brasseur, J.; Rossolini, G. M.; Spencer, J.; Dideberg, O.; Frere, J. M., Standard numbering scheme for class B beta-lactamases. *Antimicrobial Agents and Chemotherapy* **2001,** 45, (3), 660-663.

41. Beadle, B. M.; Trehan, I.; Focia, P. J.; Shoichet, B. K., Structural milestones in the reaction pathway of an amide hydrolase: Substrate, acyl, and product complexes of cephalothin with AmpC beta-lactamase. *Structure* **2002,** 10, (3), 413-424.

42. Patera, A.; Blaszczak, L. C.; Shoichet, B. K., Crystal structures of substrate and inhibitor complexes with AmpC beta-lactamase: Possible implications for substrate-assisted catalysis. *Journal of the American Chemical Society* **2000,** 122, (43), 10504-10512.

43. Usher, K. C.; Blaszczak, L. C.; Weston, G. S.; Shoichet, B. K.; Remington, S. J., Three-dimensional structure of AmpC beta-lactamase from Escherichia coli bound to a transition-state analogue: Possible implications for the oxyanion hypothesis and for inhibitor design. *Biochemistry* **1998,** 37, (46), 16082-16092.

44. Galleni, M.; Amicosante, G.; Frere, J. M., A Survey of the Kinetic-Parameters of Class-C Beta-Lactamases - Cephalosporins and Other Beta-Lactam Compounds. *Biochemical Journal* **1988,** 255, (1), 123-129.

45. Pattanaik, P.; Bethel, C. R.; Hujer, A. M.; Hujer, K. M.; Distler, A. M.; Taracila, M.; Anderson, V. E.; Fritsche, T. R.; Jones, R. N.; Pagadala, S. R. R.; van den Akker, F.; Buynak, J. D.; Bonomo, R. A., Strategic Design of an Effective beta-Lactamase Inhibitor LN-1-255, A 6-ALKYLIDENE-2 '-SUBSTITUTED PENICILLIN SULFONE. *Journal of Biological Chemistry* **2009,** 284, (2), 945-953.

46. Venkatesan, A. M.; Agarwal, A.; Abe, T.; Ushirogochi, H.; Ado, M.; Tsuyoshi, T.; Dos Santos, O.; Li, Z.; Francisco, G.; Lin, Y. I.; Petersen, P. J.; Yang, Y. J.; Weiss, W. J.; Shlaes, D. M.; Mansour, T. S., 5,5,6-fused tricycles bearing imidazole and pyrazole 6-methylidene penems as broad-spectrum inhibitors of beta-lactamases. *Bioorganic & Medicinal Chemistry* **2008,** 16, (4), 1890-1902.

47. Venkatesan, A. M.; Agarwal, A.; Abe, T.; Ushirogochi, H.; Yamamura, I.; Ado, M.; Tsuyoshi, T.; Dos Santos, O.; Gu, Y.; Sum, F. W.; Li, Z.; Francisco, G.; Lin, Y. I.; Petersen, P. J.; Yang, Y.; Kumagai, T.; Weiss, W. J.; Shlaes, D. M.; Knox, J. R.; Mansour, T. S., Structure-activity relationship of 6-methylidene penems bearing 6,5 bicyclic heterocycles as broad-spectrum beta-lactamase inhibitors: Evidence for 1,4-thiazepine intermediates with C7 R stereochemistry by computational methods. *Journal of Medicinal Chemistry* **2006,** 49, (15), 4623-4637.

48. Weiss, W. J.; Petersen, P. J.; Murphy, T. M.; Tardio, L.; Yang, Y. J.; Bradford, P. A.; Venkatesan, A. M.; Abe, T.; Isoda, T.; Mihira, A.; Ushirogochi, H.; Takasake, T.; Projan, S.; O'Connell, J.; Mansour, T. S., In vitro and in vivo activities of novel 6-methylidene penems as beta-lactamase inhibitors. *Antimicrobial Agents and Chemotherapy* **2004,** 48, (12), 4589-4596.

49. Venkatesan, A. M.; Agarwal, A.; Abe, T.; Ushirogochi, H.; Yamamura, I.; Kumagai, T.; Petersen, P. J.; Weiss, W. J.; Lenoy, E.; Yang, Y. J.; Shlaes, D. M.; Ryan,

J. L.; Mansour, T. S., Novel imidazole substituted 6-methylidene-penems as broad-spectrum beta-lactamase inhibitors. *Bioorganic & Medicinal Chemistry* **2004,** 12, (22), 5807-5817.

50. Venkatesan, A. M.; Gu, Y. S.; Dos Santos, O.; Abe, T.; Agarwal, A.; Yang, Y. J.; Petersen, P. J.; Weiss, W. J.; Mansour, T. S.; Nukaga, M.; Hujer, A. M.; Bonomo, R. A.; Knox, J. R., Structure-activity relationship of 6-methylidene penems bearing tricyclic heterocycles as broad-spectrum beta-lactamase inhibitors: Crystallographic structures show unexpected binding of 1,4-thiazepine intermediates. *Journal of Medicinal Chemistry* **2004,** 47, (26), 6556-6568.

51. Sandanayaka, V. P.; Prashad, A. S.; Yang, Y. J.; Williamson, R. T.; Lin, Y. I.; Mansour, T. S., Spirocyclopropyl beta-lactams as mechanism-based inhibitors of serine beta-lactamases. Synthesis by rhodium-catalyzed cyclopropanation of 6-diazopenicillanate sulfone. *Journal of Medicinal Chemistry* **2003,** 46, (13), 2569-2571.

52. Bitha, P.; Li, Z.; Francisco, G. D.; Rasmussen, B. A.; Lin, Y. I., 6-(1-hydroxyalkyl)penam sulfone derivatives as inhibitors of class A and class C beta-lactamases - I. *Bioorganic & Medicinal Chemistry Letters* **1999,** 9, (7), 991-996.

53. Phillips, O. A.; Czajkowski, D. P.; Spevak, P.; Singh, M. P.; HaneharaKunugita, C.; Hyodo, A.; Micetich, R. G.; Maiti, S. N., SYN-1012: A new beta-lactamase

inhibitor of penem skeleton. *Journal of Antibiotics* **1997,** 50, (4), 350-356.

54. Tondi, D.; Morandi, F.; Bonnet, R.; Costi, M. P.; Shoichet, B. K., Structure-based optimization of a non-beta-lactam lead results in inhibitors that do not up-regulate beta-lactamase expression in cell culture. *Journal of the American Chemical Society* **2005,** 127, (13), 4632-4639.

55. Newman, D. J.; Cragg, G. M.; Snader, K. M., The influence of natural products upon drug discovery. *Natural Product Reports* **2000,** 17, (3), 215-234.

56. Ness, S.; Martin, R.; Kindler, A. M.; Paetzel, M.; Gold, M.; Jensen, S. E.; Jones, J. B.; Strynadka, N. C. J., Structure-based design guides the improved efficacy of deacylation transition state analogue inhibitors of TEM-1 beta-lactamase. *Biochemistry* **2000,** 39, (18), 5312-5321.

57. Kitchen, D. B.; Decornez, H.; Furr, J. R.; Bajorath, J., Docking and scoring in virtual screening for drug discovery: Methods and applications. *Nature Reviews Drug Discovery* **2004,** 3, (11), 935-949.

58. Schuttelkopf, A. W.; van Aalten, D. M. F., PRODRG: a tool for high-throughput crystallography of protein-ligand complexes. *Acta Crystallographica Section D-Biological Crystallography* **2004,** 60, 1355-1363.

59. Gohlke, H.; Klebe, G., Approaches to the description and prediction of the binding affinity of small-molecule ligands to macromolecular receptors. *Angewandte*

Chemie-International Edition **2002,** 41, (15), 2645-2676.

60. Powers, R. A.; Morandi, F.; Shoichet, B. K., Structure-based discovery of a novel, noncovalent inhibitor of AmpC beta-lactamase. *Structure* **2002,** 10, (7), 1013-1023.

61. Abagyan, R.; Totrov, M., High-throughput docking for lead generation. *Current Opinion in Chemical Biology* **2001,** 5, (4), 375-382.

62. Babaoglu, K.; Simeonov, A.; Lrwin, J. J.; Nelson, M. E.; Feng, B.; Thomas, C. J.; Cancian, L.; Costi, M. P.; Maltby, D. A.; Jadhav, A.; Inglese, J.; Austin, C. P.; Shoichet, B. K., Comprehensive mechanistic analysis of hits from high-throughput and docking screens against beta-lactamase. *Journal of Medicinal Chemistry* **2008,** 51, (8), 2502-2511.

63. Bursulaya, B. D.; Totrov, M.; Abagyan, R.; Brooks, C. L., Comparative study of several algorithms for flexible ligand docking. *Journal of Computer-Aided Molecular Design* **2003,** 17, (11), 755-763.

64. Feng, B. Y.; Toyama, B. H.; Wille, H.; Colby, D. W.; Collins, S. R.; May, B. C. H.; Prusiner, S. B.; Weissman, J.; Shoichet, B. K., Small-molecule aggregates inhibit amyloid polymerization. *Nature Chemical Biology* **2008,** 4, (3), 197-199.

65. Coan, K. E. D.; Shoichet, B. K., Stoichiometry and physical chemistry of promiscuous aggregate-based inhibitors. *Journal of the American Chemical Society* **2008,** 130, (29), 9606-9612.

66. Seidler, J.; McGovern, S. L.; Doman, T. N.; Shoichet, B. K., Identification and prediction of promiscuous aggregating inhibitors among known drugs. *Journal of Medicinal Chemistry* **2003,** 46, (21), 4477-4486.

67. McGovern, S. L.; Shoichet, B. K., Kinase inhibitors: Not just for kinases anymore. *Journal of Medicinal Chemistry* **2003,** 46, (8), 1478-1483.

68. McGovern, S. L.; Helfand, B. T.; Feng, B.; Shoichet, B. K., A specific mechanism of nonspecific inhibition. *Journal of Medicinal Chemistry* **2003,** 46, (20), 4265-4272.

69. McGovern, S. L.; Caselli, E.; Grigorieff, N.; Shoichet, B. K., A common mechanism underlying promiscuous inhibitors from virtual and high-throughput screening. *Journal of Medicinal Chemistry* **2002,** 45, (8), 1712-1722.

70. Coan, K. E. D.; Maltby, D. A.; Burlingame, A. L.; Shoichet, B. K., Promiscuous Aggregate-Based Inhibitors Promote Enzyme Unfolding. *Journal of Medicinal Chemistry* **2009,** 52, (7), 2067-2075.

71. Feng, B. Y.; Simeonov, A.; Jadhav, A.; Babaoglu, K.; Inglese, J.; Shoichet, B. K.; Austin, C. P., A high-throughput screen for aggregation-based inhibition in a large compound library. *Journal of Medicinal Chemistry* **2007,** 50, (10), 2385-2390.

72. Coan, K. E. D.; Shoichet, B. K., Stability and equilibria of promiscuous aggregates in high protein milieus. *Molecular Biosystems* **2007,** 3, (3), 208-213.

73. Feng, B. Y.; Shelat, A.; Doman, T. N.; Guy, R. K.; Shoichet, B. K., High-throughput assays for promiscuous inhibitors. *Nature Chemical Biology* **2005,** 1, (3), 146-148.

74. Ryan, A. J.; Gray, N. M.; Lowe, P. N.; Chung, C. W., Effect of detergent on "promiscuous" inhibitors. *Journal of Medicinal Chemistry* **2003,** 46, (16), 3448-3451.

75. Urbain, J. L.; Wittich, C. M.; Campion, S. R., In vitro measurement of beta-lactamase-catalyzed ampicillin hydrolysis by recombinant Escherichia coli extracts using quantitative high-performance liquid chromatography. *Analytical Biochemistry* **1998,** 260, (2), 160-165.

76. Kumar, R. A.; Clark, D. S., High-throughput screening of biocatalytic activity: applications in drug discovery. *Current Opinion in Chemical Biology* **2006,** 10, (2), 162-168.

77. Chan, P. H.; Chan, K. C.; Liu, H. B.; Chung, W. H.; Leung, Y. C.; Wong, K. Y., Fluorescein-labeled beta-lactamase mutant for high-throughput screening of bacterial beta-lactamases against beta-lactam antibiotics. *Analytical Chemistry* **2005,** 77, (16), 5268-5276.

78. Shoichet, B. K., Interpreting steep dose-response curves in early inhibitor discovery. *Journal of Medicinal Chemistry* **2006,** 49, (25), 7274-7277.

79. Ocallagh.Ch; Shingler, A. H.; Kirby, S. M.; Morris, A., Novel Method for

Detection of Beta-Lactamases by Using a Chromogenic Cephalosporin Substrate. *Antimicrobial Agents and Chemotherapy* **1972,** 1, (4), 283-&.

80. Puckett, L. G.; Lewis, J. C.; Bachas, L. G.; Daunert, S., Development of an assay for beta-lactam hydrolysis using the pH-dependence of enhanced green fluorescent protein. *Analytical Biochemistry* **2002,** 309, (2), 224-231.

81. Jiang, T. T.; Liu, R. R.; Huang, X. F.; Feng, H. J.; Teo, W. L.; Xing, B. G., Colorimetric screening of bacterial enzyme activity and inhibition based on the aggregation of gold nanoparticles. *Chemical Communications* **2009**, (15), 1972-1974.

82. Wu, C. W.; Yarbrough, L. R.; Wu, F. Y. H., N-(1-Pyrene)Maleimide - Fluorescent Cross-Linking Reagent. *Biochemistry* **1976,** 15, (13), 2863-2868.

83. Hermanson, G. T., *Bioconjugate Techniques*. 2 ed.; ACADEMIC PRESS 2008.

84. Chan, P. H.; So, P. K.; Ma, D. L.; Zhao, Y.; Lai, T. S.; Chung, W. H.; Chan, K. C.; Yiu, K. F.; Chan, H. W.; Siu, F. M.; Tsang, C. W.; Leung, Y. C.; Wong, K. Y., Fluorophore-labeled beta-lactamase as a biosensor for beta-lactam antibiotics: A study of the biosensing process. *Journal of the American Chemical Society* **2008,** 130, (20), 6351-6361.

85. Chan, P. H.; Liu, H. B.; Chen, Y. W.; Chan, K. C.; Tsang, C. W.; Leung, Y. C.; Wong, K. Y., Rational design of a novel fluorescent biosensor for beta-lactam antibiotics from a class A beta-lactamase. *Journal of the American Chemical Society*

2004, 126, (13), 4074-4075.

86. Scripcariu, M.; Fleschin, S.; Magearu, V., Determination of Michaelis Constants for beta-lactamase reaction by spectrophotometric methods. *Roum. Biotechnol. Lett.* **2002,** 7, 661-666.

87. Minami, S.; Yotsuji, A.; Inoue, M.; Mitsuhashi, S., Induction of Beta-Lactamase by Various Beta-Lactam Antibiotics in Enterobacter-Cloacae. *Antimicrobial Agents and Chemotherapy* **1980,** 18, (3), 382-385.

88. Strynadka, N. C. J.; Adachi, H.; Jensen, S. E.; Johns, K.; Sielecki, A.; Betzel, C.; Sutoh, K.; James, M. N. G., Molecular-Structure of the Acyl-Enzyme Intermediate in Beta-Lactam Hydrolysis at 1.7 Angstrom Resolution. *Nature* **1992,** 359, (6397), 700-705.

89. Bradford, P. A., Extended-spectrum beta-lactamases in the 21st century: Characterization, epidemiology, and detection of this important resistance threat. *Clinical Microbiology Reviews* **2001,** 14, (4), 933-951.

90. Hüser, J., *High Throughput-Screening in Drug Discovery*. WILEY-VCH Verlag GmbH & Co. kGaA: 2006.

91. Cook, A.; Le, A., The Effect of Solvent and pH on the Fluorescence Excitation and Emission Spectra of Solutions containing Fluorescein. *J. Phys. Chem. Lab* **2006,** 2006, (10), 44-49.

92. Mann, M.; Wilm, M., Electrospray Mass-Spectrometry for Protein Characterization. *Trends in Biochemical Sciences* **1995,** 20, (6), 219-224.

93. Bush, K.; Sykes, R. B., Methodology for the Study of Beta-Lactamases. *Antimicrobial Agents and Chemotherapy* **1986,** 30, (1), 6-10.

94. Samuni, A., Direct Spectrophotometric Assay and Determination of Michaelis Constants for Beta-Lactamase Reaction. *Analytical Biochemistry* **1975,** 63, (1), 17-26.

95. Waley, S. G., Spectrophotometric Assay of Beta-Lactamase Action on Penicillins. *Biochemical Journal* **1974,** 139, (3), 789-790.

96. Frey, P. A.; Hegeman, A. D., *Enzymatic Reaction Mechanisms*. Oxford University Press, Inc: 2007.

97. Drake, A. F., *Circular Dichroism*. Humana Press Inc. : 1994.

98. Venyaminov, S. Y.; Yang, J. T., *Determination of Protein Secondary Structure*. Plenum Press, New York: 1996.

99. Woody, R. W.; Dunker, A. K., *Aromatic and Cystine Side-Chain Circular Dichroism in Proteins*. Plenum Press: New York, 1996.

100. Wang, X. J.; Minasov, G.; Shoichet, B. K., Noncovalent interaction energies in covalent complexes: TEM-1 beta-lactamase and beta-lactams. *Proteins-Structure Function and Genetics* **2002,** 47, (1), 86-96.

101. Palzkill, T.; Le, Q. Q.; Venkatachalam, K. V.; Larocco, M.; Ocera, H., Evolution

of Antibiotic-Resistance - Several Different Amino-Acid Substitutions in an Active-Site Loop Alter the Substrate Profile of Beta-Lactamase. *Molecular Microbiology* **1994,** 12, (2), 217-229.

102. Leung, Y. C.; Robinson, C. V.; Aplin, R. T.; Waley, S. G., Site-Directed Mutagenesis of Beta-Lactamase-I - Role of Glu-166. *Biochemical Journal* **1994,** 299, 671-678.

103. Jelsch, C.; Mourey, L.; Masson, J. M.; Samama, J. P., Crystal-Structure of Escherichia-Coli Tem1 Beta-Lactamase at 1.8-Angstrom Resolution. *Proteins-Structure Function and Genetics* **1993,** 16, (4), 364-383.

104. Fisher, J.; Belasco, J. G.; Khosla, S.; Knowles, J. R., Beta-Lactamase Proceeds Via an Acyl-Enzyme Intermediate - Interaction of the Escherichia-Coli Rtem Enzyme with Cefoxitin. *Biochemistry* **1980,** 19, (13), 2895-2901.

105. Chen, H. M.; Ahsan, S. S.; Santiago-Berrios, M. B.; Abruna, H. D.; Webb, W. W., Mechanisms of Quenching of Alexa Fluorophores by Natural Amino Acids. *Journal of the American Chemical Society* **2010,** 132, (21), 7244-+.

106. Frey, K. M.; Lombardo, M. N.; Wright, D. L.; Anderson, A. C., Towards the understanding of resistance mechanisms in clinically isolated trimethoprim-resistant, methicillin-resistant Staphylococcus aureus dihydrofolate reductase. *Journal of Structural Biology* **2010,** 170, (1), 93-97.

107. Wang, X. J.; Minasov, G.; Shoichet, B. K., Evolution of an antibiotic resistance enzyme constrained by stability and activity trade-offs. *Journal of Molecular Biology* **2002,** 320, (1), 85-95.

108. Sanders, C. C., Beta-Lactamases of Gram-Negative Bacteria - New Challenges for New Drugs. *Clinical Infectious Diseases* **1992,** 14, (5), 1089-1099.